HIV-1 gp120 AND METHAMPHETAMINE-MEDIATED INDUCTION OF PRO-INFLAMMATORY CYTOKINES / CHEMOKINES AND OXIDATIVE STRESS IN ASTROCYTES: IMPLICATIONS IN NEUROINFLAMMATION

A DISSERTATION IN
Pharmacology
and
Cell Biology and Biophysics

Presented to the faculty of the University
of Missouri-Kansas City in partial fulfillment of
the requirements for the degree

DOCTOR OF PHILOSOPHY

By

ANKIT SHAH

M.S. University of Missouri- Kansas City, 2012

Kansas City, Missouri

2013

HIV-1 gp120 AND METHAMPHETAMINE-MEDIATED INDUCTION OF PRO-INFLAMMATORY CYTOKINES/CHEMOKINES AND OXIDATIVE STRESS IN ASTROCYTES: IMPLICATIONS IN NEUROINFLAMMATION

Ankit Shah, Candidate for the Doctor of Philosophy Degree
University of Missouri-Kansas City, 2013

ABSTRACT

HIV associated neurocognitive disorder (HAND) remains a major concern for patients infected with HIV. The viral envelope protein, gp120 has been extensively studied and some of its neurotoxic effects are due to the increased expression of various proinflammatory cytokines. Additionally, it has been well documented that various drugs of abuse can exacerbate HAND, but the mechanism by which this occurs is still poorly understood. *The present study was based on the central hypothesis that HIV-1 gp120 and methamphetamine (MA) interact with each other to increase the cytotoxicity in the astrocytes, which is mediated via induction of various pro-inflammatory cytokines/chemokines and oxidative stress.* In order to test these hypothesis four different studies were designed. We also investigated the mechanism(s) and pathways involved in the functional interaction between gp120 and MA. Furthermore, in order to understand the functional implications of the interaction between MA and gp120, we examined the combined effect of MA and gp120 to produce oxidative stress and apoptotic cell death.

In the first study, we investigated the role of gp120 in the cytokine production in astrocytes. SVGA astrocytes and human fetal astrocytes were either transfected with a plasmid coding gp120 or treated with recombinant gp120 protein and the expression

levels of various cytokines at RNA and protein levels were measured. In order to better explain the role of gp120 in the induction of proinflammatory cytokines/chemokines, 3 major and highly induced cytokines/chemokines were screened and further mechanistic studies were aimed with these 3 cytokines/chemokines. We investigated the role of NF-κB pathway in the transcriptional regulation followed by studies to identify molecular mechanisms. Various MAPKs were assessed for their involvement in the gp120-mediated cytokine/chemokine production. Finally the involvement of PI3K/Akt was explored to understand the signaling pathway upstream of NF-κB.

The second study was designed to address the role of MA in the cytokine production in astrocytes. As observed with gp120, MA also showed increase in the expression of various proinflammatory cytokines. In particular, the induction of IL-6 and IL-8 was found to involve the NF-κB pathway. Furthermore, the activation of NF-κB was found to be independent of MAPKs. However, our studies with PI3K/Akt pathway and mGluR5 suggested that these signaling molecules could trigger the activation of NF-κB.

In the third part of the study, we demonstrated that astrocytes treated with both MA and gp120 increased the expression of IL-6 to levels that are much higher than when cells are treated with either agent alone. This suggested that MA and gp120 may act synergistically to increase the expression of IL-6. Furthermore, the increase in the levels of IL-6 due to treatment with both gp120 and MA was found to involve the PI3K/Akt and NF-κB pathways. Inhibition of either of these pathways could abrogate the increased expression of IL-6 due to MA or gp120 alone, and the increased expression of IL-6 when the astrocytes were treated with both gp120 and MA. Additionally, our results

demonstrated that neither MA nor gp120 utilized the JNK-MAPK and ERK1/2 pathways to increase IL-6 expression.

In the final chapter, we also demonstrated that gp120 and MA cause apoptotic cell death by inducing oxidative stress through the cytochrome P450 (CYP) and NADPH oxidase (NOX) pathways. The results showed that both MA and gp120 induced ROS production in concentration- and time-dependent manners. The combination of gp120 and MA also induced CYP2E1 expression at both mRNA and protein levels, suggesting the involvement of CYP2E1 in ROS production. This was further confirmed by using selective inhibitors of ROS (Vitamin C), CYP2E1 (DAS), NOX, diphenyleneiodonium (DPI), and FWH reaction, deferoxamine (DFO), which significantly reduced ROS production. These findings were further confirmed using specific siRNAs against NOX2 and NOX4 (NADPH oxidase family). Furthermore, gp120 and MA both induced apoptosis (as evidenced by increased caspase-3 activity and DNA lesion via TUNEL assay) and cell death (measured using MTT assay). Additionally, Vitamin C, DAS, DPI, and DFO completely abolished apoptosis and cell death, suggesting the involvement of CYP and NOX pathways in ROS-mediated apoptotic cell death.

In conclusion, we showed that both MA and gp120 independently and in combination increased the production of pro-inflammatory cytokine/chemokines via different pathways. The functional consequences for the interaction between gp120 and MA led to oxidative stress and apoptotic cell death in astrocytes. Thus, our current study provides the evidence and underlying mechanism for the neurotoxic potential of HIV protein, gp120 and substance of abuse, methamphetamine.

APPROVAL PAGE

The faculty listed below, appointed by the Dean of School of Graduate Studies have examined the dissertation titled "HIV-1 gp120 and Methamphetamine-mediated Induction of Proinflammatory Cytokines/chemokines and Oxidative Stress in Astrocytes: Implications in Neuroinflammation" presented by Ankit Shah, candidate for the Doctor of Philosophy degree, and hereby certify that in their opinion it is worthy of acceptance.

Supervisory Committee

Anil Kumar, Ph.D., Committee Chair
Division of Pharmacology & Toxicology

Russell Melchert, Ph.D.
Division of Pharmacology & Toxicology

Santosh Kumar, Ph.D.
Division of Pharmacology & Toxicology

Sullivan Read, Ph.D.
Department of Cell Biology and Biophysics

Xiao-Qiang Yu, Ph.D.
Department of Cell Biology and Biophysics

CONTENTS

TABLES

Table

ILLUSTRATIONS

Figure

ABBREVIATIONS

AD	Alzheimer ’s disease
BBB	Blood-brain barrier
CCL	Chemokine ligand
CNS	Central nervous system
CYP	Cytochrome P450
DAS	Diallylsulfide
DAT	dopamine transporters
DFO	Deferoxamine
DMEM	Dulbecco’s modified Eagle’s medium
DNPH	2,4-dinitrophenylhydrazine
DPI	Diphenyleneiodonium
FWH	Fenton-Weiss-Haber reaction
gp120	glycoprotein 120
GAPDH	Glyceraldehyde 3-phosphate dehydrogenase
HAART	Highly active anti-retroviral therapy
HAD	HIV associated dementia
HAND	HIV associated neurocognitive disorders
H_2DC-FDA	5-(and-6)-chloromethyl-2',7'-dichlorodihydrofluorescein diacetate
HFA	Human fetal astrocytes
HPRT	Hypoxanthine guanine phosphoribosyltransferase
IFN	interferon
IL	Interleukin
MCMD	Minor cognitive motor dysfunction
MDM	Monocyte derived macrophages
MA	Methamphetamine
MFI	Mean fluorescence intensity
MTT	3-(4,5-dimethylthioazol-2-yl)-2,5-diphenyl tetrazolium bromide
NAC	N-acetyl cysteine
NF-κB	Nuclear factor-kappa B
NOS	Nitric oxide synthase
NOX	NADPH oxidase
OP	Orphenadrine
PD	Parkinson’s Disease
PBS	Phosphate buffer saline
ROS	Reactive oxygen species
RT-PCR	Reverse transcriptase-polymerase chain reaction
SOD	Superoxide dismutase
TCA	Trichloroacetic acid
TNF	Tumor necrosis factor
TUNEL	Terminal deoxynucleotidyltransferase-mediated dUTP-nick end labeling
vit.C	Vitamin C
vit. E	Vitamin E

ACKNOWLEDGEMENTS

First and foremost, I would like to thank my thesis mentor, Dr. Anil Kumar for accepting me in his lab immediately after the rotation in his lab during the first semester. At the time, the lab was going through the optimization phase for several techniques. I was fortunate to have first-hand experience with his continuous support along with a then fellow student, Kalpesh Patel. Dr. Kumar's continuous faith in me and inspiration and advice to strive harder and outdo myself has always made me learn new lessons in the lab everyday. Thank you very much for providing me with such a wonderful opportunity to spark my interests into the field of neuroAIDS.

Many thanks go to my thesis committee members, Dr. Santosh Kumar, Dr. Russell Melchert, Dr. Sullivan Read and Dr. Xiao-Qiang Yu for their continuous guidance and help during the meetings, seminars and coursework as well as at the time of critical thinking for the project. The advice from all of you has always been very valuable in all the aspects and helped me develop through these years as a graduate student.

I would like to thank Dr. Bhupendra Singh and Dr. Hari Bhat who have helped me with learning a few techniques. Dr Bhupendra Singh had always been there in the times of need to troubleshoot the basic techniques such as western blotting, oxidative stress measurement etc.

I would also like to express my thanks to all the graduate students and the members of the HIV discussion group, who have continuously helped me in designing experiments, question the results in a critical manner and draw logical conclusions. I would like to mention special thanks to Dr. Silverstein for his help during preparation and proof reading of most of my manuscripts throughout these years. Of course, I must thank the whole staff of the department of Pharmacology & Toxicology, especially Ms. Yvonne McCommon for her

continuous support even before I was accepted in the program. She and Ms. Sharon Self were always available for help in all the administrative formalities right since the admission process.

I would like to convey special thanks to my friends and roommates who were always supportive, both emotionally and sometimes financially through all these years. I would also like to thank the school of graduate studies for the doctoral chancellor's fellowship and the department of Pharmacology & Toxicology for providing me with the funding and various scholarships to earn my daily allowances.

Finally, I would like to thank my parents and sister for giving me the opportunity to achieve my goals in life. It was because of their continuous support and sacrifice that helped me hang in there while I was not home and allowed me to stay focused on my studies. Without their support and encouragement it was impossible to make it this far.

DEDICATION

I would like to dedicate this dissertation to my family for all of their care and support, especially my parents who continuously encouraged me and taught me the importance of education in life.

CHAPTER-1

GENERAL INTRODUCTION

1.1 Human Immunodeficiency Virus:

The first isolation of the Human Immunodeficiency Virus (HIV) from the lymph node of a patient in 1983 provided the first clue of the etiological understanding of AIDS. The virus was found to be a retrovirus type of lentivirus due to its longer incubation periods in the human body (Ascher & Sheppard, 1988). Being a retrovirus, HIV is comprised of two single stranded RNA strands which are converted into DNA with the aid of reverse transcriptase once the virus infects the host system. The viral DNA is then integrated into the host DNA using the viral enzyme, known as integrase. This process allows successful replication of the virus. In addition to the aforementioned enzymes, the virus contains several other proteins in the genome that help the following steps of the replication cycle of the virus and it is thought that the complexity of the additional proteins in the genome attributes to the profound virulence of HIV as opposed to several other lentiviruses (Frankel & Young, 1998).

HIV can be subcategorized into two types, HIV-1 and HIV-2. While HIV-1 is the most common type of the virus that infects human subjects, HIV-2, which is closely related to Simian Immunodeficiency Virus, is highly restricted to the Western African population (Clavel, 1987; De Cock et al., 1993). HIV-1 can be subdivided into four major classes; major (M), non-M/non-O (N), Outlier (O) and Pending identification (P). The M group is comprised of various clades of the virus; i.e. A, B, C, D, E, F, G, H, I, J and K. Among these, Clade B is the most prevalent form of HIV observed in the U.S., Europe, South-East Asia and South America, whereas Clade E and C are more prevalent in Asian countries.

1.2 HIV: A global epidemic:

HIV infection is a global epidemic with a devastating 34.2 million cases all over the world. Apart from the sub Saharan region, where the prevalence is at its largest, substantial number of people are living with HIV infection in the North America (1.4 million as of 2011) (Fig. 1). However, with the advent of combinatorial antiretroviral therapies, AIDS has become rather a chronic condition which was once considered a death sentence. The ability of the virus to readily enter into the CNS results into various neurocomplications, known as HIV associated neurocognitive disorders (HAND) including the most severe form, HIV associated dementia (HAD) (Bromek, Haduch, Golembiowska, & Daniel). However, in the

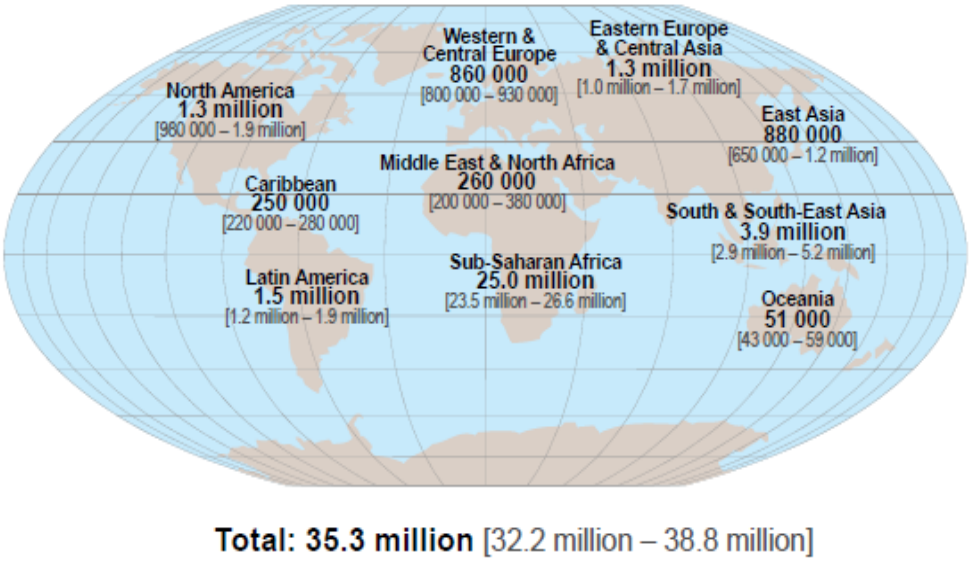

Figure 1: Adults and Children estimated to be living with HIV in Sept. 2013. (Source: UNAIDS)

post-highly active antiretroviral therapy (HAART) era, the incidences of HAD have dramatically reduced from ~60% to ~30%. Even though the life span of HIV-infected patients has improved, the quality of life has gradually deteriorated owing to the neurocognitive impairment such as minor cognitive motor dysfunction (MCMD) and other motor dysfunctions.

As per the "Trojan Horse" theory, upon entry into the CNS via the carrier monocytes/macrophages, HIV can actively infect the microglia with restricted infection in the astrocytes (Carroll-Anzinger & Al-Harthi, 2006; Carroll-Anzinger, Kumar, Adarichev, Kashanchi, & Al-Harthi, 2007). Once inside, the virus can actively replicate upon a favorable environment. The neurotoxicity of the HIV is largely attributed to the virus itself and/or the viral proteins such as gp120 and Tat, shed from the infected cells in various regions of the brain. In particular, neurotoxicity attributed to HIV-1 Tat and gp120 have been extensively studied; however, the underlying mechanism(s) are still unclear. Furthermore, HIV-1 gp120 is of great importance since the presence of gp120 on the surface of the HIV enables it to bind with the CD4 receptor present on the host cells.

1.3 HIV infection and neuropathology:

The infection of CNS takes place at an early stage soon after the HIV-1 infection (Kaul, Zheng, Okamoto, Gendelman, & Lipton, 2005). Almost 60% of HIV infected patients develop neurocomplications in their lifetime (Ozdener, 2005). The HIV patients demonstrate distinct microglial nodules and multinucleated giant cells, which are associated with variety of CNS complications (D. H. Gabuzda et al., 1986; Navia, Cho, Petito, & Price, 1986)**.** Furthermore, the presence of multinucleated giant cells, activated microglia and increased astrocytosis is used as a diagnostic characteristic for HIV-encephalitis (Anthony & Bell, 2008; Levy, Shimabukuro, Hollander, Mills, & Kaminsky, 1985). Post-mortem studies on the brains of HAD subjects were found to demonstrate decrease in the synaptic density, neuronal loss, astrocytosis, microglial nodules and blood brain barrier (BBB) impairments (Everall, Luthert, & Lantos, 1993; K. A. Thompson, McArthur, & Wesselingh, 2001). In addition, the morphometric studies have shown significant loss of the interneurons and pyramidal neurons

in the hippocampus (Fox, Alford, Achim, Mallory, & Masliah, 1997; Masliah, Ge, Achim, Hansen, & Wiley, 1992; Spargo, Everall, & Lantos, 1993) and reduction in the frontal and temporal lobe size in the HAD patients (Ketzler, Weis, Haug, & Budka, 1990; Masliah, Achim, et al., 1992). Recent approach of functional magnetic resonance imaging (fMRI) has revealed enlargement of the CSF cavities, loss of white matter and deep white matter lesions in the brains of HIV infected patients (Archibald et al., 2004; Broderick, Wippold, Clifford, Kido, & Wilson, 1993; Filippi, Ulug, Ryan, Ferrando, & van Gorp, 2001; McArthur, Brew, & Nath, 2005). Despite these evidences suggesting the cognitive impairments in the HIV patients, the exact pathology and their contributions in the behavioral abnormalities is still unclear.

In order to explain the mechanisms underlying these responses, considerable efforts have been made to understand the neuroimmune function of the brain during the HIV pathology. The alteration of cytokines/chemokines is known to be associated with the immune dysfunction. This is congruent with the findings that elevated levels of cytokines are found in the brains of HIV infected patients (Johnson, McArthur, & Narayan, 1988; Laurenzi et al., 1990; Perrella, Finelli, & Carrieri, 1992; Tyor et al., 1992). Furthermore, the presence of various chemokine receptors on the surface of various brain cells such as astrocytes, microglia and neurons suggest the role of cytokines and chemokines in the CNS (Lavi, Kolson, Ulrich, Fu, & Gonzalez-Scarano, 1998). Furthermore, the interaction of the virus with the chemokine receptors (CXCR4 and CCR5) during viral entry leads to their activation, which can activate various signaling cascades including calcium signaling and GPCR-mediated signal transduction (Davis et al., 1997; Madani, Kozak, Kavanaugh, & Kabat, 1998; Meucci et al., 1998).

In addition to the immune dysfunction, a large body of literature suggests a role of oxidative stress in the neuropathology of HIV infection. Oxidative stress may contribute to both cell death (Cohen & d'Arcy Doherty, 1987) and cell proliferation (Klaunig & Kamendulis, 2004), depending on the extent of the reactive oxygen species (ROS) production. Furthermore, the excessive ROS is shown to be associated with several neurodegenerative disorders such as Alzheimer's disease (AD), Parkinson's disease (PD), multiple sclerosis (MS), and HAD (Dasuri, Zhang, & Keller, 2013; Mollace et al., 2001). In addition to the ROS, increased levels of nitric oxide synthase (NOS) is also observed in the astrocytes and microglia of the brains of HAD patients (Adamson, Dawson, Zink, Clements, & Dawson, 1996). Clearly, the mechanisms responsible for the neuropathogenesis of HIV are multifaceted and perhaps therefore still unclear. Furthermore, the studies have shown pivotal role of individual proteins in the neurotoxicity associated with HIV. Therefore, it is of utmost importance to study the role of these viral proteins to understand their contribution to the HIV neurodegeneration.

1.4 Astrocytes in HAND:

Astrocytes are undoubtedly the largest population among the cells of CNS and are primarily known to perform functions such as providing support to the endothelial cells of the BBB, providing nutrients to the nervous tissue, maintenance of ionic balance, and release of neurotransmitters. In the context of HIV, astrocytes are largely thought to play a role as a reservoir since the infection of astrocytes is thought to be unproductive, which allows the virus to enter into latency (Gorry, Purcell, Howard, & McPhee, 1998; Nath, Hartloper, Furer, & Fowke, 1995). Although once thought to remain uninfected similar to neurons, astrocytes have been shown to get infected in recent studies (Churchill et al., 2009; Li, Bentsman,

Potash, & Volsky, 2007; Liu et al., 2004). Although the infection of astrocytes is thought to be highly restrictive, recent advances in the field suggest that upon favorable environment, the astrocytes may activate the virus and support productive replication of the virus (Carroll-Anzinger & Al-Harthi, 2006; Carroll-Anzinger et al., 2007). Once infected, astrocytes release several growth factors, cytokines/chemokines and certain toxins in the surrounding milieu, which in turn affect the neurons and other neighbouring cells. Furthermore, the release of various viral proteins from astrocytes especially Tat, Rev and Nef is well documented (Kutsch, Oh, Nath, & Benveniste, 2000; van Marle et al., 2004).

As mentioned earlier, several studies have been undertaken suggesting clinical symptoms associated with HAND. However, the severity of HAND correlates with the activation of glial cells rather than the viral load (Gonzalez-Scarano & Martin-Garcia, 2005). Therefore, it is critical to understand the neuroimmune function of the astrocytes during the pathology of HAND. The activation of astrocytes is commonly observed during HAD, which triggers a number of molecular and functional changes including release of a plethora of cytokines and chemokines (Tyor et al., 1992). The magnitude of these released cytokines and chemokines requires special attention since the overall population of astrocytes outnumbers any other types of the resident cells in the CNS. Thus the implication of astrocytes in the neuroinflammation presents a unique challenge to be addressed to explain their role in HAND.

1.5 HIV viral proteins: Role of gp120

HIV-1 is a retrovirus comprising of two single stranded RNA in its core and envelope surrounding the inner core (Fig. 2). The genetic

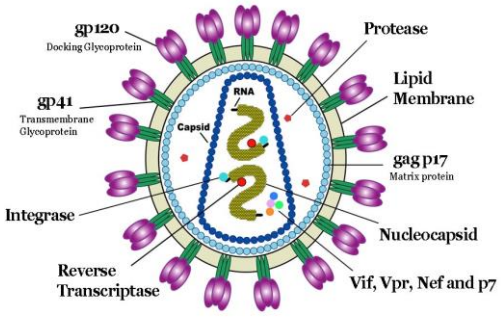

Figure 2: Structural organization of HIV-1

structure (Fig. 3) of the virus is made of accessory proteins such as Nef, Vpr, Vpu/Vpx, Vif, regulatory proteins such as Tat and Rev and the structural proteins such as Gag, Pol and Env. The Env protein is a trimeric structure made of three heterodimers comprising of gp41 and gp120. The regulatory proteins are primarily located in the nucleus of the virus and facilitate viral mRNA production and initiation and elongation of transcription whereas, the accessory

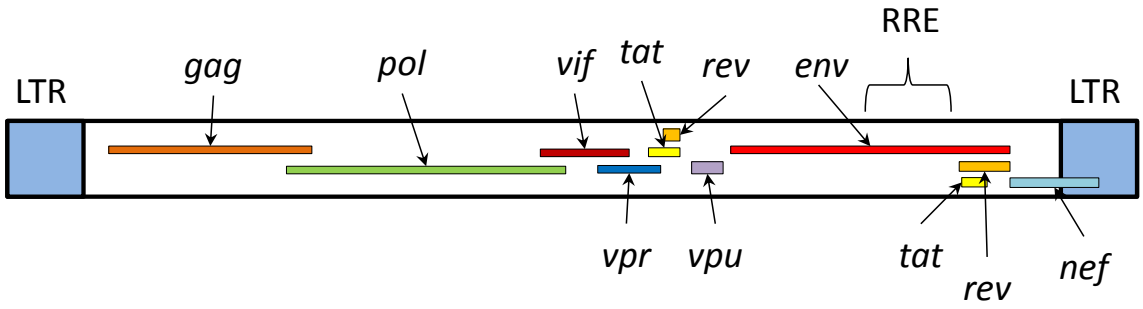

Figure 3: Genomic organization of HIV-1

proteins are located in the cytoplasm or the virion and assist in the integration, release or viral replication. The structural proteins assemble the viral structure and enable the entry of the virus into the host.

1.5.1 HIV-1 gp120 and viral entry:

HIV-1 gp120 plays an important role in the entry of the virus into the host cells (Checkley, Luttge, & Freed, 2011; Wilen, Tilton, & Doms, 2012). Although the exact mechanism is still not understood completely, the current model for the viral entry suggests an interaction between the Env protein and the surface receptors. The initial phase of the entry is facilitated by the interaction between the CD4 receptor on the host surface and viral Env protein. This interaction allows the conformational changes in the Env and the gp120 binds to the co-receptors via V3 loop. This is followed by the fusion of the membranes via gp41 and the viral contents are delivered into the host cytoplasm (Fig. 4)(Wilen et al., 2012).

In addition to the CD4 receptor, the virus interacts with the co-receptors such as CXCR4 and CCR5 found on the cell of the host cell. Depending on the interaction with the co-receptor on surface, the viral tropism is characterized into Macrophage tropic (M-tropic/R5-tropic) or T-cell tropic (T-tropic/X4-tropic). The cell tropism of HIV is largely attributable to the V3 loop and its interaction with the co-receptor. It has been previously reported that the positively charged amino acids in V3 confer a syncytium inducing (SI)

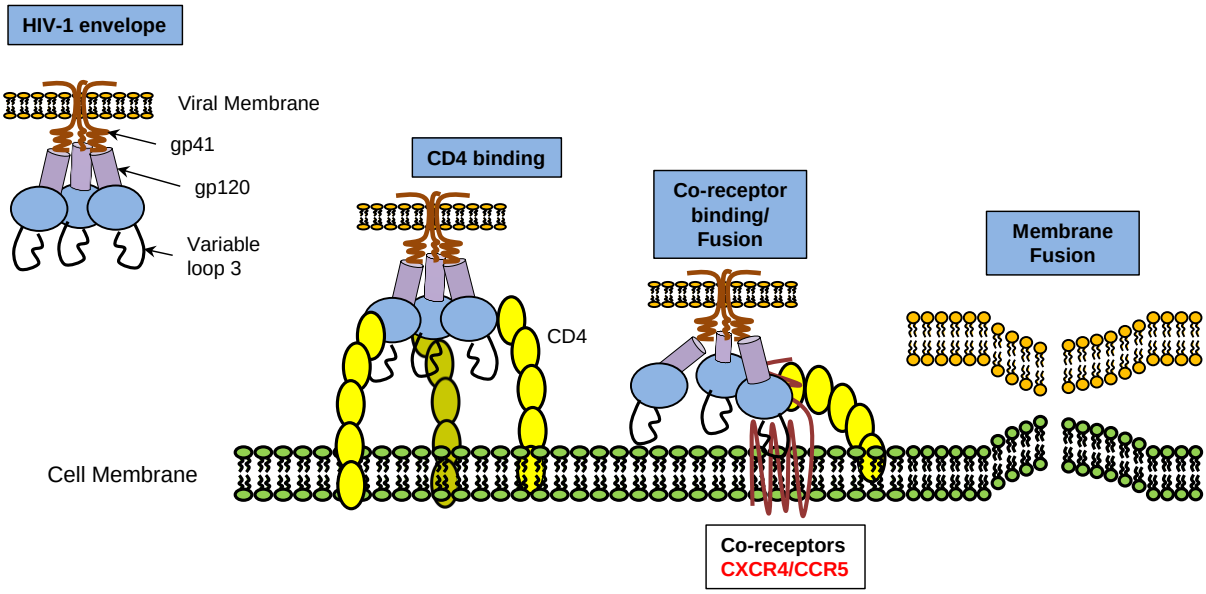

Figure 4: The viral entry into the host cell (Adopted and modified from Wilen et al. 2012).

phenotype and correlate with CXCR4 use (Clapham & McKnight, 2001). The presence of these co-receptors is highly tissue specific and cell-type specific. For example, in the CNS, M-tropic virus is thought to play an important role (D. Gabuzda & Wang, 2000); however, CXCR4 is also expressed in the CNS cells such as astrocytes and brain microvascular endothelial cells. In order to understand the difference between these two strains of the virus, several studies have been undertaken to determine the differences in the virulence and toxicity of both the strains. In particular, when injected into the brains of rats, different strains of gp120 showed neuronal apoptosis in various regions. The M-tropic gp120 showed

neuronal damage in the proximal region of the injection site, while the T-tropic gp120 showed neuronal damage in distal sites such as substantia nigra and somatosensory cortex (Bachis, Aden, Nosheny, Andrews, & Mocchetti, 2006; Bachis, Cruz, & Mocchetti, 2010). In addition to the tropism, gp120 is also important for the viral toxicity in various types of the cells. Thus, during the pathogenesis of HIV, gp120 is among one of the key players.

1.5.2 HIV-1 gp120 and oxidative stress:

In addition to its role in the viral entry, gp120 is also known to induce oxidative stress which further leads to neuronal damage. In a co-culture model containing hippocampal neurons and mixed glial cells, gp120 was shown to increase neuronal death and increased neuronal levels of intracellular calcium (Viviani, Corsini, Binaglia, Galli, & Marinovich, 2001). Furthermore, higher levels of ROS and IL-1β were observed in the glial cells upon gp120 exposure. Another study showed higher levels of ROS and decreased GSH/GSSG ratios in primary rat astrocytes treated with gp120 from an M-tropic HIV strain (HIV-$1_{96ZM651}$) (Ronaldson & Bendayan, 2008). These investigators also found increased expression and activity of MRP-1, an efflux transporter that is involved in the efflux of GSH as well as various therapeutic agents. Treatment of primary mixed glial/neuronal cultures with $gp120_{LAV}$ has also been shown to increase levels of ROS production, apoptosis, lipid peroxidation and a loss of dopaminergic neurons (Hu, Sheng, Lokensgard, Peterson, & Rock, 2009). Exposure of rat brain endothelial cells to gp120 resulted in an increase in indicators of oxidative stress including decreased GSH/GSSG ratios, as well as reduced levels of glutathione peroxidase and glutathione reductase (Price, Ercal, Nakaoke, & Banks, 2005). Injection of gp120 into the caudate-putamen of rats has been shown to induce neurotoxic effects in brain regions that extend several millimeters from the site of injection, as well as

regions more proximal to the injection site. Injection with HIV-1 Bal gp120 caused neuronal loss, loss of tyrosine hydroxylase-positive cells in the substantia nigra as well as loss of dopamine transporter-positive cells in the caudate-putamen. Delivery of antioxidant enzymes by a recombinant SV40 vector, either superoxide dismutase (SOD) or glutathione peroxidase (GPx1), prior to the gp120 treatment resulted in substantial reduction of the toxic effects of the HIV-1 protein (Louboutin, Agrawal, Reyes, Van Bockstaele, & Strayer, 2009). Subsequent studies using cultured neurons demonstrated that dopaminergic neurons were more sensitive to gp120-induced apoptosis but that transduction with a viral vector encoding either SOD or GPx1 reduced the effects of the gp120 through inhibition of ROS (Agrawal et al., 2010). Additional evidence that oxidative stress is involved in mediating the neurotoxic effects of gp120 comes from the observation that treatment of primary cultures of human astrocytes with gp120 resulted in increased expression of several genes involved in antioxidant response including Nrf2, heme oxygenase 1 and NAD(P)H dehydrogenase quinine 1 (P. V. Reddy et al., 2012). The induction of increased levels of these genes could be abrogated by pretreatment of the cells with N-acetyl cysteine and catalase prior to treatment with gp120. Furthermore, gp120 is shown to increase oxidative stress via glutathione and lipid peroxidation (Louboutin & Strayer, 2012; Ronaldson & Bendayan, 2008). The deleterious effect of gp120-mediated oxidative stress in the CNS suggests that gp120 is an important factor that is associated with the pathology of neuroAIDS.

1.5.3 HIV-1 gp120 and proinflammatory cytokines and chemokines:

In addition to various other mechanisms of neurotoxicity attributed to gp120, the increased expression of pro-inflammatory cytokines has been of interest. As mentioned above, Viviani et al. (Viviani et al., 2001) detected increased levels of IL-1β in primary glial

cells treated with gp120. In primary rat astrocytes treated with gp120, increased levels of IL-1β, TNF-α, and IL-6 were observed (Ronaldson & Bendayan, 2006). Production of these cytokines and chemokines involves multiple signal transduction pathways. In the brain microvascular endothelial cells, gp120 was shown to induce apoptosis and cytokines via p38-MAPK and ERK-MAPK pathways (Bardi, Sengupta, Khan, Patel, & Meucci, 2006; Diaz-Ruiz et al., 2001; Khan, Di Cello, Stins, & Kim, 2007) in different cells of the brain. Furthermore, the intracellular levels of Ca^{2+} due to gp120 is mediated via glutamatergic neurotransmission and IP3 pathway (Haughey & Mattson, 2002; Howard, Nakayama, Brooke, & Sapolsky, 1999). The activation of these intermediate molecules can eventually lead to the activation of transcription factors such as NF-κB and AP-1 (Ronaldson, Ashraf, & Bendayan, 2010). The involvement of NF-κB is not only restricted to the production of cytokines and chemokines. Earlier, Alvarez et al. showed involvement of NF-κB and AP-1 pathway in the production of COX-2 in neuroblastoma cells (Alvarez, Serramia, Fresno, & Munoz-Fernandez, 2005). Furthermore, gp120 was found to induce CX3CR1, a chemokine receptor, in neuronal cells and thereby led to neuronal survival (Meucci, Fatatis, Simen, & Miller, 2000). Together these findings explain the multitude of the complications associated with the gp120-mediated neurotoxicity. Obviously, despite being one of the mostly studied HIV proteins, the mechanism by which gp120 alters the neuropathology and neuronal dysfunction is still not understood.

1.6 Substance abuse among HIV-infected patients:

As per the recent report published by National Institute on Drug Abuse, the use of illicit substances in US has increased over the last decade. As of 2011, substance abuse among the overall American population aging 12 and above was reported to be at least 8.7

percent as opposed to 8.3 percent observed back in 2002. The trend was observed to be very common among the age group of 18-20 years with an average of 23 percent of all the drug abusers. These illicit drugs include alcohol, tobacco, marijuana and other psychostimulants such as cocaine, methamphetamine (MA), MDMA and opioids. In addition to oral route of administration, majority of these psychostimulants are abused via injection. Furthermore, injection drug use is reported to be the second common mode of HIV transmission in the United States. (Colfax & Guzman, 2006).

In general, the use of club drugs is observed to be common among men who have sex with men (MSM)(Cochran, Ackerman, Mays, & Ross, 2004). Particularly, MA use is observed to be common among MSM (Gonzales et al., 2009) and the prevalence of HIV was observed to be higher among MSM using MA as opposed to those who do not abuse MA (Buchacz et al., 2005). Similarly, the use of cocaine among the HIV infected patients is thought to alter the immune and CNS functions (Buch et al., 2012). Furthermore, considerable evidence exists which indicates that use of opioids modulate the immune function, thus affecting the HIV pathogenesis (Arora, Fride, Petitto, Waggie, & Skolnick, 1990). Therefore, it is imperative to think that the drugs of abuse play an important role in the pathophysiology of the HIV.

1.6.1 Methamphetamine and HIV:

Methamphetamine is a commonly used psychostimulant that is known to induce euphoria, anxiety, alertness, concentration and hallucination. Due to these properties, it presents high abusive potential. The toxicity of MA is known to involve damage to the dopaminergic neurons, which leads to potent psychosis. It is noteworthy that MA also targets the frontostriatal regions by increasing the dopamine and glutamate transmission, which

leads to neuronal loss (Davidson, Gow, Lee, & Ellinwood, 2001; Langford et al., 2003; Stephans & Yamamoto, 1996). As mentioned earlier, the CNS infection of HIV takes place within weeks after the systemic infection. Once in the CNS, the HIV can produce neurotoxicity in a variety of ways. Among various regions of the brain, basal ganglia exhibits the highest viral loads with the greatest number of infected macrophages, which eventually lead to loss of the dopaminergic neurons in the substantia nigra (Koutsilieri, ter Meulen, & Riederer, 2001; Navia et al., 1986). Furthermore, the dysfunction in the basal ganglia is associated with a number of dopaminergic disorders. Therefore the dopaminergic neurons are key components in the HIV neuropathophysiology. In addition, HIV patients with dementia demonstrate reduced levels of dopamine transporters (DAT) in the brains (Berger, Kumar, Kumar, Fernandez, & Levin, 1994). Similarly, MA-mediated neuronal loss is largely attributed to depletion in the dopamine, 5-HT and dopamine transporters (Cadet et al., 1994; Wagner et al., 1980; Xu, Zhu, & Angulo, 2005). These studies provide strong evidences suggesting a role of MA in the HIV neuroAIDS.

1.6.2 Methamphetamine and neurotoxicity:

In addition to the dopaminergic system, recent studies suggest a possibility of MA-meditated alteration in the immune function in the brain. Among various mechanisms, induction of pro-inflammatory cytokines/chemokines and production of ROS is thought to be associated with the altered immune function as a result of MA (Flora et al., 2002; Silverstein et al., 2011). A single i.p. injection of MA has been shown to induce the hippocampal levels of TNF-α and IL-6 in mice (Goncalves et al., 2010; Goncalves et al., 2008). Additionally, MA was shown to increase microglial cell death via induction of TNF-α and IL-6 (Coelho-Santos, Goncalves, Fontes-Ribeiro, & Silva, 2012). In the peripheral system, various studies

showed MA-mediated induction of TNF-α, CCR5, IL-8, IL-1β, MIP-1α, MIP-1β, IFN-α and CCL5 in human dendritic cells and monocyte derived macrophage (MDM) cells (Liang et al., 2008; Mahajan et al., 2006; Nair & Saiyed, 2011). There exists an extensive amount of literature suggesting that the MA-mediated oxidative stress is associated with dopaminergic mechanism. Furthermore, the ROS generated by MA is found to alter the blood brain barrier via alteration of various tight junction proteins (Mahajan et al., 2008; Ramirez et al., 2009). In spite of the existing literature, the mechanism underlying the MA-mediated neurotoxicity is still not clear. Furthermore, the role of MA in the neuroimmune function is still poorly understood. Therefore, the MA-mediated neurotoxicity and its implication in neuroAIDS are of utmost importance to understand the role of drugs of abuse in the HIV pathogenesis.

1.7 Significance:

Significant amount of work has been undertaken in the direction towards better understanding of HIV pathogenesis. The proposed study was designed to understand how HIV-1 gp120 and MA alter the astrocyte functions and produce cytotoxicity. Production of neuroinflammation is a multifaceted process and our study attempted to investigate into the production of cytokine/chemokines and oxidative stress. We also aimed at the mechanistic explanation underlying these alterations. The present study was based on the central hypothesis that HIV-1 gp120 and methamphetamine (MA) interact with each other to increase the cytotoxicity in the astrocytes, which is mediated via induction of various pro-inflammatory cytokines/chemokines and oxidative stress. The long-term goal of the current study is to develop a therapeutic strategy to block the uncontrolled production cytokines/chemokines or oxidative stress due to gp120 and MA, which can tackle the HAND development. The following specific aims were designed to elucidate our hypothesis:

- To measure the individual, as well as the combined, effects of MA and gp120 on the expression levels of pro-inflammatory cytokines in the SVGA astrocytic cell line as well as human fetal astrocytes (HFA).
- To investigate the role of the NF-κB pathway and dissect the signal transduction mechanisms upstream of the NF-κB pathway responsible for the effects of gp120 and MA.
- To assess the possible role of oxidative stress and the involvement of cytochrome P450 in the mechanism of gp120 and MA mediated astrocyte toxicity.

The findings in the present study are of clinical importance as understanding the molecular mechanisms of increased neuroinflammation via cytokine/chemokine secretion or oxidative stress, can lead to effective development of therapeutic strategies aimed at curbing HAND.

CHAPTER-2

GENERAL MATERIALS AND METHODS

2.1 Cell culture:

All studies were reviewed and approved by Institutional Biosafety Committee and Institutional Review Board of UMKC. SVGA, a clone of human astrocytes (SVG) (Major et al., 1985), were obtained from Dr. Avindra Nath and used in all the experiments unless specified. For experiments with human fetal astrocytes (HFA), the cells were obtained from aborted fetal brain tissue and were cultured in complete DMEM. HFA were kind gift from Dr. Anuja Ghorpade. Both, the SVGA and primary human fetal astrocytes were cultured in DMEM medium supplemented with 10% FBS, 1% L-glutamine, 1% Na_2HCO_3, 1% Non-essential amino acids and 1% gentamicin at 37°C in 5% CO2 environment. The growing cells were >98% astrocytes as defined by GFAP staining. 8 X 10^5 cells/ well in a 6-well plate were used for all the experiments. The cells were incubated overnight to allow them to adhere and treated the next morning.

2.2 Chemicals and Reagents:

The HIV gp120 plasmid, pSyn gp120 JR-FL (Catalog # 4598) was obtained from NIH AIDS research and reference reagent program. Lipofectamine 2000™, and NF-κB inhibitors (IKK-2: SC514; BAY1170-82) were obtained from Invitrogen Inc. (Carlsbad, CA) and Calbiochem (EMD Biosciences Inc., La Jolla, CA), respectively. The inhibitors for the p38 (SB203580), PI3K/Akt (LY294002), JNK (SP600125), and ERK1/2 (U0126) pathways were obtained from Cayman Chemicals (Cayman Chemicals, Ann Arbor, MI). MPEP (an mGluR5 antagonist) were obtained from Sigma (Sigma-Aldrich, St. Louis, MO). DAS was obtained from Fisher (Fisher Scientific, Pittsburgh, PA). DPI, Deferoxamine, orphenadrine,

TROLOX, vitamin E, fluoxetine and paroxetine were purchased from Sigma (Sigma-Aldrich, St. Louis, MO). The recombinant HIV-1 IIIB gp120 (Catalog # 11784), HIV-1 CN54 gp120 (Catalog # 7749), recombinant HIV-1BaL gp120 (Catalog # 4961), HIV-1 gp120 Monoclonal (2G12) (Catalog # 1476) and HIV-1 gp120 CM (Catalog # 2968) were obtained from the NIH AIDS Research and Reference Reagent Program. Monomeric gp120 SF162 and trimeric forms of gp140 SF162 were prepared as discussed earlier (Sather et al., 2009; Sellhorn, Caldwell, Mineart, & Stamatatos, 2009). The antagonist treatment was given 1 hour prior to gp120 transfection or MA treatment. The heat-inactivated gp120 was prepared by heating gp120 at 65ºC for 30 minutes. Negative control samples with gp120-immune complex treatments were also included. Monoclonal antibody gp120 (2G12) was mixed with gp120IIIB for 30 minutes in 10:1 proportion to make immune complex prior to addition to the cells. Specific siRNA against gp120 were designed using Ambion siRNA design tool. Pre-designed and validated siRNA against p50 (P/N AM51331; id 5213), p65 (P/N 4390824; id s11914), various isoform of p38 and negative silencer control (#AM4611) were obtained from Ambion Inc. (Applied Biosystems). Specific siRNA for CYP2E1, CYP2B6, CYP2D6, NOX2, NOX4 and control siRNA were purchased from Dhramacon (Thermo Fisher Scientific, Inc., MA). Vectashield Mounting Medium with DAPI was obtained from Vector laboratories (Vector Laboratories, Burlingame, CA).

2.3 MA treatment of astrocytes transfected with gp120:

Astrocytes were treated with 500 μM of MA once a day for 3 days. The cells were then reseeded in 6-well plates at 8 X 10^5 cells/well and transfected with gp120 in either the presence or absence of MA. Astrocytes that were not treated with MA previously were used for appropriate controls. The cells were grown in the transfection reagents for 5 hours

followed by incubation in complete media for 6 hours in the presence of MA. Total RNA was isolated to measure the expression of IL-6 and IL-8 at the mRNA level. The cytokines released in the supernatants were measured 48 hours post-transfection using a Bio-Rad multiplex cytokine assay. Cells were also treated with 1 dose of methamphetamine prior to gp120 transfection and cytokine expression at the level of mRNA and protein was measured.

2.4 Transfection:

Transfection of SVGA cells was performed using Lipofectamine 2000^{TM} reagent (Invitrogen Inc. Carlsbad, CA) using manufacturer's protocol. Briefly, 8 X 10^5 cells were seeded in 6-well plate and left to adhere overnight. On the following day the cells were washed with PBS and the culture medium was replaced with serum-free DMEM. The transfection reagent mixture was prepared using high glucose DMEM medium-Hyclone (Thermoscientific, Rockford, IL), Lipofectamine 2000^{TM} and the 2 μg plasmid. After 5 hours of incubation with the transfection reagent, the serum-free medium was replaced with DMEM supplemented with 10% FBS. Cells were harvested 6, 12, 24, 48 and 72 hours post-transfection and subjected to RNA isolation. Cell culture supernatants were also collected in order to measure the expression of CCL2 (MCP-1), MIP1, IL-4, IP10, IL6, IL-8, and CCL5 (RANTES) protein released in the medium. The expressions were calculated by taking the ratio of the gp120 transfected over equimolar amount of empty vector. Our transfection efficiency ranged between 55-75% as demonstrated by transfection of a plasmid encoding green fluorescent protein (GFP) followed by flow cytometric analyses. In the experiments involving siRNA-mediated gene knockdown, 20-50 nM scrambled siRNA or silencer select siRNA against specific gene were transfected 48 hours prior to gp120 transfection. After 24 hours, transfection reagents were removed and DMEM supplemented with 10% FBS was

added. Cells were trypsinized and reseeded with $8x10^5$ cells for gp120 transfection. Finally, 6 hour post-transfection, the RNA was extracted using RNeasy mini kits (QIAGEN Inc, Valencia, CA). Similarly, for protein expressions, supernatants were collected after 48 hours post-transfection.

2.5 Electroporation of primary astrocytes for transfection of gp120:

For the primary astrocytes, we used Neuclefactor II (Amaxa-Lonza) to transfect the gp120 plasmid. Transfections were performed as described in the manufacturer's protocol. Briefly, 8×10^6 cells were mixed with the transfection reagent supplied with the kit (Amaxa rat astrocyte, VPI-1006 from Lonza) and the cells were placed in a cuvette. 5µg of gp120 plasmid was added to the cells and electroporation was performed using a unique pulse program (T-020) for rat astrocyte cells which was optimized for human astrocytes. The cells were allowed to recover for 30 minutes with 500µl DMEM media in the cuvette and further diluted with DMEM followed by 30 minute incubation. With the optimum conditions, the transfection efficiency was found to be 60-70 % as measured with GFP expression (Data not shown) and the cell viability ranged from 45-60 %. 2×10^6 cells were plated per well.

2.6 Real time RT-PCR:

The cells were harvested and total RNA was extracted using RNeasy kit from Qiagen (Valencia, CA) at different time intervals as per the experimental design. The mRNA expressions were measured in Real-Time RT-PCR using the forward primer, reverse primer, and probes in a Bio-Rad iCycler using optimized PCR conditions (Sequences and PCR conditions shown in table-1). To normalize gene expression, HPRT was used as housekeeping gene. The data was analyzed using the equation $2-\Delta\Delta CT$ method as described previously (Livak & Schmittgen, 2001).

Table 1: List of primers and PCR conditions

No.	Gene	Primer Sequence	PCR Conditions			
			Reverse Transcription	Denaturation	Annealing	Extension
1	IL-6	Fwd: 5'-GGT ACA TCC TCG ACG GCA TC-3' Rev: 5'-CCA GTG CCT CTT TGC TGC TT-3' Probe: 5'-FAM-CAG CCC TGA GAA AGG AGA CAT GTA ACA GGA GGT AA-3'-BHQ1	50ºC for 30min 95ºC for 15min	95ºC for 15 Sec	57.5ºC for 1 min	
2	IL-8	Fwd: 5'-CTC TTG GCA GCC TTC CTG ATT-3' Rev: 5'-TAT GCA CTG ACA TCT AAG TTC TTT AGC A- 3' Probe: 5'-FAM-CTT GGC AAA ACT GCA CCT TCA CAC AGA-3'BHQ1	50ºC for 30min 95ºC for 15min	95ºC for 30 Sec	61ºC for 30 sec	
3	CCL5	Fwd: 5' ACC AGT GGC AAG TGC TCC A-3' Rev: 5' ACC CAT TTC TTC TCT GGG TTG GCA -3'	50ºC for 30min 95ºC for 15min	95ºC for 15 Sec	54ºC for 30 sec	76ºC for 30 sec
4	MCP-1	Fwd: 5'-GCT GCT CAT AGC AGC CAC CTT C-3' Rev: 5'-TAG CTC GCG AGC CTC TGC AC-3' Probe: 5'-FAM-TCG CTC AGC CAG ATG CAA TCA ATG CC-3'-BHQ1	50ºC for 30min 95ºC for 15min	95ºC for 30 Sec	59ºC for 30 sec	76ºC for 30 sec
5	HPRT	Fwd: 5'-GCT TTC CTT GGT CAG GCA GTA-3' Rev: 5'-CCA ACA CTT CGT GGC GTC CTT T-3'	50ºC for 30min 95ºC for 15min	95ºC for 15 Sec	55ºC for 30 sec	76ºC for 30 sec
6	MIP1α	Fwd: 5' CCC GGT GTC ATC TTC CTA ACC -3' Rev: 5' TTC TGG ACC CAC TCC TCA CTG-3'	50ºC for 30min 95ºC for 15min	95ºC for 15 Sec	54ºC for 30 sec	76ºC for 30 sec
7	IP-10	Fwd: 5' AAG CTG AGA ACC AAG ACC CAG ACA-3' Rev: 5'AAA GGC ATT CTT CAC CTG CTC CAC-3'	50ºC for 30min 95ºC for 15min	95ºC for 15 Sec	62ºC for 30 sec	74ºC for 15 sec
8	IL-4	Fwd: 5' CCA CGG ACA CAA GTG CGA TA-3' Rev: 5' CCC TGC AGA AGG TTT CCT TCT-3'	50ºC for 30min 95ºC for 15min	95ºC for 15 Sec	55ºC for 40 sec	72ºC for 30 sec
9	CYP3A4*	HS00430021_m1	37ºC for 60min 95ºC for 5min	95ºC for 15 Sec	60ºC for 1 min	
10	CYP2E1*	Hs00559367_m1				
11	CYP2D6*	Hs00164385_m1				
12	CYP2B6*	Hs03044636_m1				
13	CYP1A1*	Hs01054794_m1				
14	GAPDH*	4333764F				

* Primers for these genes were obtained from applied biosystems and the sequences were not possible to obtain. The PCR was run with two step realtime RT-PCR as per manufacturer's protocol

2.7 Western blotting:

The cells were harvested at given time points and nuclear and cytoplasmic extracts were prepared using the NE-PER Nuclear extraction kit (Pierce, Rockford, IL) as per the manufacturer's directions or using cytoplasmic buffer (10 mM HEPES, 50 mM NaCl, 0.5 M sucrose, 0.1 mM EDTA and 0.5% TritonX100) and nuclear buffer (10mM HEPES, 500 mM NaCl, 0.1mM EDTA, 0.1mM EGTA and 0.1% IGPAL). In order to collect the whole cell lysates, the cells were lysed with RIPA Buffer (Boston BioProducts, Ashland, MA), followed by homogenization for 15 sec and centrifugation at 10000 RPM for 10 minutes to eliminate cell debris. Protein concentrations were estimated using Pierce BCA protein assay (Pierce). The protein electrophoresis and transfer was performed using Mini-PROTEAN® Tetra Cell (Bio-Rad, Hercules, CA). 20-30 μg of protein was loaded on a 10-12% acrylamide gel and electrophoresed at 80V for 150 min and transferred to a PVDF membrane at 350mA for 90 min. Various primary and secondary antibodies were obtained from different sources and were used at optimized dilution for optimum results as shown in table-2. The band intensities for phosphorylated proteins were normalized using total protein. The nuclear and cytoplasmic expressions of various proteins were normalized using Lamin-B as an endogenous control for the nuclear extracts and β-tubulin/GAPDH/Actin as an endogenous control for the cytoplasmic extracts. HRP conjugated secondary antibodies were used to detect the primary antibodies and detection of protein bands was performed using BM Chemiluminescence Western Blotting Substrate (POD) (Roche Applied Sciences, Indianapolis, IN). Quantification was done using spot densitometry with FluorChem HD2 software (Alpha Innotech, San Leandro, CA).

Table 2: List of antibodies and optimal dilutions

List of Antibodies

Number	Name	Cat. No.	Company	Dilution
1	Actin mouse mAb	sc-8432	Santacruz	(1:2000)
2	NF-κB p50 Rabbit pAb	SC-7178	Santacruz	(1:1000)
3	β Tubulin mouse mAb	sc-5274	Santacruz	(1:2000)
4	Phospho-IκBα (Ser32) (14D4) Rabbit mAb	#2859	Cell Signaling	(1:750)
5	IκB-α Rabbit pAb	sc-847	Santacruz	(1:1000)
6	Lamin B Rabbit mAb	sc-6216	Santacruz	(1:2000)
7	p-Akt1/2/3 Rabbit pAb	sc-101629	Santacruz	(1:750)
8	Akt1/2 goat pAb	sc-1619	Santacruz	(1:1000)
9	gp91-phox (NOX2) goat pAb	sc-5827	Santacruz	(1:1000)
10	Nox4 Rabbit pAb	sc-30141	Santacruz	(1:1000)
11	CYP2B6 Rabbit pAb	ab69652	Abcam	(1:1500)
12	CYP2D6 Rabbit pAb	ab62204	Abcam	(1:1500)
13	p65 Rabbit pAb	ab31481	Abcam	(1:1000)
14	GAPDH goat pAb	2118L	Cell Signaling	(1:2000)
15	GFAP (GA5) Mouse mAb	3670S	Cell Signaling	(1:500)
16	Phospho-Akt (Ser473) (D9E) XP® Rabbit mAb	4060S	Cell Signaling	(1:1000)
17	Caspase-3 (8G10) Rabbit mAb	9665S	Cell Signaling	(1:1000)
18	mouse IgG (conjugated with Alexa Fluor 555)	#4409	Cell Signaling	(1:1000)
19	rabbit IgG (conjugated with Alexa Fluor 488)	#4340	Cell Signaling	(1:1000)
20	rabbit anti-IL-6	ab6672	Abcam	(1:500)
21	rabbit anti-IL-8	sc-7922	Santacruz	(1:500)
22	rabbit anti-CCL5	PA1-84182	Thermo Fisher	(1:500)
23	Ferritin heavy chain (B12)	sc-376594	Santacruz	(1:1500)
24	CYP2E1 (H-21)	sc-133491	Santacruz	(1:1000)
25	goat anti-mouse	sc-2005	Santa Cruz	(1:2000)
26	donkey anti-goat	sc-2020	Santa Cruz	(1:2000)
27	goat anti-rabbit	ab6721	Abcam	(1:2000)

2.8 Multiplex cytokine assay:

The expression of various cytokines such as IL-1β, TNF-α, CCL2, IL-6, IL-8 and CCL5 protein was measured in the cell culture supernatants of the astrocytes. The supernatants were collected at the times indicated and centrifuged twice at 2000Xg for 5 minutes to eliminate debris and stored at -86ºC until used. The concentrations of cytokines were measured using the Bio-Plex multiple cytokine assay kits (Bio-Rad, Hercules, CA) according to the manufacturer's protocol. Briefly, samples were incubated with cytokine-coupled beads for 1 hour. The buffer was removed and incubated with detection antibody for 30 minutes. Finally PE-labeled streptavidin dye was added and fluorescence was measured using Bio-Plex manager 5.0 software. The analysis was performed by 5-PL statistical analysis associated with the software to obtain the concentrations.

2.9 Immunocytochemistry:

In order to observe the intracellular expression of IL-6, IL-8 and CCL5, SVGA cells were immunostained and observed under a confocal microscope. Briefly, 3.5 X 10^5 SVGA cells were seeded in a 12 well plate containing glass coverslips at the bottom of each well. The cells were treated as indicated and incubated for 24 hours. GolgiStop^{TM} (BD biosciences, San Jose) at a concentration of 1 mg/ml was added 6 hours prior to the termination of the indicated treatment in order to prevent the release of cytokine from the cells. Upon termination, the cells were fixed with 1:1 mixture of ice-cold acetone: methanol for 20 min and incubated at -20ºC. Following fixation, the cells were washed 3X with PBS and permeabilized with PBS containing 0.1% Triton X100 (PBST) for 20 min. The coverslips were then blocked with 1% BSA in PBST for 30 min. This was followed by incubation with a cocktail of primary antibodies for overnight incubation followed by 3 washes with PBS for

5 min. The coverslips were then incubated with fluorescent-labeled secondary antibodies for 1 hour in a dark humidified chamber at room temperature. The coverslips were then washed 3X with PBS for 5 min each. Finally, the coverslips were mounted on glass slides using 10 µl vectashield containing DAPI. The slides were analyzed using confocal microscopy in order to obtain fluorescent images using a Nikon Eclipse E800 confocal microscope (Nikon Instruments, Melville, NY). The images were captured using a 60X zoom lens.

2.10 Measurement of reactive oxygen species (ROS) production:

In order to measure the oxidative stress produced in the astrocytes, the cells were treated with various agents for appropriate duration. After the termination of treatments, the cells were washed twice with PBS and incubated with 5µM 5-(and-6)-chloromethyl-2',7'-dichlorodihydrofluorescein diacetate, (CM-H2DCFDA) (Molecular probes, Carlsbad, CA) for 30 min in serum-free medium at 37°C. The cells were then washed twice with PBS to remove unloaded dye and the images were taken using Leica fluorescent microscope (DMI 3000B, Leica Microsystems Inc., Buffalo Grove, IL). Unstained cells were used as experimental controls and the fluorescent images were obtained using excitation and emission wavelengths at 485 nm and 535 nm, respectively.

In order to obtain the fluorescence intensity corresponding to ROS, the cells were collected and acquired using FITC wavelengths on FACSCanto II flow cytometer (BD Biosciences, San Jose, CA). The ROS production was measured using unstained cells as negative controls and cells treated with 500 µM H_2O_2 as positive controls. The mean fluorescence intensities (MFI) were compared between different treatments.

2.11 Cell survival assay (MTT assay):

The cell viability was measured using a colorimetric 3-(4,5-Dimethylthiazol-2-yl)-2,5-diphenyltetrazolium bromide (MTT) assay. Briefly, 2 x 10^5 astrocyte cells were seeded in 12-well plates and treated with either the inhibitor or saline with subsequent treatment with MA and/or gp120 for 48 hours. Upon termination of the treatments, the medium was replaced with 0.2 mM MTT containing medium and incubated at 37°C for 4 hours. The medium was carefully removed and purple formazan crystals were dissolved in 500µl DMSO containing 125µl of Sorenson's glycein buffer. The color formation was measured using Benchmark Microplate Reader (Bio-Rad Laboratories, Hercules, CA) with absorbance at 570 nm and reference at 650nm.

2.12 Terminal deoxynucleotidyl transferase dUTP nick end labeling (TUNEL) Assay:

The measurement of cell viability was also correlated with DNA damage using TUNEL assay as per manufacturer's protocol (GenScript, Piscataway, NJ). Briefly, 2 x 10^5 cells/well were seeded in 12-well plates and the cells were exposed to the treatments with appropriate compounds. Upon treatments, the cells were air-dried for 5 min and fixed (4% paraformaldehyde in PBS) for 30 min at room temperature. After fixation, they were incubated overnight at 4ºC and permeabilized using 1% Triton X-100. The cells were then blocked in 3% H2O2 in methanol and labeled with TUNEL reaction mixture (Biotin-11-dUTP and TdT) and streptavidin-FITC. The smear of cells were washed with PBS to remove excess of labeling reagents and incubated with POD-conjugated Anti-FITC substrate. Finally, 3,3'-diaminobenzidin (DAB) working reagent was added and the cells were observed under light microscope. The images were taken using Leica DMI 300B (Leica Microsystems Inc., Buffalo Grove, IL).

2.13 Caspase-3 activity assay:

The caspase-3 activity was measured using caspase-3 colorimetric assay kit (BioVision Inc., Milpitas, CA) as per the manufacturer's protocol. Briefly, apoptosis was induced as per the treatments under investigation and the cells were lysed using lysis buffer. The protein concentration in the lysates were measured using BCA Protein Assay Kit (Pierce Biotechnology, Rockford, IL) and 50µl of lysates containing 200µg protein was used for caspase-3 activity. The lysates were mixed with 2X reaction buffer containing 10µM DTT and DEVD-pNA substrate and incubated at 37ºC for 2 hours. Finally, the absorbance was measured using Benchmark Microplate Reader (Bio-Rad Laboratories, Hercules, CA) at 405 nm and the caspase activity was calculated with relative standard curve obtained using substrate alone.

2.14 Protein carbonylation assay:

The measurement of carbonylated protein was performed using protein carbonyl colorimetric assay kit (Cayman Chemicals, San Francisco, CA) as per manufacturer's protocol. Briefly, the cells were treated and lysed with RIPA lysis buffer. The protein samples were checked for the absence of nucleic acid contamination and 200 µg proteins were used for the assay. The lysates were mixed with DNPH and incubated in dark for 1 hour followed by consecutive treatments with 20% TCA and 10% TCA. This was followed by 3 washes with ethanol:ethyl acetate (1:1 mixture and finally the pellet was re-suspended in guanidine hydrochloride. The absorbance of the supernatants was measured at 370nm using a microplate reader and carbonylated protein content was calculated.

2.15 Statistical Analysis:

The statistical analysis was performed to represent the data in Mean ± SE values. Results were based on at least 3 separate experiments unless specified with each experiment

performed in triplicates. For the comparison between mock/control group and treatments were performed with two-tailed student's t-test was applied to calculate p-values and p-value ≤ 0.05 was considered significant. The p-value ≤ 0.05 was shown by * and ≤ 0.01 was shown by ** in the bar graphs. Experiments involving two variables were analyzed using general linear model to address, whether they interact with each other in synergistic manner. In order to examine dose-dependent effect of the inhibitors results were analyzed using p-value for trend test using general linear model. No adjustments were done in the statistical analysis for multiple comparisons.

CHAPTER-3

EVALUATION OF THE ROLE OF HIV-1 gp120 IN THE EXPRESSION OF PROINFLAMMATORY CYTOKINES/CHEMOKINES AND THE UNDERLYING MECHANISM(S).

3.1 Introduction:

The neurotoxic effect of the HIV-1 is largely attributed to the viral particles as well as its proteins shed from the virus in brain microenvironment. Therefore, it is essential to understand the neurotoxic potential of gp120. Among various mechanisms for its neurotoxic role (Iskander, Walsh, & Hammond, 2004), HIV-1 gp120 is thought to increase oxidative stress (Agrawal et al., 2010; Ronaldson & Bendayan, 2008), activate macrophage/microglia (Hesselgesser et al., 1998; Kaul, Ma, Medders, Desai, & Lipton, 2007) and alter expression of cytokines/chemokines (Ronaldson & Bendayan, 2006; Viviani et al., 2006). Furthermore, it is well established that increased levels of various cytokines are responsible for the pathology of a variety of CNS complications (Eggert et al., 2009; Jaerve & Muller, 2012; Monji, Kato, & Kanba, 2009; Schoeniger-Skinner et al., 2007; Viviani et al., 2006; Ziebell & Morganti-Kossmann, 2010; Zink et al., 2001). In particular, the pro-inflammatory cytokines/chemokines such as IL-6, IL-8, CCL2, TNF-α and CCL5 have been found in the brains of HIV-1 infected patients. We, therefore, wished to determine if gp120 increased pro-inflammatory cytokines and chemokines.

Low levels of cytokines and chemokines are constitutively expressed by microglia in the CNS and these can be induced to higher levels by inflammatory mediators (Farber & Kettenmann, 2005; Mennicken, Maki, de Souza, & Quirion, 1999). However, astrocytes are undoubtedly the most abundant cell type in the brain with ~50-60% of the total cell

population. They regulate synaptic transmission, maintain the integrity of the blood-brain barrier (BBB), and protect neurons by clearing toxic compounds (Ricci, Volpi, Pasquali, Petrozzi, & Siciliano, 2009). Furthermore, astrocytes are known to regulate the levels of numerous pro- and anti-inflammatory cytokines (Miljkovic, Timotijevic, & Mostarica Stojkovic, 2011). The HIV-1 infection in the brain is predominantly observed in the microglia, where the virus can actively replicate. On the other hand, the neurons remain unaffected due to lack the CD4 receptor for gp120. The viral infection in the astrocytes is largely known to be a reservoir mechanism however, recent studies demonstrate that the infection in astrocytes can become productive in a supportive environment (Carroll-Anzinger & Al-Harthi, 2006; Li et al., 2007).

The current understanding of the mechanism(s) responsible for gp120-mediated neurotoxicity is very limited and requires further studies. Therefore, we sought to determine if gp120 can induce the expressions of various proinflammatory cytokines/chemokines and if so, the signaling pathways involved for the same. The results from this study will provide essential information regarding the molecular mechanism(s) underlying the gp120-mediated toxicities in the astrocytes.

3.2 Results:

3.2.1 HIV-1 gp120 induces various cytokines/chemokines in SVGA astrocytes.

Previously it has been shown that astrocytes express variety of cytokines/chemokines (Miljkovic et al., 2011). In order to determine whether gp120 induces various cytokines/chemokines in the SVGA astrocytes, we screened at least 7 different cytokines/chemokines at mRNA and protein levels (Fig. 5). Among these, the mRNA expressions of IL-6, IL-8 and CCL5 were observed to be strikingly higher than the others.

Similarly, the expressions at protein levels for IL-1β and TNF-α were lower than the minimal detectable range when measured using bio-plex multiple cytokine assay. Therefore, all our follow-up studies were focused on IL-6, IL-8 and CCL5 for gp120-mediated cytokine/chemokine expression and the mechanistic studies of the underlying signaling pathways responsible for the induction these cytokines/chemokines.

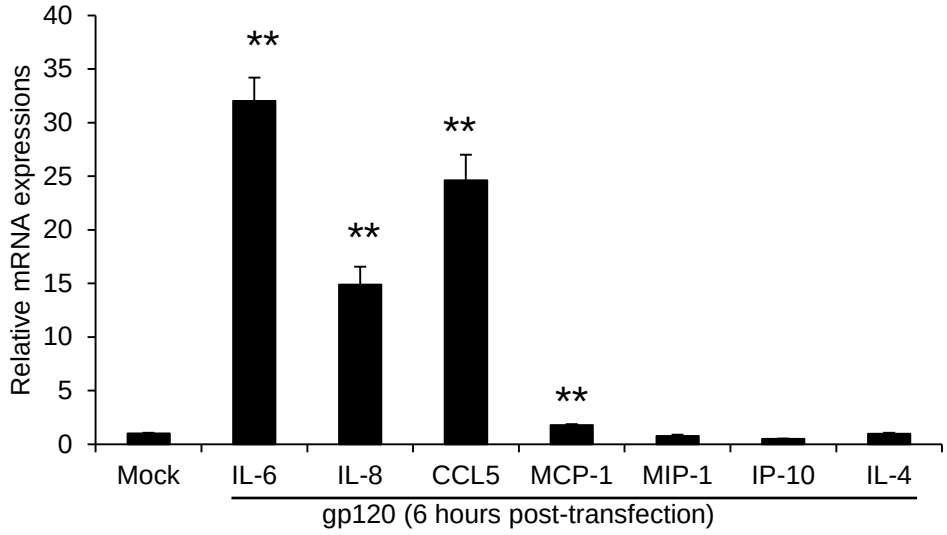

Figure 5: gp120-mediated increase of cytokine expression in SVGA astrocyte cells. $1x10^6$ SVGA astrocytes were transfected with 2 µg gp120 JR-FL (R5 tropic) DNA using Lipofectamine™ 2000. The cells were harvested 6 hours post-transfection. Mock transfection was performed with transfection of equal amount of empty human vector pcDNA3.1. The mRNA expressions were measured using real time RT-PCR and levels are presented as fold difference between gp120 transfected cells and mock-transfected control. Each bar represents mean ± SE of 3 experiments with each experiment done in triplicates. The statistical significance was calculated using student's t-test and ** denotes p value ≤ 0.01.

3.2.2 HIV-1 gp120 induces the expressions of IL-6 in SVGA astrocytes in time-dependent manner.

SVGA cells were transfected with a gp120-expressing plasmid for different durations and the cells were harvested after 6, 12, 24, 48 and 72 hours post-transfection. IL-6 mRNA was found to be increased and peak level (51.3 ± 2.1 fold) was observed at 6 hours after transfection (Fig. 6A). The levels of IL-6 expression reduced after 6 hours and was found to be 33.8 ± 1.1, 12.3 ± 2.4, 3.6 ± 0.4 and 2.7 ± 0.4 fold higher than in empty vector-transfected mock controls after 12, 24, 48 and 72 hour post-transfection, respectively (Fig. 6A). We also quantified IL-6 protein concentrations at these time points, which were observed to be significantly elevated. The levels were increased as soon as 6 hours post-transfection in supernatants of gp120-transfected cells compared to that in mock-transfected controls (3.418 ± 0.708 vs 0.370 ± 0.068 ng/ml) (Fig. 6B). The protein levels of IL-6 increased in both, control and gp120-transfected cells over time. However, gp120-transfected cells showed significantly elevated levels compared to the control. The IL-6 concentration was 4.8 to 11.6 fold-higher in gp120-transfected cells as compared to their respective controls during the observed time-intervals (Fig. 6B).

Previous studies have reported that astrocytes express both the CCR5 and CXCR4 chemokine receptors but not CD4 (Hesselgesser & Horuk, 1999; Lavi et al., 1998). Therefore, we used various strains of gp120 that can bind to CCR5 or CXCR4. In particular, gp120IIIB which can bind to CXCR4 was used in the present study in order to study the effect of exogenous gp120 on astrocytes. Briefly, SVGA cells were treated with 20nM gp120IIIB and increased levels of IL-6 expression were found as soon as 1 hour, which gradually declined over the next 5 hours (Fig. 6C).

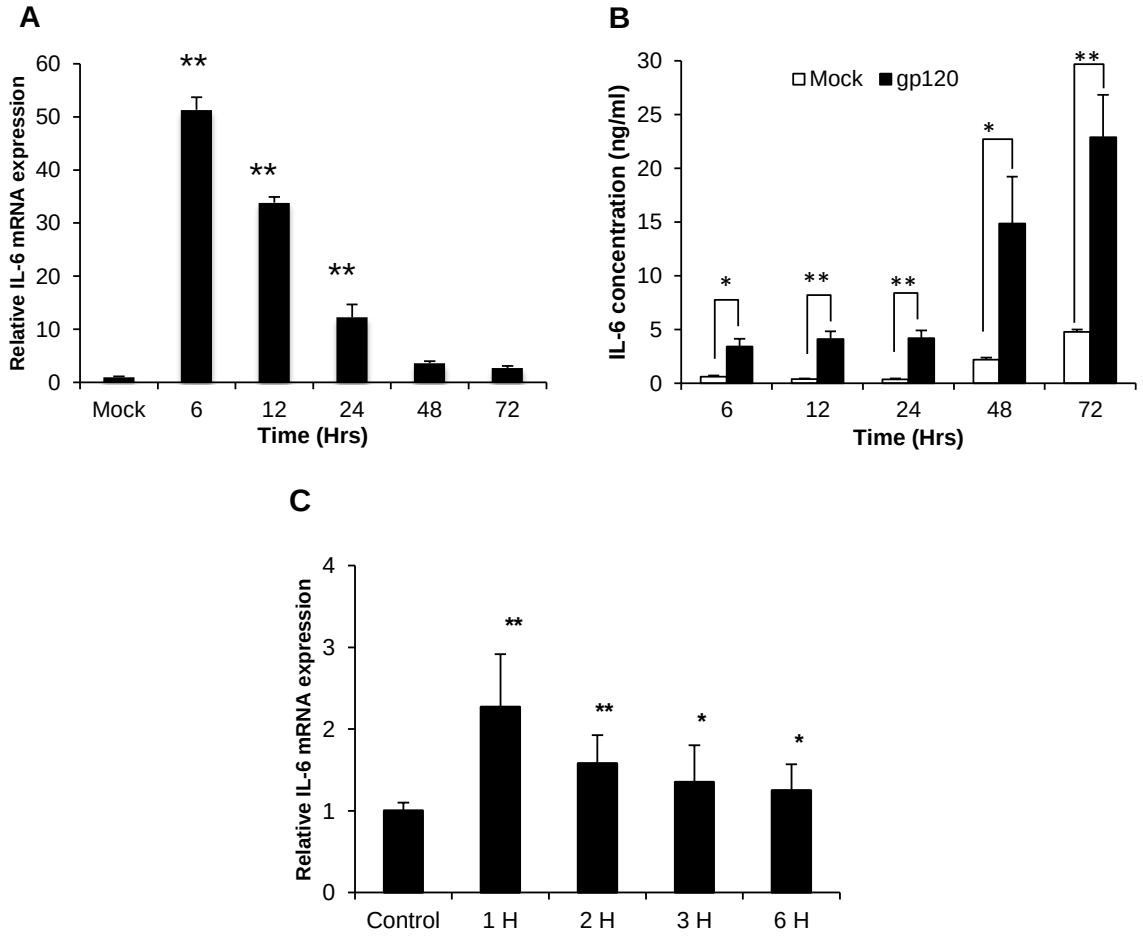

Figure 6: gp120-mediated increase of IL-6 expression in SVGA astrocyte cells. $1x10^6$ SVGA astrocytes were transfected with 2 µg gp120 JR-FL (R5 tropic) DNA using Lipofectamine™ 2000. The cells were harvested at the times described in the text. Mock transfection was performed with transfection of equal amount of empty human vector pcDNA3.1. All times noted on the figure and listed in the text are the times at which cells and supernatants were harvested after the end of the 5 hour transfection protocol. IL-6 mRNA (A) and IL-6 protein (B) expression levels were measured using real time RT-PCR and bioplex assays respectively. In (B), open bars show empty-vector transfected mock controls and closed bars show gp120 transfected samples. (C) shows the effect of exogenous gp120 on SVGA cells. SVGA were exposed to 20nM recombinant gp120IIIB for various lengths of time and total mRNA was isolated. IL-6 expression levels were measured using real time RT-PCR. The mRNA levels are presented as fold difference between gp120 transfected cells and control cells transfected with empty plasmid. The protein concentration is presented as ng/ml protein in supernatant. Each bar represents mean ± SE of 3 experiments with each experiment done in triplicates. The statistical significance was calculated using student's t-test and * and ** denotes p value of ≤ 0.05 and ≤ 0.01, respectively.

3.2.3 HIV-1 gp120 induces the expressions of IL-8 in SVGA astrocytes in time-dependent manner.

Similar to IL-6, we measured the levels of IL-8 after different time intervals post-transfection. The IL-8 mRNA levels increased within hours and the peak levels were observed at 6 hours post-transfection (14.9 ± 3.27 Fold). This was followed by gradual decline in a time dependent fashion from this peak level and was found to be 7.1 ± 1.04, 4.3 ± 0.89, 5.5 ± 1.9 and 2.1 ± 0.14 folds after 12, 24, 48 and 72 hour post-transfection, respectively (Fig. 7A).

We further measured the protein expression in the supernatants at different time points. The protein levels were altered significantly as soon as 6 hours post transfection as compared to control (279.7 ± 22.6 vs 183.9 ± 22.6 pg/ml). The concentration gradually increased in both control and gp120 transfected cells however, gp120 transfected cells showed significant increase in the IL-8 expression. IL-8 over-expression was observed to be 1.52 to 2.41 fold higher in gp120 transfected cells as compared to those in control wells (Fig. 7B). Thus, in spite of the lag phase between the peaks for mRNA and protein expression, both the results demonstrated the time dependent increase in the gp120 mediated IL-8 expression in astrocytes.

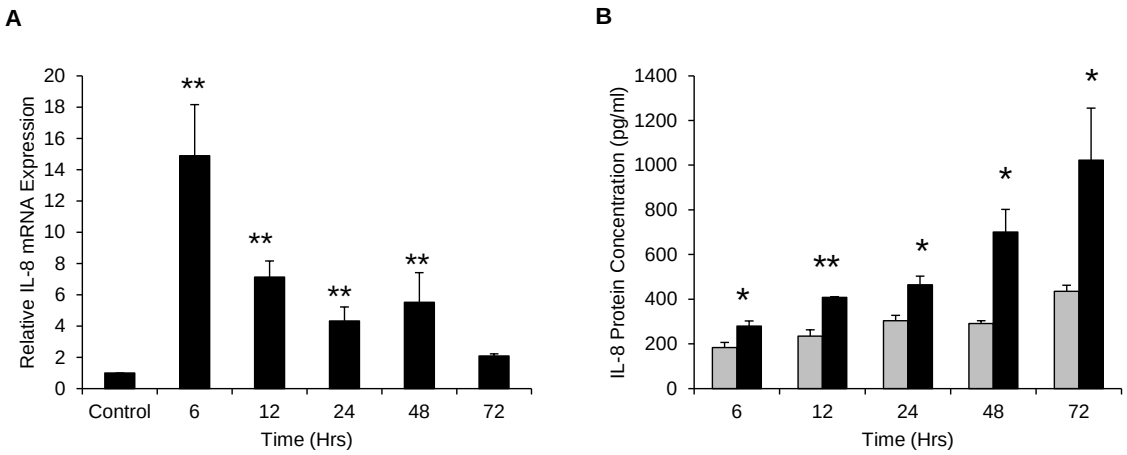

Figure 7: gp120-mediated increase of IL-8 expression in SVGA astrocyte cells. $1x10^6$ SVGA astrocytes were transfected with 2 µg gp120 JR-FL (R5 tropic) DNA using Lipofectamine™ 2000. The cells were harvested at the times described in the text. Mock transfection was performed with transfection of equal amount of empty human vector pcDNA3.1. All times noted on the figure and listed in the text are the times at which cells and supernatants were harvested after the end of the 5 hour transfection protocol. IL-8 mRNA (A) and IL-8 protein (B) expression levels were measured using real time RT-PCR and bioplex assays respectively. In (B), greybars show empty-vector transfected mock controls and black bars show gp120-transfected samples. Each bar represents mean+SE of 3 independent experiments with each experiment done in triplicates. Student's t-test was used to calculate statistical analysis and the significance were denoted as * (p value < 0.05) and ** (p value < 0.01).

3.2.4 HIV-1 gp120 induces the expressions of CCL5 in SVGA astrocytes in time-dependent manner.

The role of CCL5 in inflammation has been widely accepted. It has been shown to increase HIV-1 infection in several reports (Gordon et al., 1999; Trkola et al., 1999). Although the role of CCL5 in HIV-1 infection is controversial, CCL5 in the form of aggregates due to oligomerization on the cell surface is a potent modulator of inflammation (Dairaghi et al., 1998; McDermott et al., 2000). The expression levels of CCL5 in mRNA and protein were measured after 6, 12, 24, 48 and 72 hours. As shown in Fig. 8A, peak levels of CCL5 were observed at 6 hours (24.6 ± 2.67 fold), which gradually reduced till 72 hours (14.3 ± 1.2 fold at 12 hours, 6.2 ± 0.2 fold at 24 hours, 0.9 ± 0.0 fold at 48 hours and 1.4 ± 0.1 fold at 72 hours). Clearly, the mRNA expression of CCL5 due to gp120 was time dependent. Similarly, when measured in the culture supernatants as released protein, CCL5 increased as soon as 6 hours post transfection (0.5 ± 0.21 ng/ml) with a peak response at 48 hours (3.0 ± 0.5 ng/ml) due to gp120 (Fig. 8B).

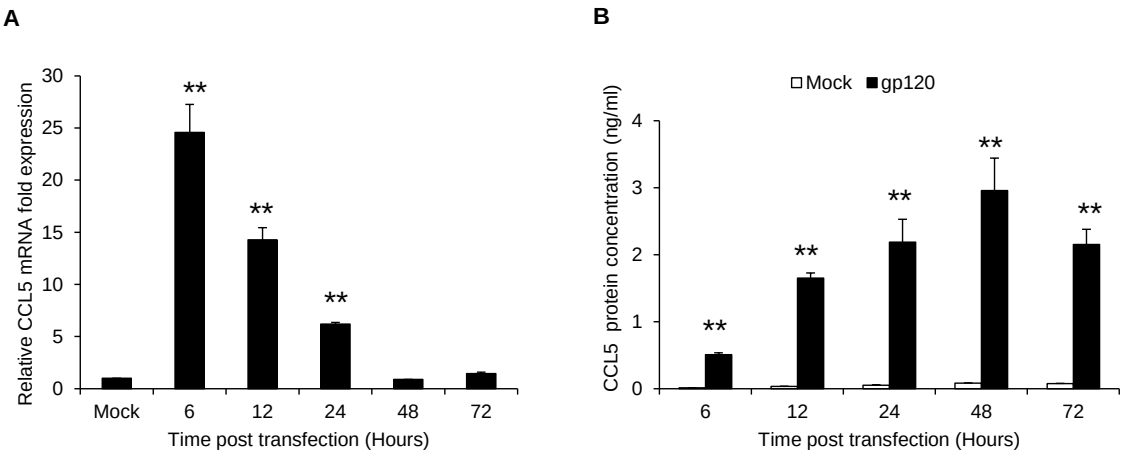

Figure 8: gp120-mediated increase of CCL5 expression in SVGA astrocyte cells. $1x10^6$ SVGA astrocytes were transfected with 2 µg gp120 JR-FL (R5 tropic) DNA using Lipofectamine™ 2000. The cells were harvested at the times described in the text. Mock transfection was performed with transfection of equal amount of empty human vector pcDNA3.1. All times noted on the figure and listed in the text are the times at which cells and supernatants were harvested after the end of the 5 hour transfection protocol. CCL5 mRNA (A) and CCL5 protein (B) expression levels were measured using real time RT-PCR and bioplex assays respectively. In (B), open bars show empty-vector transfected mock controls and closed bars show gp120 transfected samples. Each bar represents mean+SE of 3 independent experiments with each experiment done in triplicates. Student's t-test was used to calculate statistical analysis and the significance were denoted as ** (p value < 0.01).

3.2.5 Role of gp120 in the induction of IL-6 and IL-8 expression in human fetal astrocytes.

To confirm the expression of IL-6 and IL-8 due to gp120 in human primary astrocytes, we obtained at least 3 different donors and they were treated with 20nM gp120IIIB for various lengths of time that ranged from 30 min to 12 hours, after which mRNA and cell culture supernatants were collected. Expression levels of IL-6 mRNA peaked at 1 hour (Fig. 9A) followed by a gradual decline, while protein expression in the supernatants peaked at 6 hours (Fig. 9B). Similar to IL-6, a time-dependent trend was observed in the case of IL-8, although the peak expressions for mRNA and protein were observed at 2 hours and 6 hours, respectively (Fig. 9C-D). In order to determine whether the observed response was specific for gp120, astrocytes were treated with heat-inactivated gp120. The expressions were not significantly different in the treatment with heat-inactivated gp120 compared to the untreated control. We also treated astrocytes with a gp120 protein-antibody complex, and this further confirmed the specificity of gp120 as the gp120-immune complex did not induce IL-6 and IL-8 expression (Fig. 9E-F).

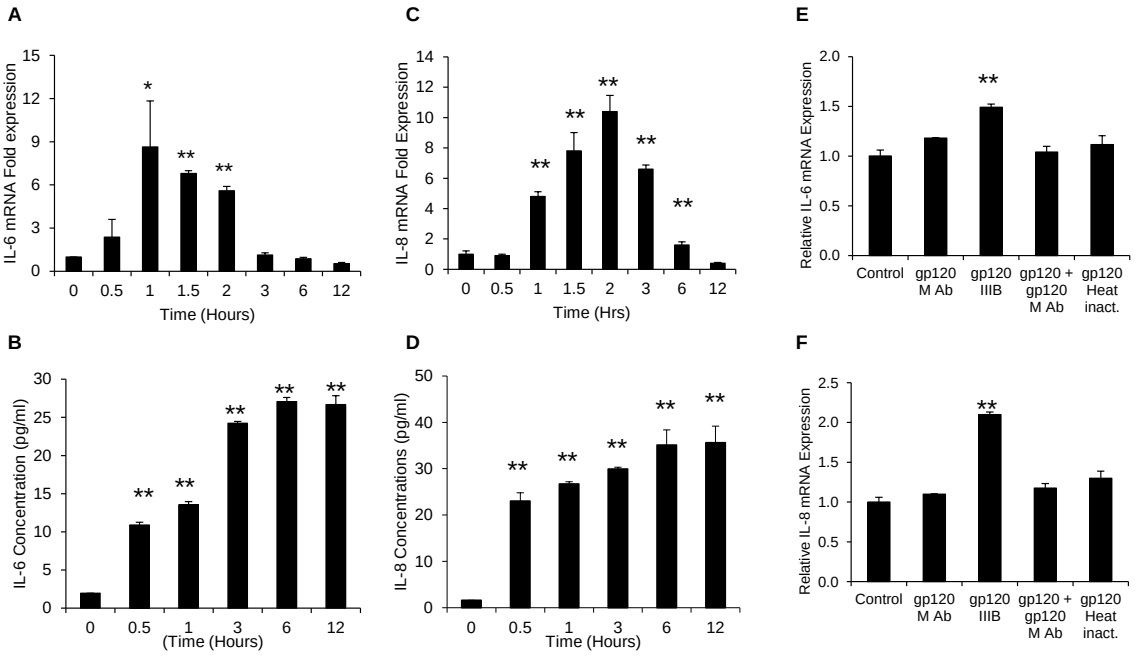

Figure 9: gp120 mediated increased levels of IL-6 & IL-8 in primary human fetal astrocytes. $1x10^6$ primary human fetal astrocytes from each of three different donors were treated with 20nM gp120 IIIB for specific lengths of time and the cells were harvested to obtain mRNA. The cell culture supernatants were collected at the times indicated and used to quantify the level of IL-6 protein expression using a Bio-Plex assay. Levels of IL-6 mRNA expression as measured by real-time RT-PCR peaked at 1 hour (A) and IL-6 protein expressions peaked at 6 hours (B). Similarly, levels of IL-8 mRNA expression as measured by real-time RT-PCR peaked at 2 hour (C) and IL-8 protein expressions peaked at 6 hours (D). Monoclonal antibody for gp120 was used to negate the gp120 mediated response and thus served as another control. Heat inactivated gp120 and monoclonal antibody conjugated with gp120 was used as controls to show gp120 specific IL-6 (E) and IL-8 (F) expressions. Each bar represents mean ± SE of 3 independent experiments with each experiment done in triplicates. Student's t-test was used to calculate statistical analysis and the significance were denoted as * (p value ≤ 0.05) and ** (p value ≤ 0.01).

In addition to CXCR4, gp120 can also bind to CCR5 as a co-receptor. Astrocytes have been reported to express CCR5 in addition to CXCR4 on their surface (Avdoshina, Biggio, Palchik, Campbell, & Mocchetti, 2010; Ronaldson et al., 2010; K. A. Thompson et al., 2004). In order to determine the differential effect of various strains of gp120 based on its tropism, primary astrocytes were treated with 20nM of either gp120 CN54, gp120 CM or gp120 Bal. gp120 CN54, CM and Bal strains are M-tropic strains and all showed over expression of IL-6 and IL-8 (Fig. 10A-B) at variable levels (2.2 ± 0.2, 3.3 ± 0.1 and 1.4 ± 0.1 fold IL-6 for gp120 CN54, CM and Bal, respectively and 1.7 ± 0.2 and 3.5 ± 0.6 fold for gp120 CN54 and CM, respectively). Earlier studies have shown that the trimeric form of gp120 elicited a potent neutralizing response as compared to monomeric gp120 (Grundner et al., 2005), thus providing a better immunogen for vaccination. In order to determine the inflammatory response of astrocytes to both of the forms of gp120, we used monomeric and trimeric forms of the gp120 and gp140 from SF162 strain. Both monomeric and trimeric forms increased the expression of IL-6 (1.2 ± 0.1 and 1.3 ± 0.1 fold respectively) (Fig. 10C) to similar levels. However, they did not elicit any effect on the expression of IL-8 mRNA (Fig. 10D).

Furthermore, in order to determine the effect of transfection on the primary astrocytes, a plasmid encoding gp120 was transfected via electroporation. The expression levels of IL-6 (2.4 ± 0.4 fold) and IL-8 (1.7 ± 0.1 fold) in the transfected cells were comparable to those observed when gp120 was added exogenously (Fig. 10E-F).

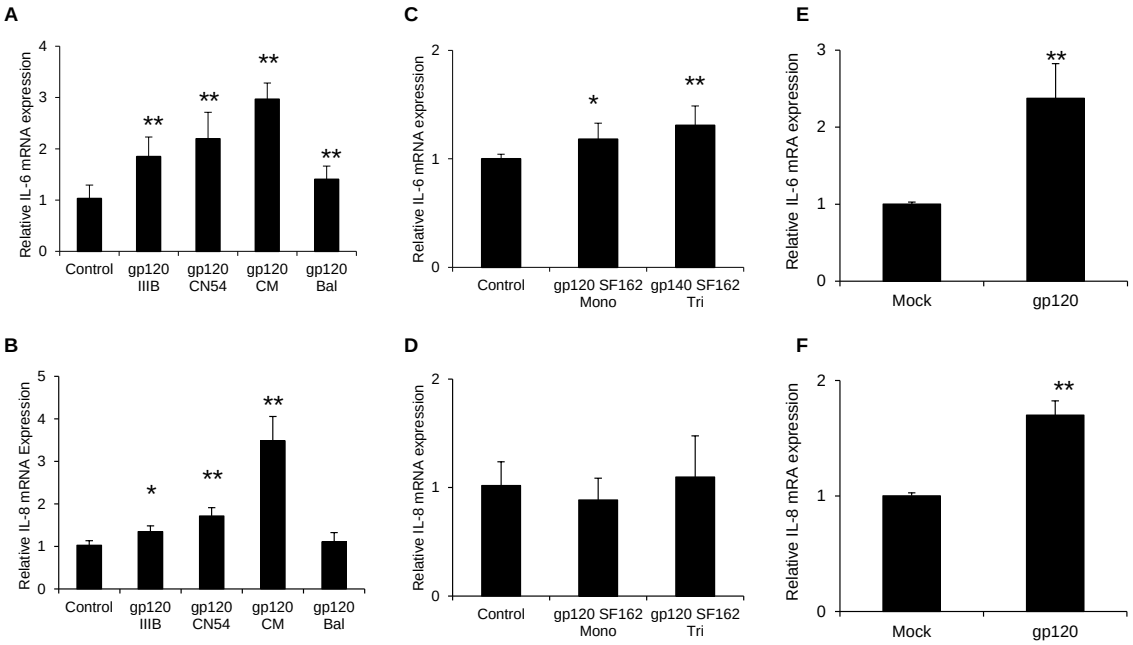

Figure 10: Strain specific response of gp120 on IL-6 & IL-8 in primary human fetal astrocytes. $1x10^6$ primary human fetal astrocytes from each of three different donors were treated with 20nM gp120 from various strains and IL-6 mRNA (A) and IL-8 mRNA (B) expressions were measured. Similarly, gp120SF162 in monomeric and trimeric form were exposed to the primary astrocytes and the levels of IL-6 (C) and IL-8 (D) mRNA were measured. The primary astrocytes were transfected with a plasmid coding for gp120 using electrophoresis method and the expressions of IL-6 (E) and IL-8 (F) were measured post-transfection. Each bar represents mean+SE of 3 independent experiments with each experiment done in triplicates. Student's t-test was used to calculate statistical analysis and the significance were denoted as * (p value < 0.05) and ** (p value < 0.01).

3.2.6 HIV-1 gp120-mediated induction of intracellular protein expression of various cytokines/chemokines.

In order to further confirm HIV-1 gp120-mediated increased expressions of IL-6, IL-8 and CCL5, SVGA astrocytes were immunostained after transfection with a gp120 plasmid. The cells were incubated with a cocktail of GFAP and CCL5 specific antibodies. These proteins were visualized by staining with a secondary antibody labeled with alexafluor 488 and alexafluor 555 for GFAP and the respective cytokine, respectively. DAPI staining was used to visualize the nuclei of the cells. Distinct accumulation in the axons of astrocytes was observed for IL-6 (Fig. 11A-I), IL-8 (Fig. 12A-I) and CCL5 (Fig. 13A-I) in the astrocytes transfected with gp120 as opposed to empty vector transfected mock or untransfected control.

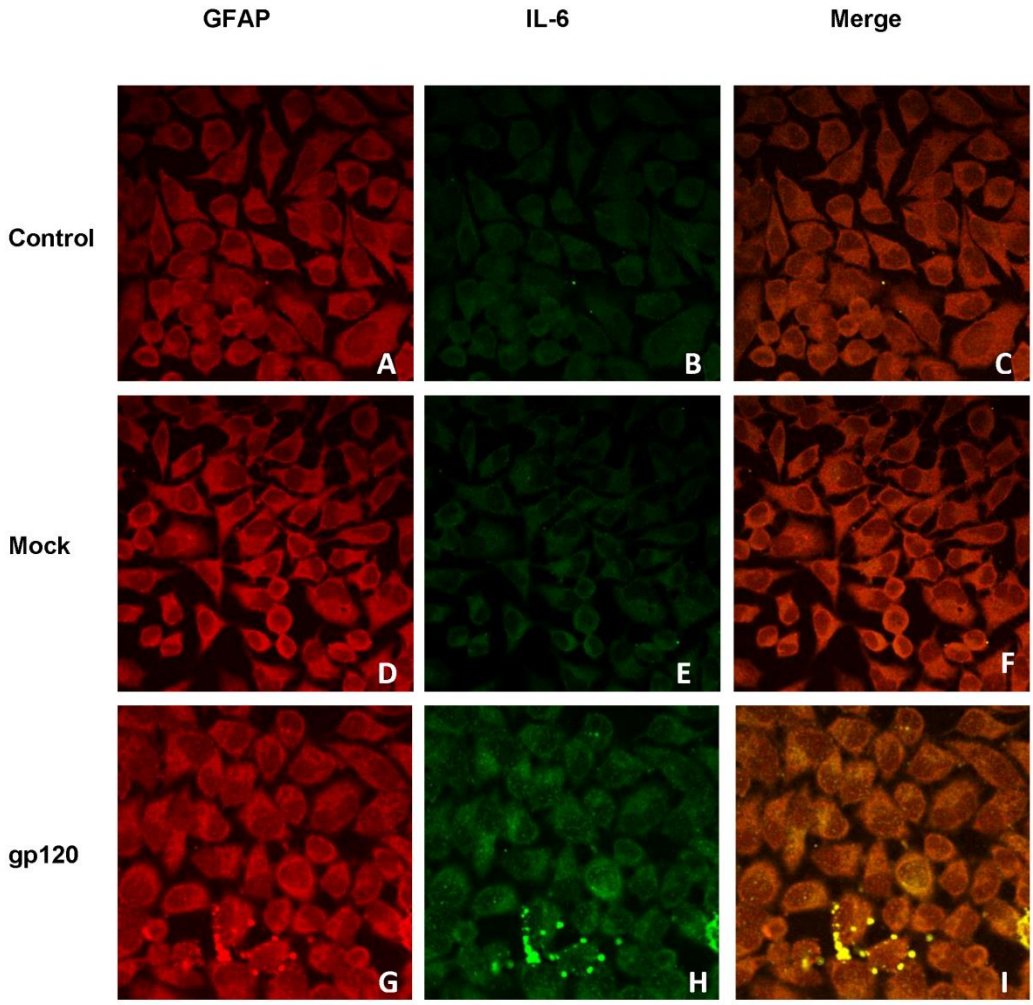

Figure 11: gp120 mediated increased intracellular levels of IL-6 in SVGA astrocytes. SVGA astrocytes were grown on cover slips and transfected with a plasmid encoding gp120. The media was supplemented with golgi-plus during the transfection and the cells were fixed 6 hours post-transfection. The cells were washed, permeabilized, and blocked in PBST containing 1% BSA for 30 minutes and co-stained for GFAP (red) and IL-6 (green). The cells were then incubated with anti-mouse conjugated with Alexa Fluor 555 (for GFAP) and anti-rabbit conjugated with Alexa Fluor 488 antibodies (For IL-6), following which cover slips were mounted using Vectashield mounting medium with DAPI. Individual images for different fluorophores were captured using confocal microscopy and merged using EZ C1 confocal mircroscope software. The non-transfected control showed basal levels of IL-6 and GFAP (A-C). Mock-transfected astrocytes exhibited a marginal increase in IL-6 expression as compared to the control (D-F), while gp120-transfected astrocytes demonstrated stronger accumulation of IL-6 in the processes of astrocytes that colocalized with GFAP (G-I). (Magnification - 60X in A-I)

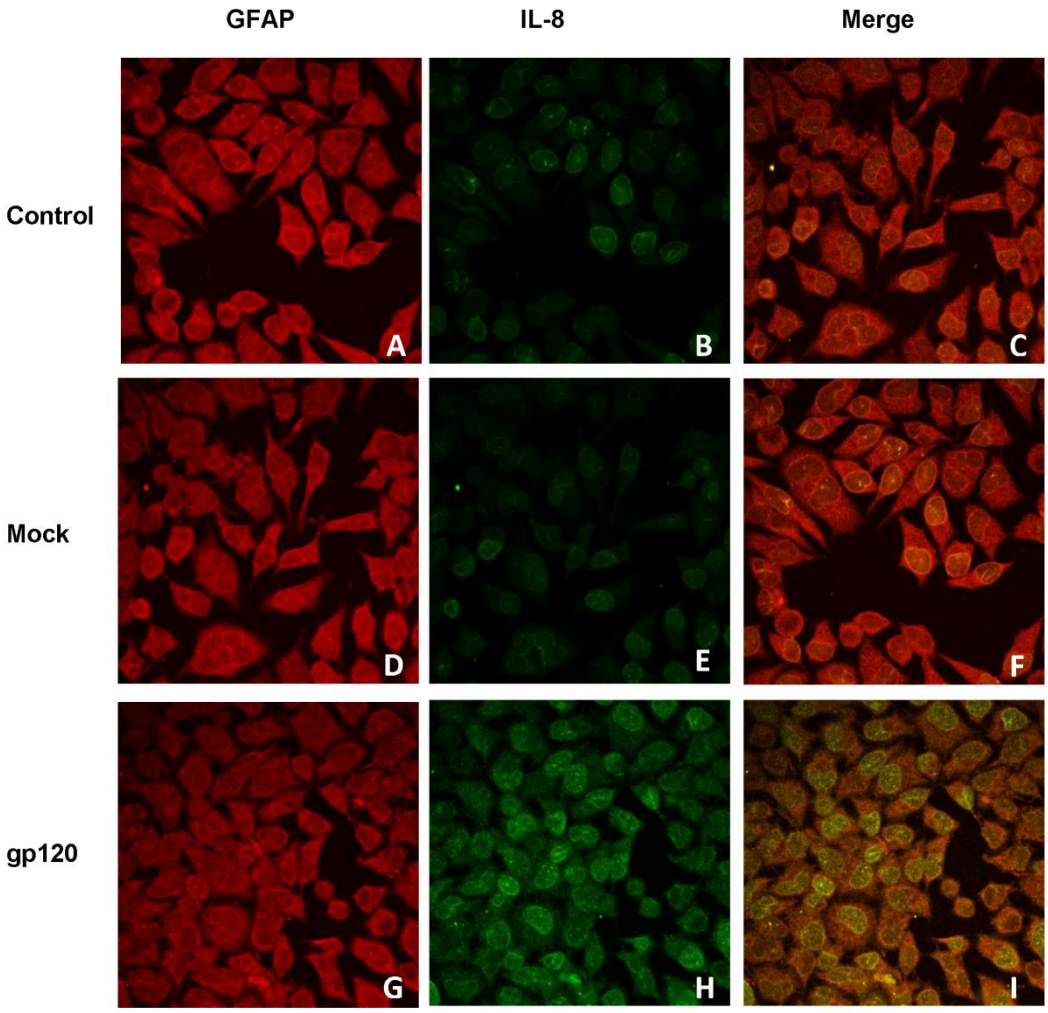

Figure 12: gp120 mediated increased intracellular levels of IL-8 in SVGA astrocytes. SVGA astrocytes were grown on cover slips and transfected with a plasmid encoding gp120. The media was supplemented with golgi-plus during the transfection and the cells were fixed 6 hours post-transfection. The cells were washed, permeabilized, and blocked in PBST containing 1% BSA for 30 minutes and co-stained for GFAP (red) and IL-8 (green). The cells were then incubated with anti-mouse conjugated with Alexa Fluor 555 (for GFAP) and anti-rabbit conjugated with Alexa Fluor 488 antibodies (For IL-8), following which cover slips were mounted using Vectashield mounting medium with DAPI. Individual images for different fluorophores were captured using confocal microscopy and merged using EZ C1 confocal mircroscope software. The non-transfected control showed basal levels of IL-8 and GFAP (A-C). Mock-transfected astrocytes exhibited a marginal increase in IL-8 expression as compared to the control (D-F), while gp120-transfected astrocytes demonstrated stronger accumulation of IL-8 in the processes of astrocytes that colocalized with GFAP (G-I). (Magnification - 60X in A-I)

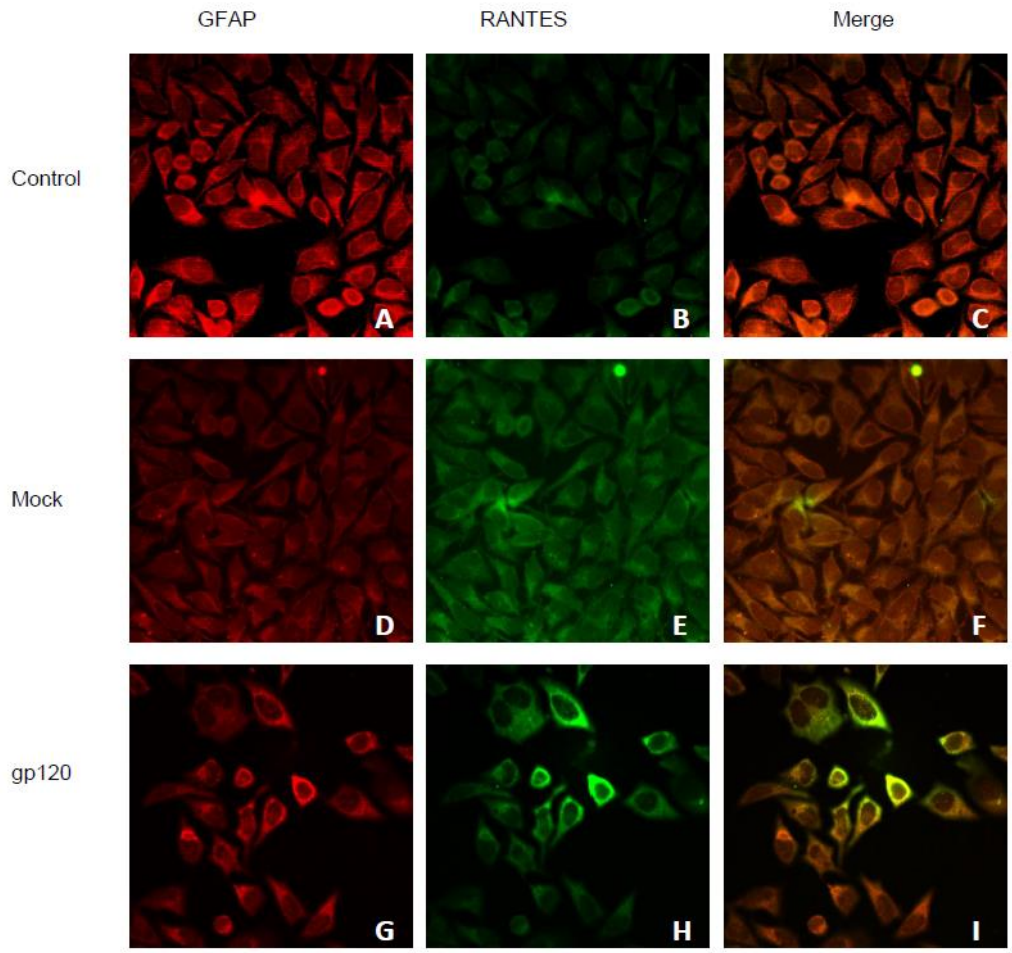

Figure 13: gp120 mediated increased intracellular levels of CCL5 in SVGA astrocytes. SVGA astrocytes were grown on cover slips and transfected with a plasmid encoding gp120. The media was supplemented with golgi-plus during the transfection and the cells were fixed 6 hours post-transfection. The cells were washed, permeabilized, and blocked in PBST containing 1% BSA for 30 minutes and co-stained for GFAP (red) and CCL5 (green). The cells were then incubated with anti-mouse conjugated with Alexa Fluor 555 (for GFAP) and anti-rabbit conjugated with Alexa Fluor 488 antibodies (For CCL5), following which cover slips were mounted using Vectashield mounting medium with DAPI. Individual images for different fluorophores were captured using confocal microscopy and merged using EZ C1 confocal mircroscope software. The non-transfected control showed basal levels of CCL5 and GFAP (A-C). Mock-transfected astrocytes exhibited a marginal increase in CCL5 expression as compared to the control (D-F), while gp120-transfected astrocytes demonstrated stronger accumulation of CCL5 in the processes of astrocytes that colocalized with GFAP (G-I). (Magnification - 60X in A-I)

3.2.7 HIV-1 gp120 increased the activation and translocation of NF-κB in SVGA astrocytes.

Having demonstrated that gp120 can induce the expression of IL-6, IL-8 and CCL5 in astrocytes, we wished to determine the underlying signal transduction pathway. We examined the NF-κB pathway because its role in the induction of inflammatory cytokines, including IL-6 and IL-8, has been well documented (Beg & Baltimore, 1996; Saile, Matthes, El Armouche, Neubauer, & Ramadori, 2001; Siebenlist, Franzoso, & Brown, 1994). Nuclear translocation of p50 and/or p65 (RelB) has been shown to be associated with NF-κB activation. Inhibitory kappa B kinase is an enzyme that phosphorylates and releases IκBα from the p50/p65 heterodimer, thus yielding active NF-κB. Therefore, we measured the levels of p-IκBα to determine whether NF-κB activation plays a role in the induction of the cytokines/chemokines. Primary astrocytes were treated with exogenous gp120 IIIB and the levels of phosphorylated IκBα were measured in whole cell lysates. Although the peak levels were observed at different times for both the donors, the phosphorylation of IκB-α showed a time-dependent increase as compared to total IκBα in astrocytes from both the donors (Fig. 14A & 14B). Peak levels of phosphorylated IκBα were observed at 10 min (1.94 fold higher) for donor-1 and 45 min (2.52 fold higher) for donor-2.

In order to measure the translocation of NF-κB, SVGA cells were transfected with either the plasmid encoding gp120 or empty vector. When compared for the levels of p50 in the cytoplasm and the nucleus, gp120-transfected cells showed 2.74 fold higher p50 translocation as compared to mock-transfected cells ($p<0.001$) (Fig. 14C). The mock transfected cells showed 1.76 ± 0.03 fold difference between nuclear and cytosolic fractions,

($p<0.05$), whereas gp120 transfected cells showed relative levels to be 4.91 ± 0.15 fold ($p<0.001$) higher in the nucleus.

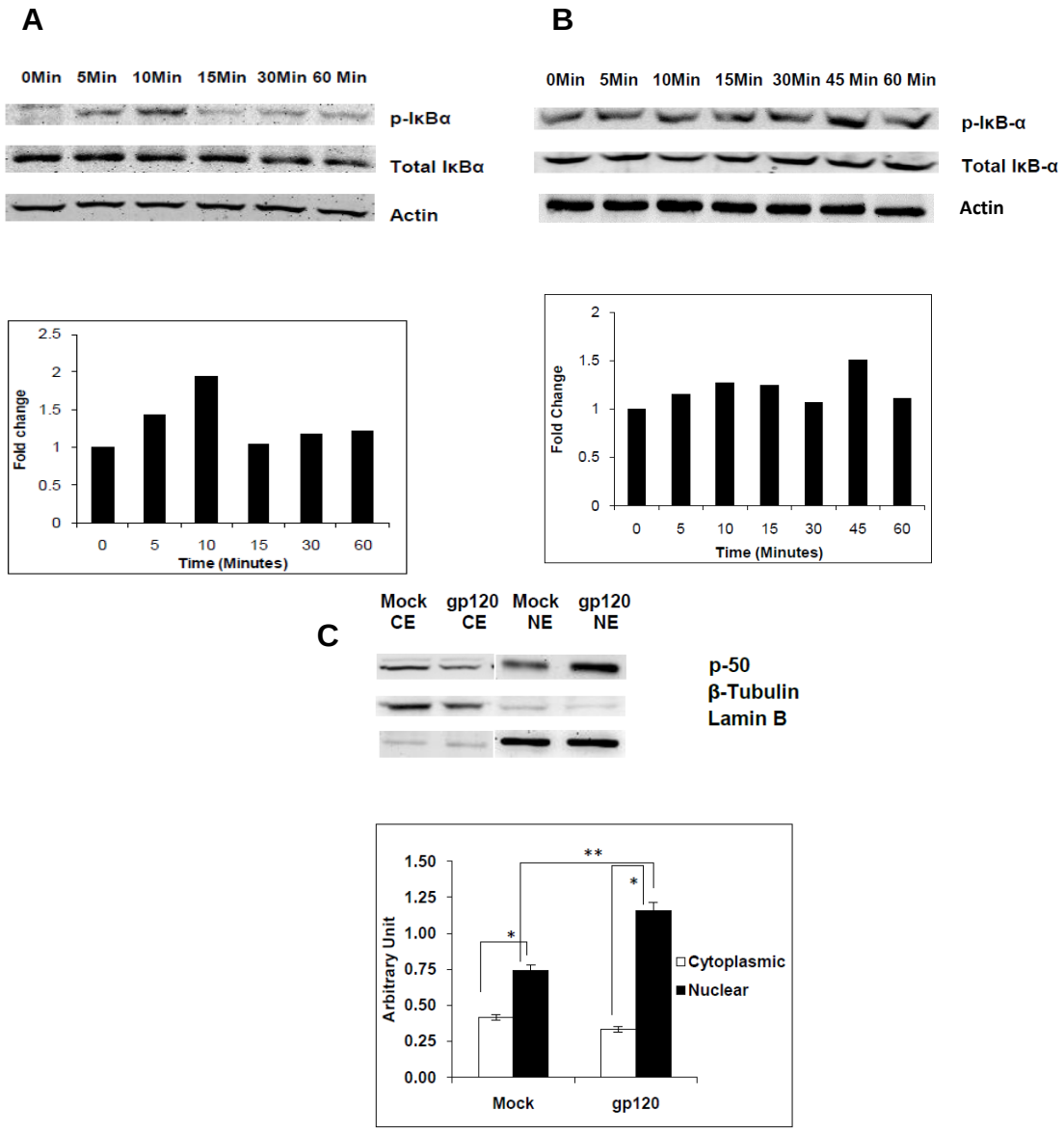

Figure 14: HIV-1 gp120 increased the activation and translocation of NF-κB in astrocytes. Primary human astrocytes from two donors were treated with 20nM gp120 IIIB, cells were collected and lysed using RIPA buffer at different times. These proteins were electrophoresed on 10% SDS gel and transferred to PVDF membrane. Antibodies against p-IκBα, total IκBα and β-actin were used for western blotting and membrane was read on densitometer. Values below the lanes show band intensities of the respective bands for both the donors (A & B). The increase in p-IκB-α was estimated by calculating the ratios of p-IκB-α to total IκB-α. Actin was used as loading control. (C) SVGA cells were either mock-transfected or were transfected with gp120 plasmid for a period of 6 hours followed by separation of cytosolic and nuclear fractions. These proteins were electrophoresed on 10% SDS gel and transferred to PVDF membrane. A representative western blot with lane-1 (mock-transfected SVGA cytosolic fraction), lane-2 (gp120-transfected SVGA cytosolic fraction), lane-3 (Mock-transfected SVGA nuclear fraction) and lane-4 (gp120-transfected SVGA nuclear fraction) is shown. The expression levels of p50 were normalized to their respective compartmental housekeeping genes (LaminB for nucleus and β-tubulin for cytoplasm) as loading controls. The bars, shown in the chart show normalized values of the band intensities for p50 over loading controls for appropriate compartments (LaminB for nucleus and β-tubulin for cytoplasm). The bar chart represents the Mean ± SE of the ratios of p50 to the appropriate housekeeping gene (i.e. laminB for nuclear extracts and β-tubulin for cytoplasmic extracts). The means and SE values are from 3 independent experiments. The statistical significance was calculated using student's t-test and * and ** denotes p value of ≤ 0.05 and ≤ 0.01, respectively.

3.2.8 Role of NF-κB in gp120-mediated induction of cytokines/chemokines in SVGA astrocytes.

Having shown that gp120 induced activation and translocation of NF-κB in astrocytes, we sought to determine if it plays any role in the gp120-mediated induction of cytokines/chemokines. We used SC514 and BAY11-7082, specific inhibitors for Inhibitory kappa B Kinase (P. V. Reddy et al.), which is the enzyme responsible for the phosphorylation of IκBα. SVGA astrocytes were treated with 10 μM of either IKK-2 (SC514: IC50=14.5 μM) or IKKβ (BAY11-7082: IC50=11.2 μM) inhibitors for 24 hours prior to transfection with gp120 and maintained with inhibitors throughout the experiment. The concentration of the inhibitor was determined based on the IC50 as well as the viability of the cells, which were ~90% viable at the inhibitor concentration that was used (data not shown). Expressions of IL-6, IL-8 and CCL5 at mRNA levels were determined at 6 h post-transfection and protein levels were measured at 48 h post-transfection. Both SC514 and BAY11-7082 successfully inhibited gp120-mediated expression of IL-6 mRNA by 56.5 ± 10.5 percent and 60.8 ± 7.3 percent, respectively (Fig. 15A). Similarly, IL-6 protein levels were also reduced by 51.3 ± 12.4% and 34.8 ± 13.3 %, respectively by SC514 and BAY11-7082 (Fig. 15B). When tested for IL-8, both SC514 and BAY11-7082 successfully inhibited gp120-mediated expression of IL-8 at mRNA levels by 27.5 ± 11.5 percent and 42.5 ± 15.9 percent respectively, (Fig. 15C). Similarly, IL-8 protein level was also reduced by 67.3 ± 12.6% and 58.6 ±15.4 % by SC514 and BAY11-7082, respectively (Fig. 15D). When tested for CCL5, SC514 but not BAY11-7082 reduced the CCL5 expression by 44.6 ± 4.2 % at mRNA level and 53.0 ± 20.2 % at protein levels (Fig. 15E & F).

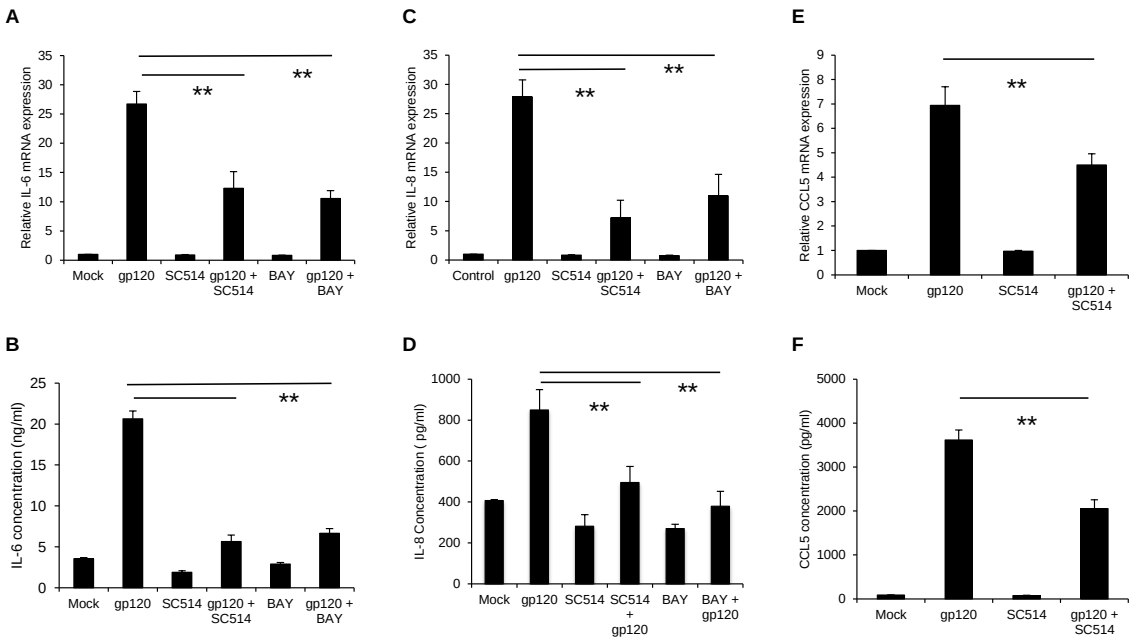

Figure 15: Inhibition of gp120-induced cytokine/chemokine expression by chemical inhibitors for the NF-κB pathway. SVGA astrocytes were treated with 10 µM SC514 or BAY11-7082 for 24 hours prior to the transfection. $1x10^6$ SVGA astrocytes were transfected with 2 µg gp120 DNA in the presence of inhibitor, which was also maintained throughout experiments. The mRNA levels of IL-6 (A), IL-8 (C) and CCL5 (E) were measured at 6 hours post-transfection and protein levels of IL-6 (B), IL-8 (D) and CCL5 (F) were measured at 48 hours post-transfection. Each bar represents mean ± SE of 3 experiments with each experiment done in triplicates. The statistical significance was calculated using student's t test and ** denotes p value ≤ 0.01.

In order to further confirm the involvement of the NF-κB pathway, we knocked down p50 (NF-κB1) and p65 (RelA) subunits using siRNA. The SVGA astrocytes were transfected using 50nmoles of siRNA 48 hours followed by gp120 transfection. The expressions of various cytokines/chemokines were measured at mRNA and protein levels. Both p50 and p65 specific siRNA reduced the expressions of IL-6 by 64.8 ± 4.5 % and 67.4 ± 2.2 % at mRNA levels, respectively (Fig. 16A). Similarly the IL-6 at protein levels were found to be reduced by 95.0 ± 0.1 % and 93.8 ± 0.1 %, respectively (Fig. 16B). When measured for IL-8, the reduction at mRNA level was found to be 63.1 ± 0.8 % and 57.4 ± 3.3 % with p50 and p65 siRNA, respectively (Fig. 16C). The reduction in the IL-8 protein levels was found to be 78.4 ± 5.2 % and 74.8 ± 4.8 %, respectively (Fig. 16D). Similarly the effect of NF-κB siRNA was observed on the gp120-mediated expressions of CCL5. However, unlike IL-6 and IL-8, the siRNA against p50 but not p65 showed reduction in the CCL5 expressions and the % reduction was observed to be 71.0 ± 6.8 % at the level of mRNA (Fig. 16E) and 52.2 ± 3.2 % at the protein level (Fig. 16F). Altogether, these experiments confirmed our observations with the chemical inhibitors and suggested that NF-κB did play an important role in the induction of the cytokines/chemokines at the transcriptional level.

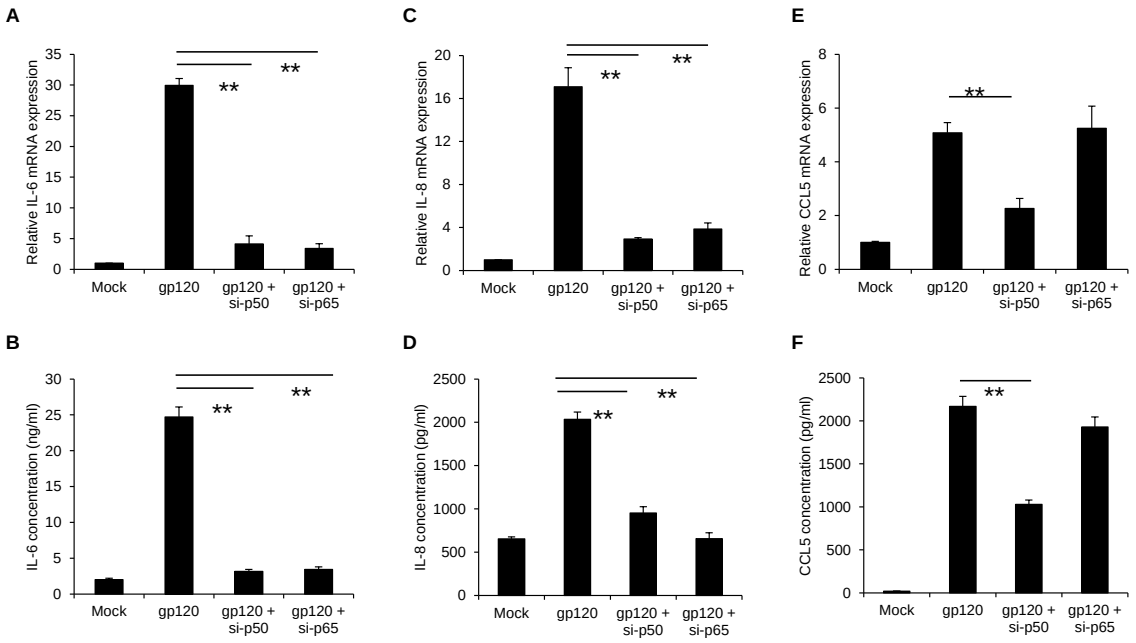

Figure 16: Inhibition of gp120-induced cytokine/chemokine expression by NF-κB siRNA. SVGA astrocytes were transfected with the siRNA against p50 and p65 subunits of NF-κB for 48 hours prior to the gp120 transfection. A scrambled sequence of siRNA was used as a control to measure non-specific knockdown of the target. $1x10^6$ SVGA astrocytes were transfected with 2 µg gp120 The mRNA levels of IL-6 (A), IL-8 (C) and CCL5 (E) were measured at 6 hours post-transfection and protein levels of IL-6 (B), IL-8 (D) and CCL5 (F) were measured at 48 hours post-transfection. Each bar represents mean ± SE of 3 experiments with each experiment done in triplicates. The statistical significance was calculated using student's t-test and ** denotes p value ≤ 0.01.

3.2.9 Specific siRNA against gp120 reduced the gp120-mediated induction of cytokines/chemokines in SVGA astrocytes.

In addition to the inhibition of NF-κB pathway, we determined whether gp120 siRNA would reduce the expression of various cytokines/chemokines. We designed 4 siRNA sequences against gp120 (Table-3) using a commercially available siRNA design tool. The SVGA cells were transfected with different siRNA, 48 hour prior to gp120 transfection and the levels of IL-6, IL-8 and CCL5 mRNA and protein expression were determined. All 4 siRNAs inhibited IL-6 mRNA and protein expression with different efficiency of individual siRNAs and siRNA1 was the most effective followed by siRNA2, 3 and 4 (Fig. 17A-B). However, when analyzed for IL-8, all except siRNA3 reduced the expressions at RNA and protein (Fig. 17C-D). Similarly, for CCL5, all except siRNA1 reduced the levels at RNA and protein (Fig. 17E-F).

Table 3: Sequences of small interfering RNA (siRNA) targeted for gp120

siRNA	Sequences*
gp120 siRNA-1	5'-UGU GAC UGA GCA CUU CAA Ctt-3'
gp120 siRNA-2	5'-UGA CAC CCU GAA GCA GAU Utt-3'
gp120 siRNA-3	5'-GCA GAU UGU GAU CAA GCU Gtt-3'
gp120 siRNA-4	5'-AGC AUA UGA UAC AGA GGU Att-3'
* The sequences shown above are sense strands of the siRNA	

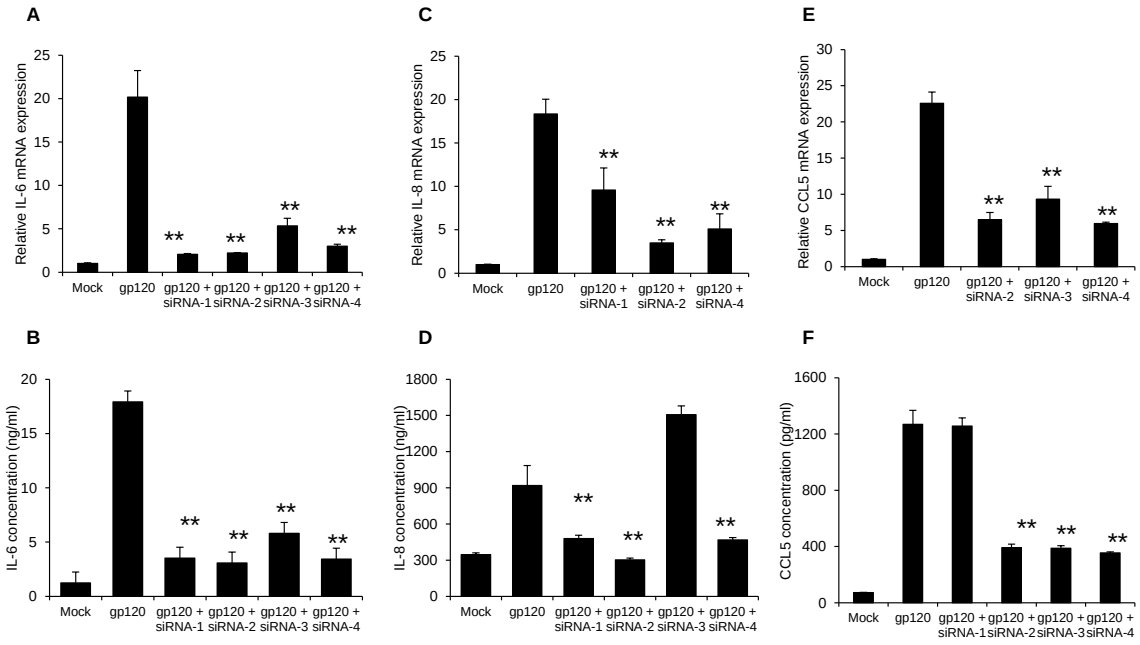

Figure 17: Inhibition of gp120-induced cytokine/chemokine expression by gp120 siRNA. SVGA astrocytes were transfected with 50 nmoles each of the 4 different siRNA for 48 hours before gp120 transfection. A scrambled sequence of siRNA was used as a control to measure non-specific knockdown of the target. $1x10^6$ SVGA astrocytes were transfected with 2 µg gp120 The mRNA levels of IL-6 (A), IL-8 (C) and CCL5 (E) were measured at 6 hours post-transfection and protein levels of IL-6 (B), IL-8 (D) and CCL5 (F) were measured at 48 hours post-transfection. Each bar represents mean ± SE of 3 experiments with each experiment done in triplicates. The statistical significance was calculated using student's t-test and ** denotes p value ≤ 0.01.

3.2.10 Role of various MAPK family molecules in gp120-mediated induction of cytokines/chemokines in SVGA astrocytes.

In order to further investigate the mechanisms involved in the induction of these cytokines, we investigated the possible roles of the p38-MAPK, ERK1/2- MAPK, and JNK-MAPK pathways. In order to investigate the role of p38-MAPK pathway, SVGA astrocytes were treated with 10μM of the specific inhibitor (SB203580) 1 hour prior to gp120 transfection. The dose of SB203580 was determined based on the cell viability as determined by trypan blue staining (data not shown). Treatment of the cells with SB203580 could reduce gp120-mediated expression of both IL-6 (Fig. 18A) and IL-8 (Fig. 18B) by 74.4 ± 2.2 % and 65.6 ± 1.9 %, respectively. We also determined the protein levels of the cytokines released in the supernatants using a multiplex cytokine bead assay and found similar results that SB203580 was able to reduce gp120-mediated expression of IL-6 (Fig. 18C) by 50.6 ± 1.6 % and IL-8 (Fig. 18D) by 43.2 ± 1.5%. In order to further confirm the involvement of p38 in gp120-mediated induction of IL-6 and IL-8, we used siRNA for various isoforms of p38. All of the p38-specific siRNAs could inhibit gp120-mediated mRNA expression of IL-6 and IL-8 by more than 70% as shown in Fig. 18E and 18F, respectively. Together, these results suggest involvement of the p38-MAPK pathway in gp120-mediated induction of IL-6 and IL-8. In addition to p38α and p38β, which lead to activation of the transcription factor NF-κB, we found that p38γ and p38δ are also involved in gp120-mediated induction of IL-6. The other isoforms of p38 may activate additional transcription factors such as STAT1, CHOP, Max, ATF2 and AP-1(reviewed in Coulthard, White, Jones, McDermott, & Burchill, 2009), which are known to play roles in variety of physiological responses such as ER-stress and production of cytokines/chemokines.

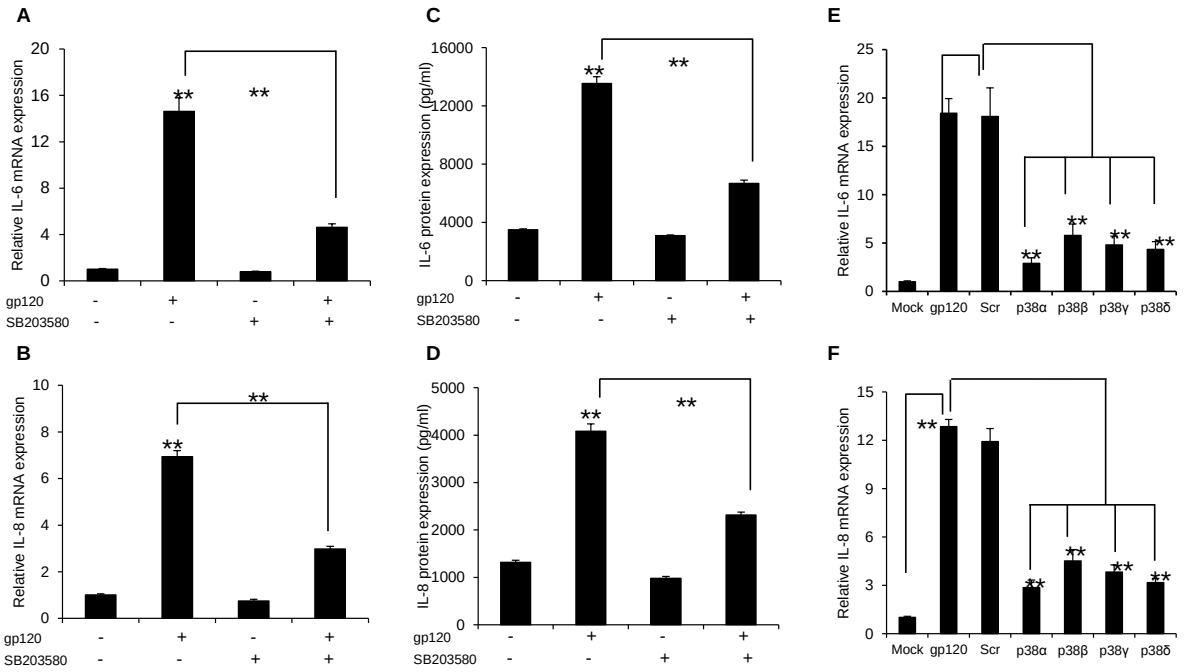

Figure 18: HIV-1 gp120–mediated induction of IL-6 and IL-8 involved the p38 pathway. (A-D) 8 X 10^5 SVGA astrocytes, seeded in each well of 6-well plate, were treated with 10μM of SB203580 1 hour prior to transfection with gp120 plasmid. The cells were transfected in serum-free medium with 2 μg of plasmid expressing gp120. The cells were incubated for 5 hours followed by replacement of the transfection mix with complete medium. The cells were harvested 6 hours post-transfection to determine the mRNA expression levels of IL-6 (A) and IL-8 (B). Identically treated cells were harvested at 24 hours post-transfection to determine protein expression levels of IL-6 (C) and IL-8 (D). SVGA astrocytes were transfected with 50nM of various siRNA against p38α, p38β, p38γ and p38δ for 48 hours (E-F). Following siRNA transfection, the cells were reseeded at 8 X 105 cells/well in a 6-well plate and transfected with 2 μg of gp120 plasmid. The cells were harvested 6 hours post-transfection and mRNA expression levels of IL-6 (E) and IL-8 (F) were determined. The bars represent mean ± SE of 3 independent experiments with each treatment in triplicates. The p-value ≤ 0.01 (**) was considered to be statistically significant using student's t-test.

We also investigated the involvement of ERK1/2-MAPK and JNK-MAPK in the gp120-mediated induction of IL-6 and IL-8. Similar to previous experiments with the inhibitors, the astrocytes were pre-treated with the inhibitors 1 hour prior to the gp120 transfection. We used 20 μM of ERK1/2-MAPK inhibitor, U0126 and JNK-MAPK inhibitor, SP600125 since these doses have been previously shown to be optimal for inhibition of their specific targets with minimal toxicity (Hsieh, Wang, Wu, Chu, & Yang, 2010; Warny et al., 2000). As shown in Fig. 19A and 19B, both the inhibitors failed to abrogate the gp120-mediated expression of IL-6 and IL-8, which suggested that p38 but not ERK1/2 or JNK-MAPK pathway is involved in the gp120-mediated induction of IL-6/IL-8.

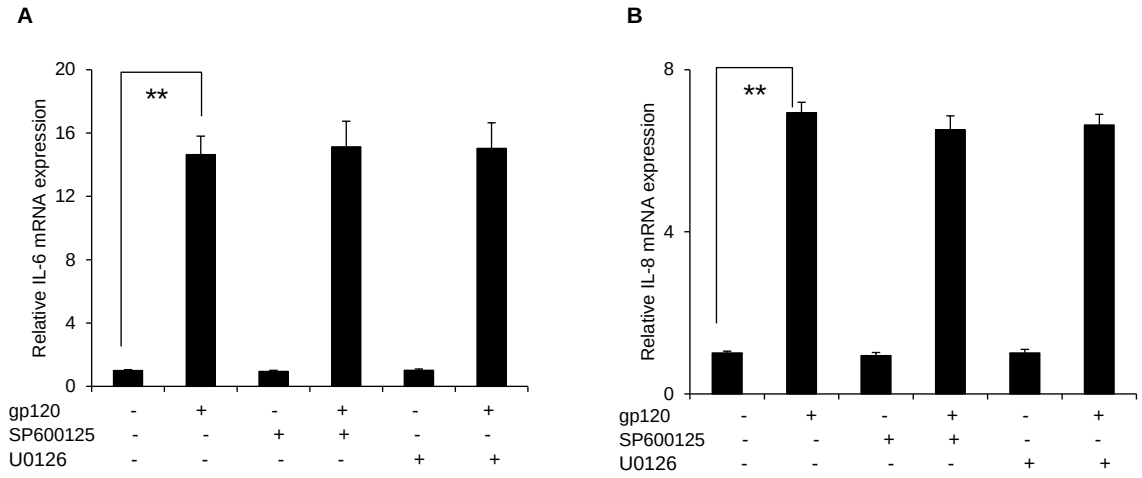

Figure 19: HIV-1 gp120–mediated induction of IL-6 and IL-8 is independent of ERK1/2 and JNK-MAPK pathways. (A-B) 8 X 10^5 SVGA astrocytes, seeded in each well of 6-well plates, were transfected with 2μg of gp120 plasmid. The cells were treated with SP600125 (a JNK-MAPK inhibitor) or U0126 (an ERK1/2-MAPK inhibitor) 1 hour prior to transfection with gp120 and the expression levels of IL-6 and IL-8 mRNA were determined. The bars represent mean ± SE of 3 independent experiments with each treatment in triplicates. The p-value ≤ 0.01 (**) was considered to be statistically significant using student's t-test.

3.2.11 Role of various MAPK family molecules in gp120-mediated induction of cytokines/chemokines in SVGA astrocytes.

Having established the involvement of various MAPK pathway, we wished to examine signaling events upstream of the NF-κB pathway. Involvement of the PI3K/Akt pathway in inducing IL-6 in an NF-κB-mediated pathway has been reported in microglia (Lu et al., 2009). Thus, we wished to study the possible role of the PI3K/Akt pathway in gp120-mediated induction of IL-6 and IL-8. In order to do so, we used a specific inhibitor LY294002 to block the PI3K/Akt pathway. SVGA astrocytes were treated with 20 μM of LY294002 1 hour prior to gp120 transfection. The dose of LY294002 was determined based on the cell viability as determined by trypan blue staining (data not shown). The abrogation of gp120-mediated induction of IL-6 and IL-8 at the mRNA level was measured using real time RT-PCR. The inhibitor could reduce gp120-mediated expression of IL-6 by 56.3 ± 7.5% (Fig. 20A) and IL-8 by 70.1 ± 8.5% (Fig. 20C). Thus, our results suggest involvement of both p38-MAPK and PI3K/Akt pathways in gp120-mediated increased expression of IL-6 and IL-8 in astrocytes. Furthermore, these results were confirmed at the protein level as shown in Fig. 20B and 20D for IL-6 and IL-8, respectively. The PI3K/Akt inhibitor abrogated gp120-mediated IL-6 and IL-8 expression at the level of protein by more than 90%.

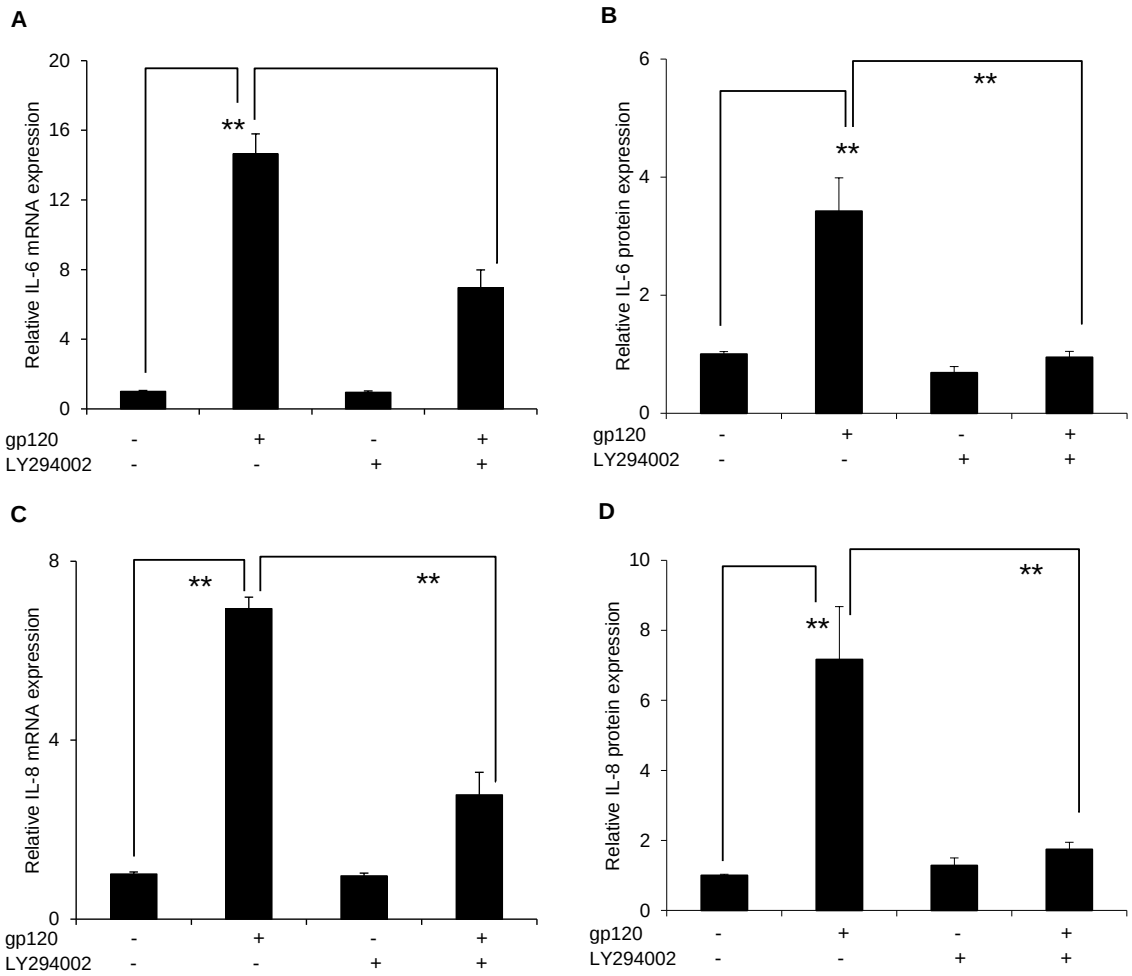

Figure 20: HIV-1 gp120–mediated induction of IL-6 and IL-8 involved the PI3K/Akt pathway. 8 X 10^5 SVGA astrocytes, seeded in each well of 6-well plate, were treated with 20μM of LY294002, a PI3K/Akt inhibitor, 1 hour prior to transfection with gp120. The cells were transfected with 2 μg of gp120 plasmid for 5 hours in serum-free media. Following this, the cells were incubated with complete medium for 6 hours in order to determine the expression levels of IL-6 and IL-8 mRNA (A & C). Identically treated cells were harvested at 24 hours in order to determine the expression levels of IL-6 and IL-8 protein (B & D). The expression levels of IL-6 and IL-8 were compared to the gp120-mediated expression levels of IL-6 and IL-8. The bars represent mean ± SE of 3 independent experiments with each treatment in triplicates. The p-value ≤ 0.01 (**) was considered to be statistically significant using student's t-test.

3.3 Discussion:

HIV-1 gp120 plays an essential role in the viral attachment and entry into the host cells. However, apart from its role in the viral entry, gp120 has been proposed to exhibit neurotoxic role during HIV-1 infection (Iskander et al., 2004; Wallace, Dodson, Nath, & Booze, 2006). Among various mechanisms responsible for the neurotoxicity, oxidative stress (Agrawal et al., 2010; Ronaldson & Bendayan, 2006), production of pro-inflammatory cytokines such as TNF-α and IL-1β (Cheung, Ravyn, Wang, Ptasznik, & Collman, 2008; C. Lee, Tomkowicz, Freedman, & Collman, 2005; Viviani et al., 2006) and damage of blood brain barrier have been explored as possible mechanisms.

In the present study, gp120-mediated induction of IL-6, IL-8 and CCL5 has been demonstrated to be dependent upon the NF-κB pathway. In our study using a human astrocyte cell line we observed that IL-6, IL-8 and CCL5 RNA expression reached their peak level at 6 h after transfection with gp120 plasmid. Furthermore, these observations were further confirmed in human fetal astrocytes, which showed increase in the levels of IL-6 and IL-8 with their peak levels at 1 h and 3 h, respectively after the treatment with gp120 protein. These results are consistent with the previous studies by Ronaldson and Bendayan (Ronaldson & Bendayan, 2006) who have found similar kinetics with respect to IL-1β, TNF-α and IL-6 after treatment of rat astrocytes with gp120. In addition, HIV-1 gp120 was shown to induce IL-6 via indirect evidence (Li et al., 2007), wherein the wild type VSV/NL4-3 was capable of inducing IL-6 in human fetal astrocytes, whereas the gp120-truncated mutant failed to do so.

Our study in the human fetal astrocytes with exogenous gp120 demonstrating the induction of IL-6 and IL-8 clearly suggested that the gp120-mediated expression of

cytokine/chemokine is a result of direct involvement of gp120. In addition to CXCR4, astrocytes are reported to express CCR5 (Avdoshina et al., 2010; Ronaldson et al., 2010; K. A. Thompson et al., 2004). We showed differential expression levels of IL-6 in response to various strains of gp120. In the present study gp120IIIB was used as an X4 strain of gp120, while gp120 CN54, gp120 CM and gp120Bal were used as R5 stains. Our results clearly demonstrate that in addition to the gp120IIIB (X4 Strain), gp120 CN54, gp120CM and gp120Bal significantly altered IL-6 expression to various extents. Earlier studies by Zheng et al (Zheng et al., 1999) demonstrated a difference between the toxic response due to X4 and R5 specific strains on neuronal apoptosis and demonstrated the most profound effects with the X4 strains, intermediate effects with the dual tropic strain, and the lowest level of apoptosis with the R5 strains. In addition, gp120-mediated signal transduction pathways showed similar strain-dependent trend. Thus, our findings with respect to the induction of cytokines/chemokines are in accordance with the previous study and provide additional line of evidence suggesting strain specific differences in the cytotoxicity.

Using siRNA targeted against gp120, we showed reduction in the gp120-mediated expressions of IL-6, IL-8 and CCL5. Interestingly, we observed differential regulation of IL-6 mRNA and protein expression after siRNA knockdown of gp120. Although gp120 siRNA1 was the most effective siRNA in blocking expression of IL-6 mRNA, gp120 siRNA4 was the most effective siRNA in blocking IL-6 expression at the level of protein. Similar traits were observed with IL-8 and CCL5 as well. The reason for this discrepancy could be attributed to the fact that mRNA expression was monitored within 6 h after transfection whereas protein was monitored 48 h after transfection and these siRNAs might have required more than 6 h to exhibit full effect.

The NF-κB pathway has been shown to be involved in myriad of cellular responses such as cell death, apoptosis and inflammation (Beg & Baltimore, 1996; Saile et al., 2001; Siebenlist et al., 1994). In rat astrocytes, induction of both MCP-1 and MCP-3 has been shown to be dependent upon NF-κB (W. L. Thompson & Van Eldik, 2009). Ronaldson, et al. showed that pretreatment of astrocytes with a peptide inhibitor of NF-κB, SN-50 dramatically reduced the level of TNF-α elicited by gp120 treatment (Ronaldson et al., 2010). Furthermore, IL-6 production has also been found to be mediated though the NF-κB pathway in patients with rheumatoid arthritis (Lazzerini et al., 2007), retinal microglia (A. L. Wang et al., 2007), lung pericytes (Edelman, Jiang, Tyburski, Wilson, & Steffes, 2007) and mice splenocytes treated with LPS (Zhang et al., 2008). In our study, we sought to address whether NF-κB activation is involved in mediating gp120-induced IL-6, IL-8 and CCL5 expression. We demonstrated that there is increased phosphorylation of IκBα along with significant translocation of p50 from the cytoplasm to the nucleus that is dependent upon gp120. Similar to the present study, a report by Saha et al.(Saha & Pahan, 2003) demonstrated that gp120 can activate the NF-κB pathway and lead to nuclear translocation of p50. Results obtained from pharmacological inhibitors and siRNA approach also confirmed that induction of the observed cytokines/chemokines was dependent on the NF-κB pathway. Taken together, the evidence presented in the present study along with results from other reports strongly suggests the involvement of NF-κB in the gp120-mediated expressions of pro-inflammatory cytokines.

Along with its role in inducing inflammatory cytokines, NF-κB has also been demonstrated to be involved in regulating the responses to oxidative stress in astrocytes (Bowie & O'Neill, 2000; Sinke et al., 2008). Oxidative stress has been widely demonstrated

as an important mechanism through which gp120 affects astrocytes (Visalli et al., 2007). Thus, activation of NF-κB by gp120 could be an important mechanism to induce oxidative stress associated with viral infection of the CNS.

In the present work we have shown that the PI3K/Akt and p38 MAPK pathways also play a role in gp120-mediated induction of IL-6. The involvement of the p38MAPK pathway was confirmed through the use of siRNA targeted against p38 homologs. This is in accordance with the earlier reports that documented the role of the p38MAPK pathway in gp120-induced neurotoxicity and release of neurotoxins in monocytes and mixed cerebrocortical cultures (Kaul & Lipton, 1999; Medders, Sejbuk, Maung, Desai, & Kaul, 2010). Using a rat astrocyte model, Yang et al. has shown that gp120-mediated cellular toxicity involves the MAPK pathway (Yang, Yao, Lu, Wang, & Buch, 2010). However, unlike the report from Yang et al., in our system we did not detect any involvement of either the ERK1/2-MAPK or JNK-MAPK pathways in the induction of IL-6 by gp120. This discrimination could be attributed to the fact that source of astrocytes in our study was human and not rat as used in previous study. It is also possible that the ERK1/2-MAPK and JNK-MAPK pathways may have a role in gp120-mediated apoptosis of astrocytes, but not in the increased expression of IL-6 and IL-8. In the present study, we also demonstrate a role for the PI3K/Akt pathway in gp120-mediated induction of IL-6 and IL-8. The PI3K/Akt pathway, acting in conjunction with other factors, is known to increase the activation of the NF-κB pathway by phosphorylation of IKK (S. A. Reddy, Huang, & Liao, 2000; Tang, Chiu, Tan, Yang, & Fu, 2007). Similarly, activation of PI3K/Akt may also lead to the activation of p38-MAPK pathway (Kao et al., 2005). Thus, our study indicates involvement of both the PI3K/Akt and the p38-MAPK pathways in the induction of cytokines by gp120. Both p38-

MAPK and PI3K/Akt may function to further activate the NF-κB pathway; as such an activity has been described for both of these pathways (S. A. Reddy et al., 2000; Vanden Berghe et al., 1998). Furthermore, numerous studies have shown that NF-κB can promote transcription of various cytokines and chemokines. Together, our study provides a detailed insight into the mechanisms in gp120-mediated induction of cytokines.

Our data on the induction of the cytokines/chemokines by gp120 are consistent with previously reported results. It should be noted that the results that we have observed using both the models for astrocyte exposure to gp120 (i.e. intracellular production of gp120 vs. extracellular administration of the protein) are somewhat different from each other in terms of kinetics and levels of IL-6 induction observed. These differences can be attributed to 2 basic differences in the models; one model utilizes extracellular exposure of primary astrocytes and the other model utilizes transfection of an immortalized cell line. We have utilized both models in order to determine the effects of gp120 on astrocytes regardless of the route of exposure. Our results not only confirm what other laboratories have reported with regard to extracellular exposure of astrocytes to gp120, but we have also shown that non-productive infection of astrocytes by HIV-1 may be a significant and persistent source of IL-6, IL-8 and CCL5 in the CNS.

Taken together, the results in the present study suggest that gp120-mediated activation of the NF-κB pathway may be critical therapeutic target for the treatment of HIV-related neuroinflammation (Fig. 21). One approach that could be explored would be to try to interfere with the interaction between NF-κB and its binding site in the promoter of these cytokines/chemokines in astrocytes. Recent advances suggest that small RNAs or miRNA might be a useful tool for silencing promoters/enhancers (Hawkins, Santoso, Adams, Anest,

& Morris, 2009; Mette, Aufsatz, van der Winden, Matzke, & Matzke, 2000; Younger & Corey, 2011), and such an approach might be applied to the IL-6/IL-8/CCL5 promoter in astrocytes. Also, recently Kim et al. have employed a novel approach to target specific cell types using antibody-based strategies (Kim, Subramanya, Peer, Shimaoka, & Shankar, 2011). Using their approach, they were able to efficiently target delivery of siRNA specifically to T-cells via the CD67 receptor. Similarly, Wu et al. used microRNA delivery to astrocyte specific promoter as a tool for cancer therapy (C. Wu et al., 2009). Such an approach might be further exploited in astrocytes by targeting these cells using GFAP to deliver siRNA/miRNA for NF-κB or the promoter of the cytokines/chemokines. Since successful antiretroviral treatment has extended the lifespan of those infected with HIV, the importance of finding novel treatments for the HIV-associated morbidities caused by chronic inflammation and oxidative stress, such as HAND, has become increasingly critical. Identification of a critical therapeutic target, as has been presented in this study, is an important step towards the development of more effective therapeutic regimens for neuroAIDS.

3.4 Acknowledgement:

Chapter 3 contains figures and text of the manuscript accepted in Journal of neuroinflammation 2010 by Shah et. al., PLOSONE 2011 by Shah e. al. Biochemistry Biophysics Research Communications 2011 by Shah et. al. and Current HIV research 2012 by Silverstein et. al. The dissertation author was the lead author of the first 3 and co-author of the 4th published manuscripts.

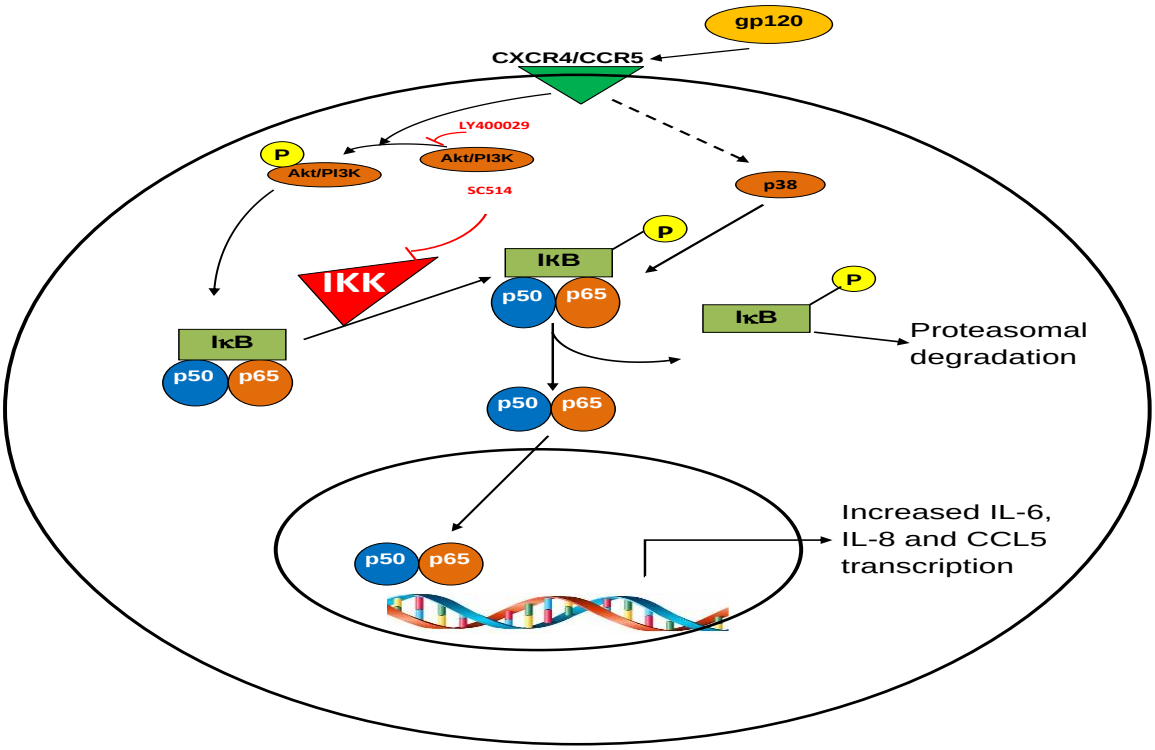

Figure 21: Schematic of the signaling pathways involved in gp120-mediated induction of IL-6, IL-8 and CCL5. Treatment of astrocytes with gp120 results in the binding of gp120 by the CCR5 or CXCR4 chemokine receptors and the subsequent activation of PI3K/Akt and p38-MAPK. The activation of these two pathways may lead to increased activation of NF-κB. The activated NF-κB then translocates into the nucleus and increases the transcription of IL-6, IL-8 or CCL5.

CHAPTER-4

EVALUATION OF THE ROLE OF METHAMPHETAMINE ON THE EXPRESSION OF IL-6 AND IL-8 IN ASTROCYTES AND THE UNDERLYING MECHANISM(S)

4.1. Introduction:

Methamphetamine (MA) is a psychostimulant in the amphetamine class of drugs and is one of the most commonly abused agents by illicit-drug users. The effects of MA are primarily attributed to its action on dopamine (DA) receptors and transporters (Fumagalli, Gainetdinov, Valenzano, & Caron, 1998; Xu et al., 2005). Furthermore, the interaction of MA with DA receptors and transporters has been shown to be associated with oxidative stress, which is among the several different mechanisms believed to be responsible for the CNS toxicity associated with MA (Jayanthi, Ladenheim, & Cadet, 1998; LaVoie & Hastings, 1999; Ramirez et al., 2009). In addition to oxidative stress, MA has been shown to increase mitochondrial dysfunction, excitotoxicity (Yamamoto & Raudensky, 2008), BBB damage (Persidsky, Ramirez, Haorah, & Kanmogne, 2006; Silva et al., 2010; Yamamoto & Raudensky, 2008), monocyte infiltration into the central nervous system (CNS) (Bowyer & Ali, 2006) along with increased levels of inflammatory markers such as IL-6 and TNF-α (Goncalves et al., 2008).

The proinflammatory cytokines/ chemokines IL-6 and IL-8 are among the inflammatory responses associated with various neurological disorders including PD (Nagatsu, Mogi, Ichinose, & Togari, 2000), AD (McGeer & McGeer, 1998), and Amyotrophic lateral sclerosis (ALS) (Iskander et al.) (Kuhle et al., 2009). A single high dose of MA has been shown to induce IL-6 and TNF-α in the striatum and hippocampus of mice

(Goncalves et al., 2010; Sriram, Miller, & O'Callaghan, 2006) and IL-1β in the hypothalamus of rats (Yamaguchi et al., 1991). However, the specific molecular mechanism(s) involved in the increased expression of these proinflammatory cytokines is still unknown. It is generally accepted that MA induces oxidative stress, which can increase proinflammatory cytokines by increasing the activities of transcription factors such as NF-κB, AP-1 and CREB (Y. W. Lee, Hennig, Yao, & Toborek, 2001; Y. W. Lee et al., 2002). Furthermore, the role of dopamine receptors and transporters in MA-mediated oxidative stress and neuroinflammation has been extensively investigated (Guillot et al., 2008; Pu & Vorhees, 1995). A more direct cytotoxic role of MA has been demonstrated to be mediated by JNK-MAPK pathway followed by the activation of caspase cascade and the induction of apoptosis (Zhang et al., 2008). However, the role of astrocytes has been relatively unexplored in terms of the regulation of inflammatory cytokines and the mechanisms underlying MA-mediated expression of proinflammatory cytokines.

Low levels of cytokines and chemokines are constitutively expressed by microglia in the CNS in order to maintain the immunological homeostasis and these cytokines/chemokines can be induced to higher levels by inflammatory mediators (Farber & Kettenmann, 2005; Mennicken et al., 1999). However, astrocytes constitute the major cell type present in the brain. Astrocytes are also involved in regulation of numerous pro- and anti-inflammatory cytokines (Miljkovic et al., 2011). Oxidative stress in astrocytes is found to be mediated via PI3K/Akt, Nrf2 and NF-κB pathways (E. Lee, Yin, Sidoryk-Wegrzynowicz, Jiang, & Aschner, 2012). Increased inflammatory markers released from astrocytes is associated with a variety of CNS complications such as AD (Zhao, O'Connor, & Vassar, 2011), multiple sclerosis, glaucoma (Morgan, 2000) and PD (Kato, Araki, Imai,

Takahashi, & Itoyama, 2003). Furthermore, astrocyte activation has been shown to be critical in the regulation of the rewarding effects induced by drugs of abuse (Narita et al., 2006). Thus, it is important to consider the role of astrocytes in neuroinflammatory signaling induced by MA. Our present study was undertaken to address whether MA induced proinflammatory cytokines in astrocytes and to determine the mechanisms responsible for MA-mediated expression of these cytokines.

4.2. Results:

4.2.1. MA increases the expression of proinflammatory cytokines/chemokines in astrocytes.

The neurotoxic effects of MA have been attributed to its potential for inducing oxidative stress through dopamine (DA) receptor and dopamine transporter (DT) dependent mechanisms reviewed in (Cadet & Krasnova, 2009; Kita, Miyazaki, Asanuma, Takeshima, & Wagner, 2009; Silverstein et al., 2011). In order to determine the effect of MA on the cytokine expression, we used similar approach as we did for gp120. As discussed in chapter 3, we treated the astrocytes with MA and measured the RNA expressions of 7 different cytokines/chemokines. However, unlike gp120, MA demonstrated induction of 2 cytokines, IL-6 and IL-8 among all. Therefore all our future studies with regards to MA was focused on IL-6 and IL-8. In order to determine whether MA could increase the expression of proinflammatory cytokines/chemokines such as IL-6 and IL-8 in astrocytes, SVGA astrocytes were treated with 250μM, 500μM and 1000μM of MA for 24 hours. The dose of methamphetamine was calculated using blood levels of methamphetamine in conjunction with tissue/serum compartmentalization ratios reported in the literature (Melega, Cho, Harvey, & Lacan, 2007; Riviere, Gentry, & Owens, 2000; Talloczy et al., 2008). It has been previously extrapolated that 250mg-1g binge methamphetamine administration as single dose could produce between 164-776 μM concentrations in the brain (Talloczy et al., 2008). The mRNA expression levels of IL-6 and IL-8 showed a dose-dependent increase. The MA-induced expression of IL-6 and IL-8 was found to be 1.7 ± 0.1, 2.7 ± 0.1, and 4.2 ± 0.2 fold and 1.4 ± 0.1, 3.5 ± 0.2 and 5.6 ± 0.2 fold, respectively for 250μM, 500μM and 1000μM of MA, respectively (Fig. 22A-B). Furthermore, we also wanted to determine the effect of

chronic exposure of MA on astrocytes. We treated the astrocytes with 500μM MA for 3 days, once a day, as the dose is relevant to the levels found physiologically in MA abusers (Talloczy et al., 2008). The chronic treatment with MA resulted in increased expression of IL-6 and IL-8 by 4.6 ± 0.2 fold and 3.5 ± 0.2 fold, respectively (Fig. 22C-D). These results clearly indicate that MA can increase the expression of proinflammatory cytokines/chemokines like IL-6 and IL-8.

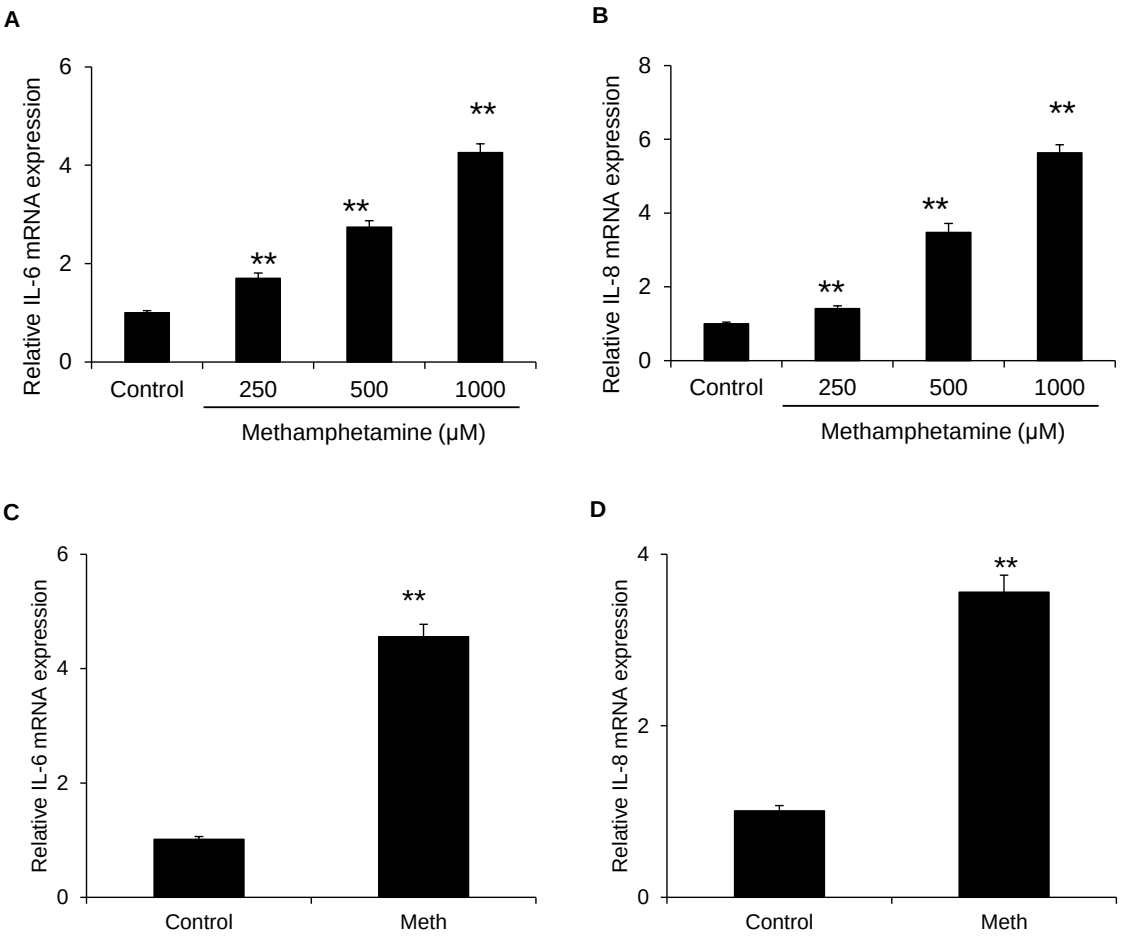

Figure 22: Methamphetamine increases the expression of IL-6 and IL-8 in astrocytes. 8 x 10^5 SVGA astrocytes were treated with different doses of MA for 24 hours and total mRNA was isolated. The relative expression levels of IL-6 (A) and IL-8 (B) were measured using real time RT-PCR as compared to untreated control. 0.8 x 106 SVGA were treated with 500μM of MA for 3 days in flasks and the cells were harvested 24 hours after the last dose. Total mRNA was isolated and the relative levels of IL-6 (C) and IL-8 (D) were determined using real time RT-PCR as compared with untreated control. Each bar represents the mean ± SE of 3 experiments with each experiment performed in triplicate. The statistical significance was calculated using student's t-test and ** denotes p value of ≤ 0.01.

4.2.2. MA increases intracellular levels of IL-6 and IL-8.

After determining that MA increased levels of IL-6 and IL-8 mRNA we wanted to confirm that increased levels of RNA were reflected in increased production of IL-6 and IL-8 protein. SVGA astrocytes were treated with 500 µM MA for 24 h and intracellular levels of IL-6 and IL-8 proteins were observed using immunhistochemistry. Although in the control cells there were only minor amounts of IL-6 or IL-8 proteins, in cells treated with MA for 24 h increased levels IL-6 and IL-8 proteins were clearly visible (Fig. 23A-B).

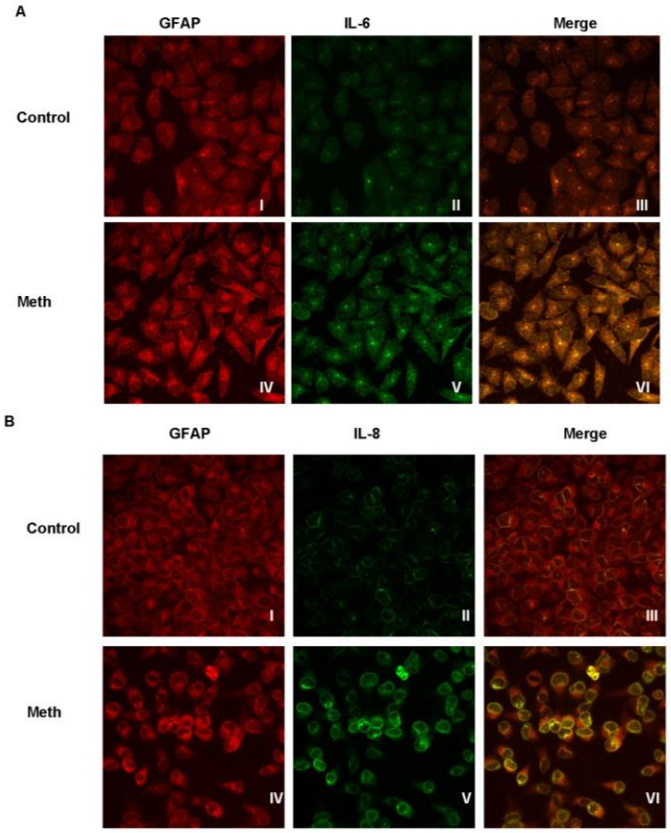

Figure 23: Methamphetamine treatment increased the intracellular expression of IL-6 and IL-8 in the astrocytes. SVGA astrocytes were grown on coverslips and were treated with 500 µM of MA for 24 hours followed by methanol-fixation. Golgi-StopTM was added 6 hours prior to fixing in order to block the release of the cytokines from the cells into the supernatants. The coverslips were blocked, and then incubated with primary antibody for IL-6/IL-8 and GFAP and secondary antibodies conjugated with Alexafluor488 to detect IL-6 and IL-8 and an antibody conjugated with Alexafluor555 to detect GFAP. The coverslips were then mounted using medium containing DAPI and were observed under a confocal microscope to determine the localization and expression of IL-6 (A) and IL-8 (B). Untreated cells were stained individually for IL-6, IL-8 and GFAP and did not show any non-specific fluorescence (data not shown).

4.2.3. MA-mediated induction of proinflammatory cytokines/chemokines is mediated via NF-κB pathway.

We then wished to determine the signaling mechanism involved in MA-mediated increased expression of IL-6 and IL-8. The potential involvement of the NF-κB pathway was investigated because the promoters for both IL-6 and IL-8 contain a binding site for NF-κB and this transcription factor is known to be involved in neurological disorders associated with increased inflammation (Beg & Baltimore, 1996; Kaltschmidt, Baeuerle, & Kaltschmidt, 1993; Kunsch & Rosen, 1993; Sparacio, Zhang, Vilcek, & Benveniste, 1992). In order to determine whether MA can induce NF-κB activation and translocation, SVGA astrocytes were treated with 500μM MA over a time period of 0 to 6 hours. The cytoplasmic and nuclear fractions of the astrocytes were collected and the levels of p50 in cytoplasmic and nuclear fractions were measured in MA treated cells and compared to untreated controls (Fig. 24A-B). Clearly, MA-treated cells showed a time-dependent increase in p50 translocation from the cytoplasm to the nucleus, with the greatest translocation observed at 3 hours (2.2 ± 0.1 fold).

In order to further confirm these results we measured the phosphorylated form of IκBα in the whole cell lysates of the astrocytes treated with 500μM of MA over a period of 0-120 min. Consistent with the previous results, MA treatment was found to increase the phosphorylation of IκBα, as evidenced by the increased levels of p-IκBα in MA treated astrocytes at 10 min (Figure 24C).

Furthermore, we also evaluated the effect of SC514, a specific inhibitor of Inhibitory Kappa B Kinase (P. V. Reddy et al.) on the expression levels of IL-6 and IL-8 in MA-treated astrocytes. The cells were treated with 10μM SC514 (IC50 = 14.5μM) 1 hour prior to each

MA treatment over the three-day course of the experiment. The mRNA expression levels of IL-6 and IL-8 were measured using real time RT-PCR and the percent inhibition of MA-mediated expression levels of IL-6 and IL-8 were found to be 56.7 ± 5.1 % and 78.4 ± 7.8 %, respectively (Fig. 24D-E). Together, all these results strongly suggest that induction of IL-6 and IL-8 by MA involves the activation and translocation of NF-κB.

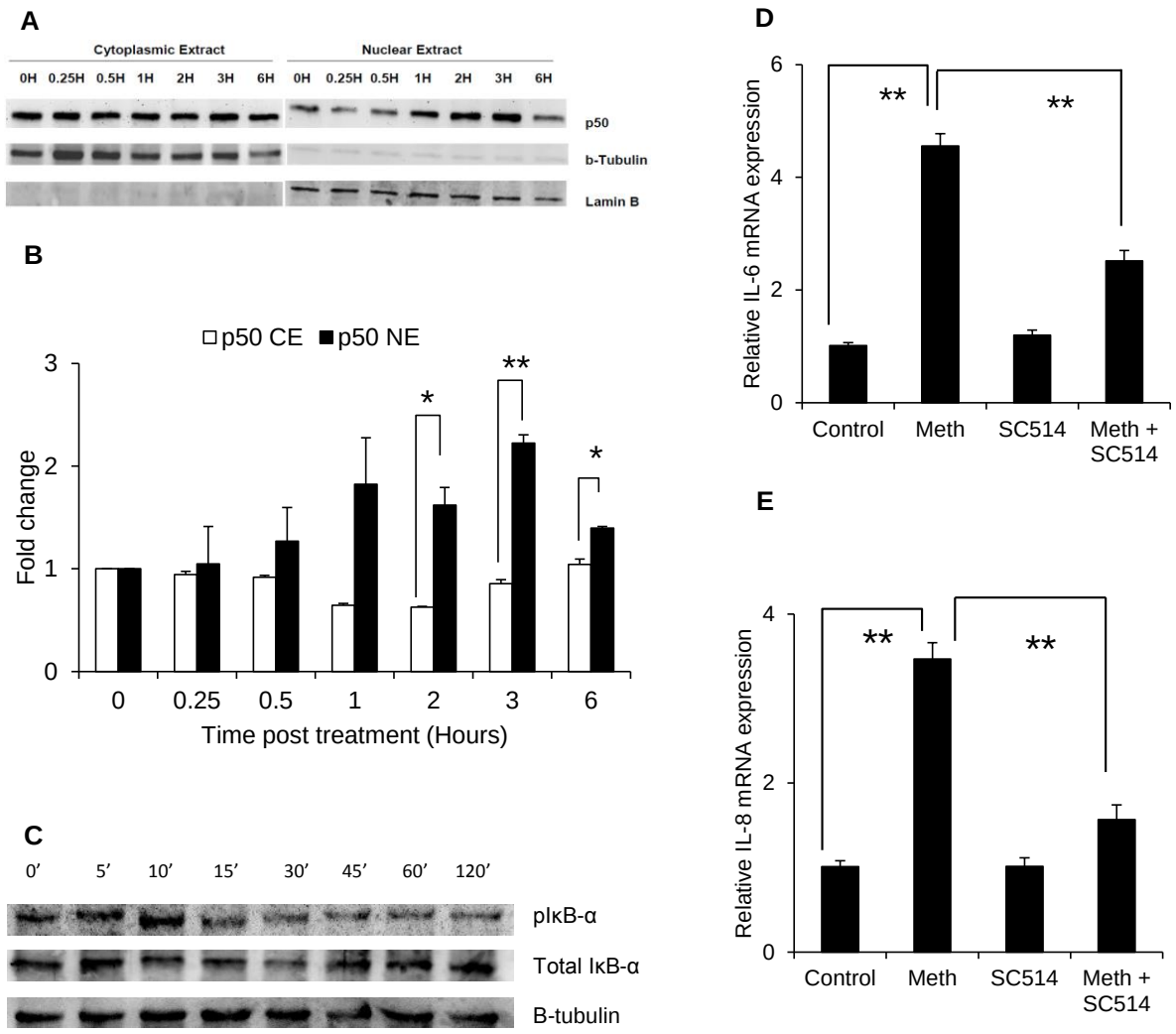

Figure 24: Methamphetamine induction of IL-6 and IL-8 is mediated via NF-κB pathway. (A) The proteins from nucleus and cytoplasm of SVGA cells were collected after various time-periods as indicated and the translocation of p50 was measured by comparing the expression in nucleus and cytoplasm. The expression in the nucleus and cytoplasm were normalized with laminB and β-Tubulin, respectively, as housekeeping genes. (B) The bar chart represents the mean ± SE of 3 independent experiments and the blot is a representation of 3 experiments. (C) SVGA cells were treated with 500μM of MA for the specified time and the total cell lysates were collected as mentioned in Materials and Methods. Total IκB-α was used as an experimental control and actin was used as a loading control. The blot is representative of 3 independent experiments. SVGA astrocytes were treated with 10μM of SC514 for 1 hour prior to MA treatment every day for 3 days and the total mRNA was isolated 24 hours after the last dose. The expression levels of IL-6 and IL-8 were measured with real time RT-PCR and the % mRNA expression of IL-6 (D) and IL-8 (E) were calculated relative to MA-mediated expression levels. SC514-treated cells did not alter the basal expression levels of IL-6 and IL-8 (data not shown). Each bar represents the mean ± SE of 3 experiments with each experiment performed in triplicate. The statistical significance was calculated using student's t-test and * and ** denotes p value of ≤ 0.05 and ≤ 0.01, respectively.

4.2.4. MA-mediated induction of IL-6 and IL-8 does not involve the p38-MAPK or JNK-MAPK pathways.

In order to further explore the signaling mechanism(s) responsible for MA-mediated expression of proinflammatory cytokines, we investigated the potential roles of the JNK-MAPK and p38-MAPK pathways, as both pathways have the capability of activating the NF-κB transcription factor. We treated SVGA astrocytes with 500 μM MA once a day for 3 days. The cells were treated with 10 μM of specific inhibitors for either JNK-MAPK (SP600125) or p38-MAPK (SB203580) pathway as described in materials and methods. As seen in Fig.-25, neither of the inhibitors could abrogate the MA-mediated expression of IL-6 (Fig. 25A) and IL-8 mRNA (Fig. 25B). Thus, we conclude that neither the JNK-MAPK nor the p38-MAPK pathways are involved in the MA-mediated induction of cytokines/chemokines.

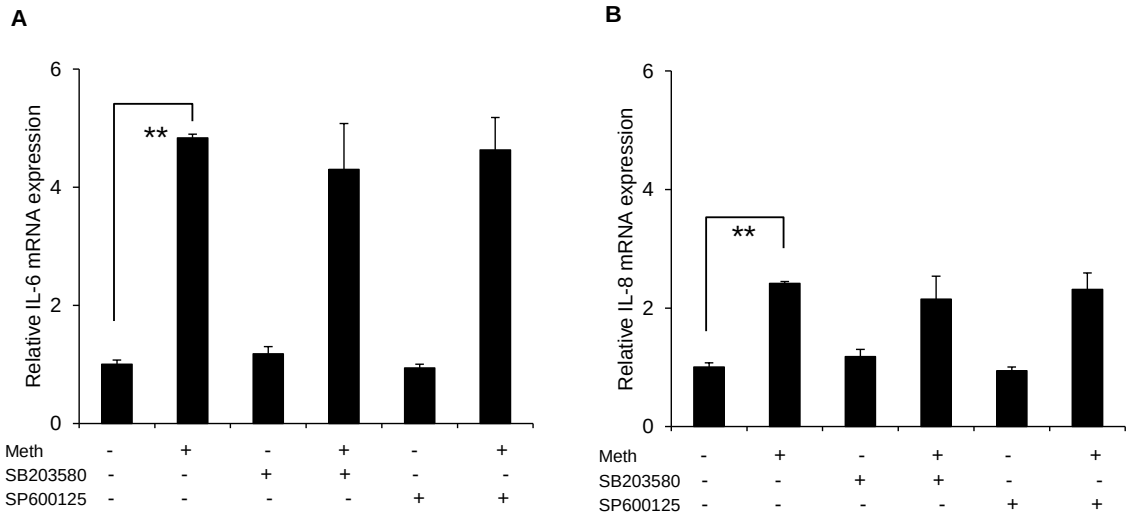

Figure 25: Methamphetamine-mediated induction of IL-6 and IL-8 does not involve the p38-MAPK or JNK-MAPK pathways. SVGA astrocytes were seeded at 8 X 10^5 cells in 6-well plate. The cells were treated once every day with 500μM of MA for 3 days. Cells were treated with inhibitors alone or inhibitors and MA. Treatments with 10μM of either SB203580 or SP600125 were started 1 hour prior to the MA treatment. The cells were harvested 24 hours after the last treatment of MA and total mRNA was isolated using an RNeasy mini kit. The RNA was analyzed using real time RT-PCR in order to quantify the expression levels of IL-6 (A) and IL-8 (B). Each experiment was repeated at least 3 times with triplicates of each treatment. The p-value ≤ 0.01 (**) was considered statistically significant when calculated with student's t-test.

4.2.5. Role of mGluR5 and PI3K/Akt in MA-mediated expression of proinflammatory cytokines / chemokines:

Having established the role of the NF-κB pathway in the induction of IL-6 and IL-8 by MA, we were interested in the receptor involved in mediating this response. There is an extensive body of literature demonstrating that many of the effects of MA are mediated through the DA receptor /DA transporter (DT). However, recent reports also suggest the possible involvement of metabotropic glutamate receptors in MA-mediated neurotoxicity and/or cognitive impairment (Battaglia et al., 2002; Golembiowska, Konieczny, Wolfarth, & Ossowska, 2003; Reichel, Schwendt, McGinty, Olive, & See, 2011). In order to determine whether the metabotropic glutamate receptor-5 (mGluR5) plays a role in the MA-mediated increase in IL-6 and IL-8 levels in astrocytes, we treated the astrocytes with 25μM of MPEP, a specific inhibitor of mGluR5, 1 hour prior to MA treatment for 3 days once in a day (o.i.d). The dose of MPEP was determined based on the cell viability as observed by trypan blue staining (data not shown). We observed that MPEP abrogated the MA-induced expression levels of IL-6 and IL-8 by 42.6 ± 5.8 % and 58.1 ± 2.9 %, respectively (Fig. 26A-B). Thus, these results clearly indicate an interaction of the mGluR5 receptor with MA, which leads to increased expressions of proinflammatory cytokines/chemokines.

In order to determine the downstream signaling cascade leading to the NF-κB pathway, we investigated the potential role of the PI3K/Akt pathway. The metabotropic glutamate receptor pathway requires the activation of the PI3K/Akt signaling cascade for its activity (Hou & Klann, 2004; Ribeiro, Paquet, Cregan, & Ferguson, 2010; Ribeiro, Paquet, Ferreira, et al., 2010). Therefore, we treated the astrocytes with 10μM of LY294002, a specific inhibitor of PI3K/Akt, for 1 hour prior to MA treatment for each of 3 days. The dose

of LY294002 was determined based on the cell viability as observed by trypan blue staining (data not shown). As per our hypothesis, LY294002 did abrogate the MA-mediated expression levels of IL-6 and IL-8 by 77.9 ± 6.6 % and 81.4 ± 2.6 %, respectively (Fig. 26C-D). Thus, these results provide strong evidence for the involvement of the PI3K/Akt signaling mechanism in the induction of IL-6 and IL-8 by MA.

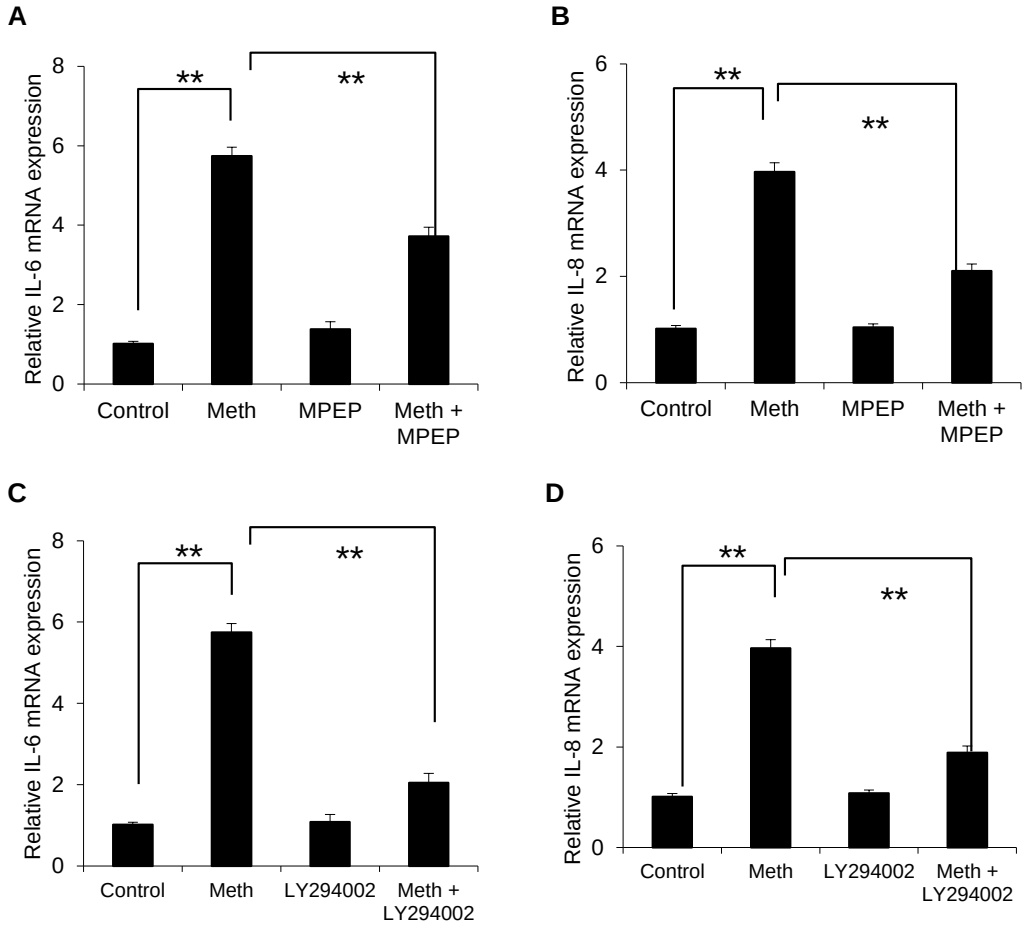

Figure 26: Role of mGluR5 and PI3K/Akt in MA-mediated expression of IL-6 and IL-8. SVGA astrocytes were treated with 25μM of MPEP or 10μM of LY294002 for 1 hour prior to the MA treatment every day for 3 days and the total mRNA was isolated 24 hours after the last treatment of MA. The relative mRNA expression levels were measured for IL-6 and IL-8 using real time RT-PCR and the effect of MPEP on MA-mediated expressions of IL-6 and IL-8 (A, B, respectively) and LY294002 (C, D, respectively) were determined. Each bar represents the mean ± SE of 3 experiments with each experiment performed in triplicate. The statistical significance was calculated using student's t-test and ** denotes p value of ≤ 0.01.

4.3. Discussion:

In the CNS, astrocytes are the most abundant cells and they are associated with several functions including metabolic support of neurons and modulation of neurotransmission. In the present study, we investigated the role of astrocytes in neuroinflammation produced by MA. We found that MA treatment of astrocytes can result in increased levels of IL-6 and IL-8 in a dose dependent manner. Furthermore, we demonstrated that the increases in IL-6 and IL-8 expression observed at the level of RNA were consistent with our observation of increased expression of IL-6 and IL-8 proteins. A single dose of MA in mice has been found to be associated with neurotoxicity mediated by increased expression of proinflammatory cytokines such as TNF-α, IL-1β and IL-6 (Goncalves et al., 2010; Goncalves et al., 2008). In this study, we investigated the effect of multiple doses of MA on the expression of proinflammatory cytokines in astrocytes. Our results demonstrated that MA can produce neuroinflammation in prolonged treatments. Furthermore, the expression of these cytokines is more pronounced with increasing doses of MA, indicative of increased neurotoxicity at higher doses of MA.

We next investigated the signaling mechanisms responsible for the MA-mediated increases in expression of IL-6 and IL-8. MA-mediated oxidative stress and mitochondrial dysfunction are found to play a major role in its neuroinflammatory effects (Potula et al., 2010; Tata & Yamamoto, 2007; Yamamoto & Raudensky, 2008). The induction of neuroinflammatory response due to MA has been shown to be associated with increased activities of certain transcription factors, including STAT1, STAT3, AP1, CREB and NF-κB (Hebert & O'Callaghan, 2000; Y. W. Lee et al., 2002). Since, NF-κB has also been found to be associated with multiple neurological disorders and neuroinflammatory complications; we

investigated whether NF-κB plays any role in the increased cytokine expression induced by MA. Our studies clearly showed multiple lines of evidence that support our hypothesis that the MA-mediated increase of proinflammatory cytokines/chemokines is dependent on the NF-κB pathway. To our knowledge, this is the first demonstration that MA-induced increases in proinflammatory cytokines/chemokines are mediated through the NF-κB pathway. Thus, the NF-κB pathway appears to be involved in mediating the induction of proinflammatory cytokines/chemokines by MA, as well as in mediating the response to oxidative stress induced by MA. The role of the dopamine receptor and transporters has been extensively studied to address the neuroinflammatory roles of MA in the CNS (Cadet & Krasnova, 2009; Kita et al., 2009; Silverstein et al., 2011). However, recently the effect on the excitatory neurotransmitter via glutamate receptors has also been shown to be responsible for MA-mediated cognitive impairments (Reichel et al., 2011). Furthermore, inhibition of the metabotropic glutamate receptors, mGluR5 in particular, has been shown to reduce the self-administration of MA in rats. (Osborne & Olive, 2008). MA-mediated extracellular glutamate is found to augment the excitotoxicity in the striatums of rats (Tata & Yamamoto, 2008). Furthermore, our results in the present study clearly demonstrate that mGluR5 plays a role in MA-mediated induction of IL-6 and IL-8. Thus, our study suggests a possible link between the oxidative stress and mGluR5 activity since both phenomena are due to MA treatment. Furthermore, recent studies in spinal cord injury and neonatal excitotoxic lesions have suggested the potential utilization of mGluR5 as a therapeutic target (Drouin-Ouellet et al., 2011; Pajoohesh-Ganji & Byrnes, 2011). Our findings also suggest mGluR5 as a therapeutic target for abrogation of MA-mediated expression of neuroinflammatory cytokines/chemokines. Furthermore, we sought to investigate a link between the effects of

MA on mGluR5 and NF-κB activation. Since, the classical Huntington disease pathway involves activation of the PI3K/Akt pathway, which is mediated via the mGluR5 receptor (Ribeiro, Pires, & Ferguson, 2011); we hypothesized a role for PI3K/Akt in the signaling cascade induced by MA. Our results support this hypothesis, because the antagonist for PI3K/Akt abrogated MA-mediated expression of IL-6 and IL-8.

In conclusion, we demonstrated that MA could increase the expression of proinflammatory cytokines/chemokines in astrocytes in a dose-dependent manner. MA alters the mGluR5 receptor activity, which activates the PI3K/Akt cascade. This may further activate the phosphorylation of IκBα via the kinase activity of IKK releasing the free form of the heterodimeric NF-κB (p50-p65). Finally the active NF-κB then translocates from cytoplasm to the nucleus and promotes the transcription of IL-6 and IL-8 (Fig. 27). The temporal relationship between the pathways that is presented in Fig. 27 is based upon reports in the literature. The activation of PI3K/Akt has been shown to be mediated through mGluR5 (Chen et al., 2012; Hou & Klann, 2004). Furthermore, involvement of the NF-κB pathway in the regulation of various pro-inflammatory cytokines/chemokines has been well reported (Beg & Baltimore, 1996; Kaltschmidt et al., 1993; Kunsch & Rosen, 1993; Sparacio et al., 1992). In our study, we demonstrated abrogation of MA-mediated IL-6 expression with the use of both, mGluR5 and PI3K/Akt inhibitors. Thus, in addition to the current paradigm presented in the literature, our study provides essential evidence suggesting involvement of these pathways with regard to MA-mediated signaling. Thus, our present study provides vital information to better understand the role of MA in the expression of proinflammatory cytokines/chemokines in astrocytes and provides an insight in the development of therapeutic strategies to counteract MA-mediated inflammation.

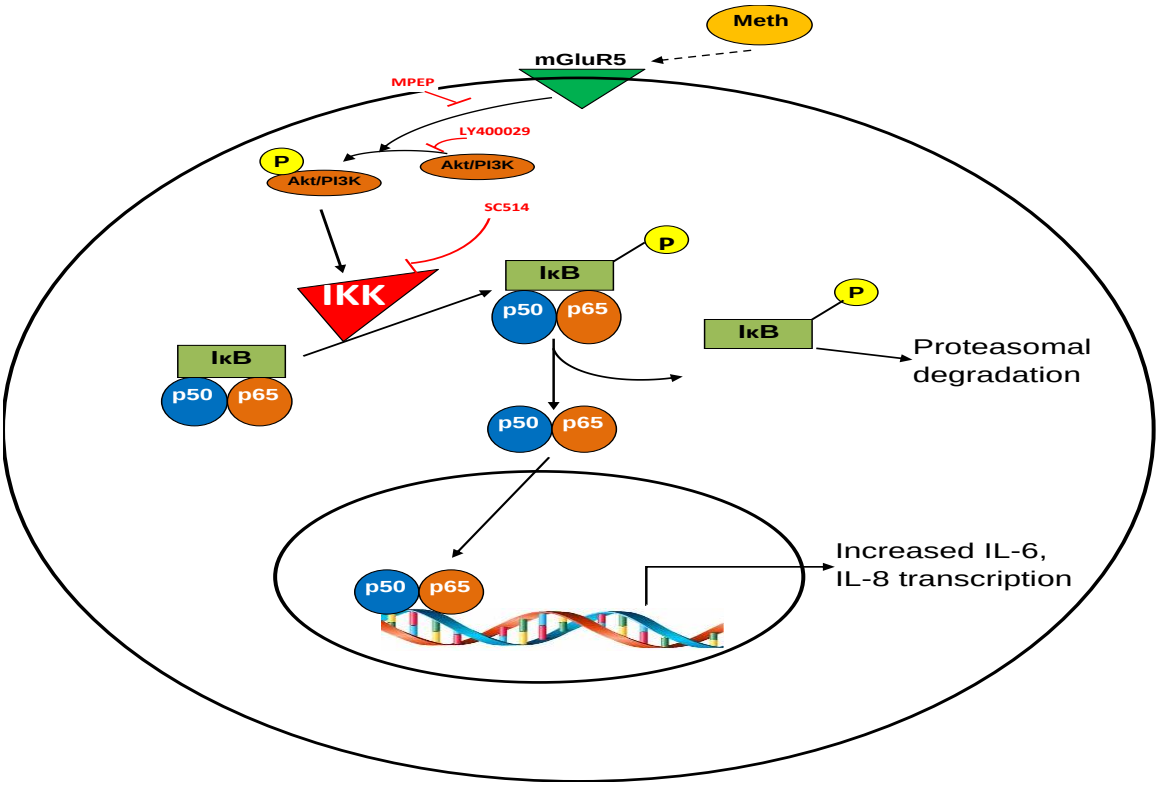

Figure 27: Schematic of the signaling pathways involved in MA-mediated induction of IL-6 and IL-8. Exposure to MA leads to the activation of excitatory neurotransmitters and leads to mGluR5-mediated activation of PI3K/Akt signaling pathways. Activated PI3K/Akt phosphorylates IKK which results in the phosporylation of p-IκB and releases the heterodimeric NF-κB (p50/p65) in the cytoplasm. NF-κB then translocates from the cytoplasm to the nucleus and leads to enhance IL-6 and IL-8 expression in astrocytes.

4.4. Acknowledgement:

Chapter 4 contains figures and text of the manuscript accepted in Journal of neuroinflammation 2012 by Shah et. al. The dissertation author was the lead author of the published manuscript.

CHAPTER-5

SYNERGISTIC COOPERATION BETWEEN METHAMPHETAMINE AND HIV-1 gp120 THROUGH THE PI3K/Akt PATHWAY INDUCES IL-6 BUT NOT IL-8 EXPRESSION IN ASTROCYTES

5.1. Introduction:

Increasing evidence suggests that drug abuse is a common risk factor in the acquisition of HIV infection. Drugs such as cocaine, methamphetamine (MA) and morphine have also been shown to exacerbate neurotoxicity (Aksenov et al., 2006; Turchan et al., 2001; Yang et al., 2010; Zou et al., 2011). MA is a potent psycho-stimulant and one of the most commonly abused drugs in the United States. MA is known to produce long-lasting dopaminergic insults to the brain (Wagner et al., 1980). Furthermore, exposure to MA has also been demonstrated to alter the integrity of the BBB (Mahajan et al., 2008; Ramirez et al., 2009). Several reports document MA-induced expression of various cytokines such as TNF-α, IL-1β and IL-6, which confirms the inflammatory role of MA in the CNS (Goncalves et al., 2008; Sriram et al., 2006; Tocharus, Khonthun, Chongthammakun, & Govitrapong, 2010). Furthermore, oxidative stress induced by MA has been demonstrated to alter BBB integrity (Ramirez et al., 2009) and exacerbates the neurotoxicity associated with viral toxins like Tat and gp120 (Banerjee, Zhang, Manda, Banks, & Ercal, 2010; Mahajan et al., 2008). Recently methamphetamine has been shown to act in synergy with gp120 to induce oxidative stress (Banerjee et al., 2010). However it is not known if a synergy exists at the level of induction of proinflammatory cytokines. In spite of the increased understanding of the toxicities produced by both viral proteins and MA, the mechanisms underlying the interactions between gp120 and MA are still unclear.

In our earlier studies, we demonstrated that the gp120-mediated increase in the expression levels of IL-6, CCL5 and IL-8 is due to an NF-κB dependent mechanism (Shah & Kumar, 2010; Shah, Singh, Buch, & Kumar, 2011; Shah, Verma, et al., 2011). Furthermore, we have also shown that MA increases the expression of IL-6 and IL-8 through the NF-κB and Akt/PI3K pathways (Shah, Silverstein, Singh, & Kumar, 2012). In the present study, we investigated the effects of MA and gp120 on IL-6 and IL-8 in astrocytes. In order to study the interactions between MA and gp120, we looked at possible mechanisms such as the Akt/PI3K, p38-MAPK and NF-κB pathways. Using our astrocyte model of neuroinflammation, we sought to identify the mechanisms responsible for the interactions observed between MA and gp120 that act to exacerbate neuroinflammation through increased cytokine production. To our knowledge, this is the first report that MA exacerbates gp120-induced inflammatory cytokine expression in astrocytes.

5.2. Results:

5.2.1. MA exacerbates gp120-mediated induction of IL-6 but not IL-8 in astrocytes.

Based on our earlier studies with either MA or gp120 administered alone, it was evident that there were overlapping mechanisms involved in the induction of cytokine levels in astrocytes (Shah & Kumar, 2010; Shah et al., 2012; Shah, Singh, et al., 2011; Shah, Verma, et al., 2011; Silverstein et al., 2012). Furthermore, MA has been shown to exacerbate the toxicity of tat and gp120 via multiple mechanisms such as increasing oxidative stress (Banerjee et al., 2010), dopaminergic insult (Cass, Harned, Peters, Nath, & Maragos, 2003; Theodore, Stolberg, Cass, & Maragos, 2006), and alteration in BBB integrity (Mahajan et al., 2008). Therefore, we hypothesized that there might be interaction between pathways governing induction of cytokines by MA and gp120 in astrocytes. Our data demonstrate that

astrocytes treated with both MA and gp120 increased the expressions of IL-6 to levels that are much higher than when cells were treated with either agent alone. This was observed for astrocytes treated with either 1 dose or 3 doses of MA given over 3 days at the levels of both, mRNA (Fig. 28A and 28B) and protein (Fig. 28C and 28D).

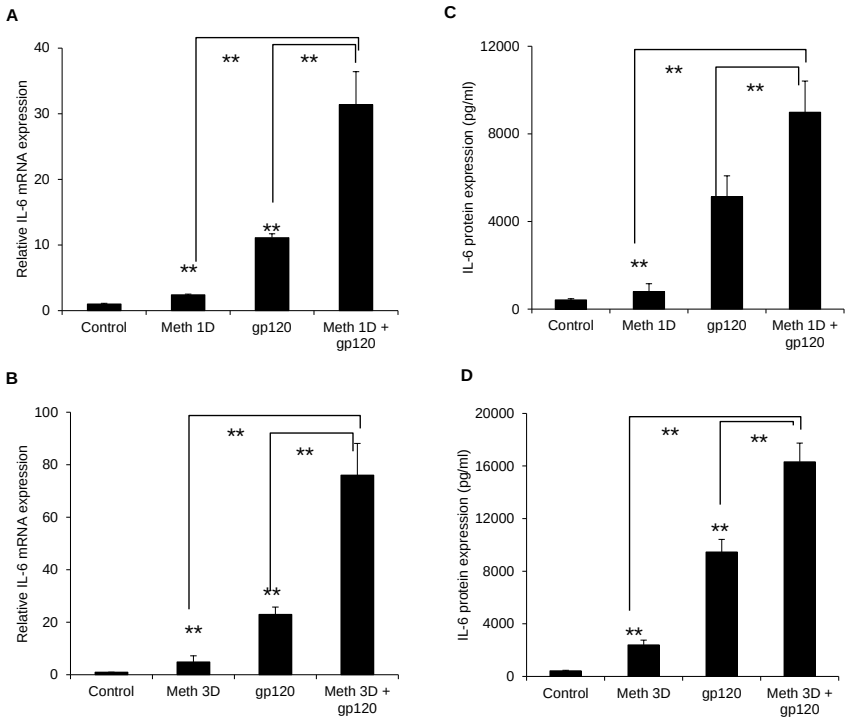

Figure 28: MA exacerbates the induction of IL-6 by gp120 in astrocytes. SVGA astrocytes were treated with 500 μM of MA for either 24 hours (1 dose) or 72 hours (3 doses). The cells were seeded at 8 x 10^5 cells/well in 6-well plates. The cells were transfected with 2 μg of a plasmid expressing gp120. The cells were harvested 6 hours post-transfection for the determination of mRNA and protein levels for IL-6 after single dose of MA (A and C) and 3 doses of MA (B and D). The response to combined treatment with both MA and gp120 was compared with the levels obtained due to treatment with either MA or gp120 alone. The bars represent the mean ± SE of 3 independent experiments with each treatment in triplicates. The p-values ≤ 0.01 were considered statistically significant when calculated using student's t-test.

However, we did not observe the same effects upon IL-8 expression either at the levels of mRNA (Fig. 29A and 29B) or protein (Fig. 29C and 29D). Although, astrocytes treated with either MA or gp120 alone increased the level of IL-8 expression, treatment with both MA and gp120 simultaneously did not show levels of expression that would suggest synergy. Furthermore, astrocytes treated with MA and gp120 for 3 days exhibited lower expression levels of IL-8 mRNA ($p<0.05$) as compared to astrocytes treated with gp120 alone. However, when IL-8 expression in these two groups was compared at the level of protein, the difference between the groups was not significantly different. We therefore did not pursue the mechanism(s) involved in regulating IL-8 expression in response to simultaneous treatment with both MA and gp120.

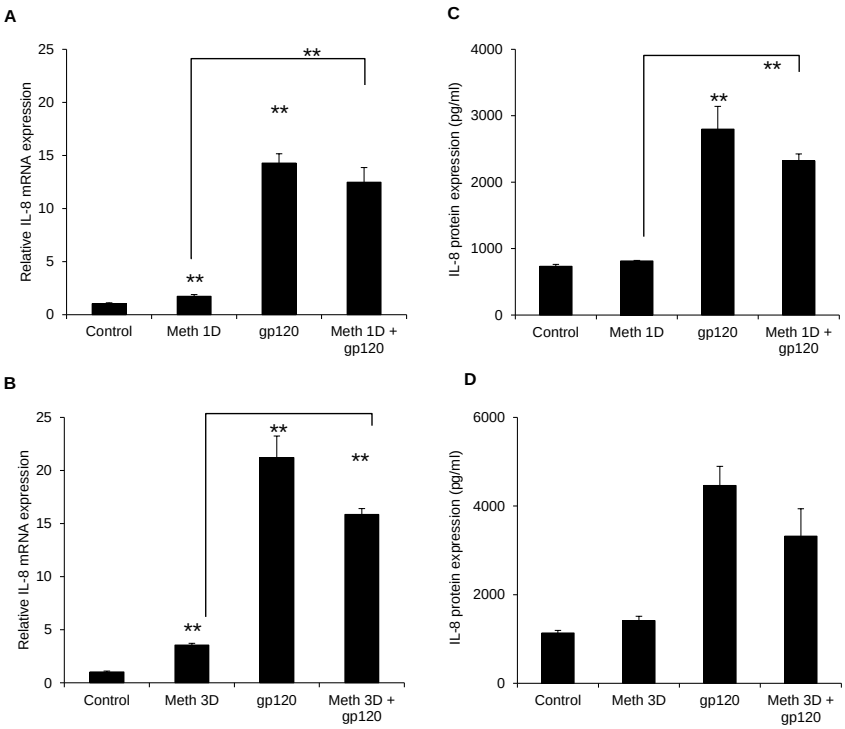

Figure 29: MA does not alter the expressions of IL-8 induced by gp120 in astrocytes. SVGA astrocytes were treated with 500 μM of MA for either 24 hours (1 dose) or 72 hours (3 doses). The cells were seeded at 8 x 10^5 cells/well in 6-well plates. The cells were transfected with 2 μg of a plasmid expressing gp120. A and C how the mRNA and protein level of IL-8 after single dose of MA for 24 hours and B and D shows the IL-8 expressions after 3 doses of MA. The response to combined treatment with both MA and gp120 was compared with the levels obtained due to treatment with either MA or gp120 alone. The bars represent the mean ± SE of 3 independent experiments with each treatment in triplicates. The p-values ≤ 0.01 were considered statistically significant when calculated using student's t-test.

In order to confirm these results, we also used immunofluorescent staining as described in the materials and methods. As shown in Fig. 30 treatment of cells with either MA or gp120 increased the expression of IL-6. However, when cells were treated with both gp120 and MA the levels of IL-6 were much higher than the levels observed when treatment was with either agent alone. Thus, our results suggest a possible synergistic interaction between MA and gp120 in terms of the expression of IL-6 at the levels of both mRNA as well as protein.

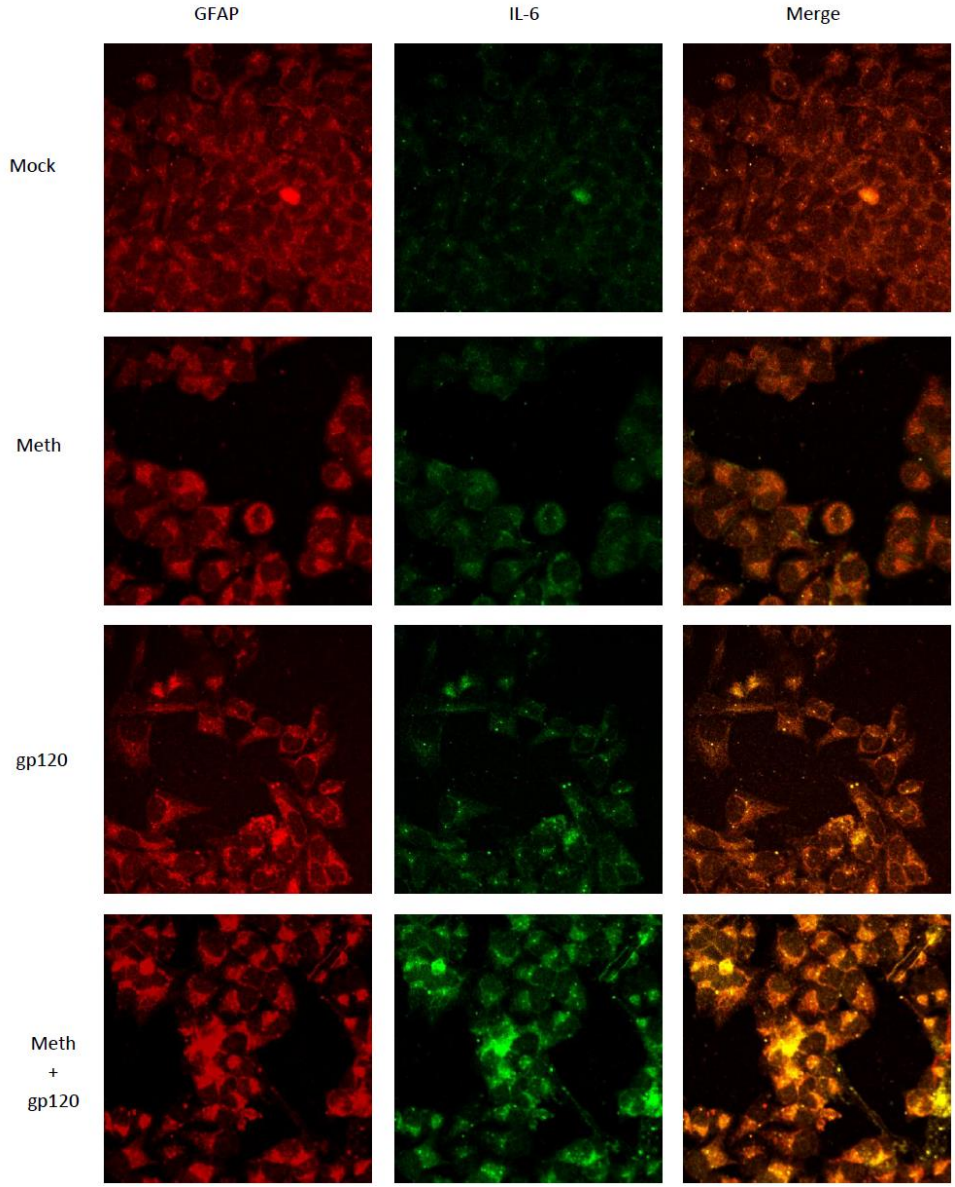

Figure 30: MA and gp120 increase the expression of IL-6 in SVGA astrocytes. SVGA astrocytes were grown on a coverslip and allowed to adhere. The cells were then treated with 500μM of MA for 24 hours followed by transfection with 2 μg of plasmid encoding gp120. The cytokine release in the supernatant was blocked with the treatment of the cells with GolgiStopTM 6 hours prior to termination. The cells were fixed 24 hours post-transfection with 1:1 methanol:acetone. The cells were permeabilized with 0.1% PBS-Triton X-100 for 10 min and blocked with 1% BSA in PBS. After blocking, the coverslip was incubated with a primary rabbit antibody against IL-6 and a primary mouse antibody against GFAP for 1 hour. This was followed by washes with PBST and incubation with fluorescently labeled secondary antibodies for 1 hour. Anti-rabbit Alexafluor488 and anti-mouse Alexafluor555 (red) were used to detect IL-6 and GFAP, respectively. The cells were washed with PBST and the coverslips were mounted on a glass slide using mounting solution. The cells were observed using confocal microscopy. The images shown here, obtained using EZ C1 confocal microscope software, are 60X magnification.

5.2.2. The PI3K/Akt and NF-κB pathways are involved in the induction of IL-6 expression by MA and gp120:

Having established that MA exacerbates the expression of IL-6 induced by gp120, we wished to investigate the mechanisms governing this interaction. We hypothesized that the NF-κB pathway was likely to be involved in this interaction because both MA and gp120 utilized this transcription factor to increase expression of IL-6. In order to confirm the signaling mechanism, we measured the p-IκBα in the whole-cell lysates and translocation of p50 from the cytoplasmic to nuclear compartment. In order to measure the phosphorylation of IκBα, SVGA cells were treated either with MA or recombinant gp120 alone or gp120+MA for 0, 5, 10, 20, 40 and 60 min. The whole-cell lysates were prepared and the expression of p-IκBα was measured using western blotting (Fig. 31A). The phosphorylation of IκBα was observed within 5 minutes with peak at 40 min for MA and 10 min for gp120. Cells treated with gp120 and MA showed increase in p-IκBα at 5 min and the expressions remained significantly high throughout observation period of 60 min. We have already shown in our previous study that both MA and gp120 can independently increase the translocation of p50 within 3 hours and 6 hours, respectively (Shah et al., 2012; Shah, Singh, et al., 2011). In order to measure the translocation of p50, SVGA astrocytes were treated with either MA or gp120-transfection alone or both MA and gp120-transfection for 6 hours and the p50 expression was measured using western-blotting (Fig. 31B). The translocation of p50 was observed in the samples treated with MA or gp120 and MA+gp120, however, there was no significant difference between gp120 transfection and gp120 transfection/MA treatment. Furthermore, SVGA astrocytes were treated with 20 μM SC514 1 hour prior to the MA treatments and gp120 transfection. The cells were harvested 6 hours post-transfection as

described in materials and methods. Treatment with an NF-κB antagonist abrogated MA and gp120-mediated expression of IL-6 when cells were treated with either agent alone.

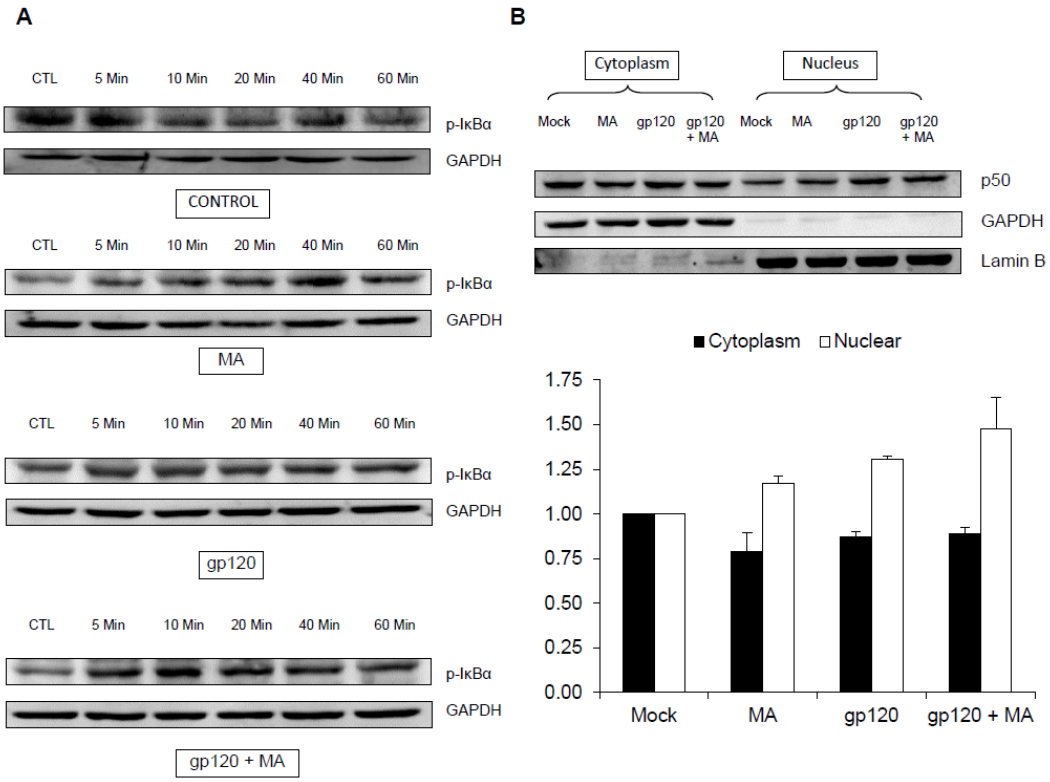

Figure 31: gp120 and/or MA activates IκBα and increases the translocation of p50 in SVGA astrocytes. (A) SVGA astrocytes were treated with 500μM MA and/or 50ng/ml recombinant gp120 protein for 0, 5, 10, 20, 40 and 60 minutes and the whole cell lysate was prepared by lysing the cells with RIPA buffer. The proteins were separated using SDS-PAGE electrophoresis as mentioned in the Materials and Methods section. The p-IκBα was determined in western blotting. GAPDH was used as housekeeping control. (B) SVGA astrocytes were treated with MA and/or transfected with gp120 for 6 hours. The translocation of p50 was measured from cytoplasm to nucleus as described in the Materials and methods. GAPDH was again used as loading control for cytoplasmic extracts and LaminB was used as loading control for nuclear extracts. The bar charts below the representative images show the densitometry values corresponding to the respective treatments. The housekeeping proteins were used to normalize the protein expressions of various genes.

Furthermore, it also abrogated the increase of IL-6 induced by simultaneous treatment with both MA and gp120 at the levels of mRNA (Fig. 32A) and protein (Fig. 32B).

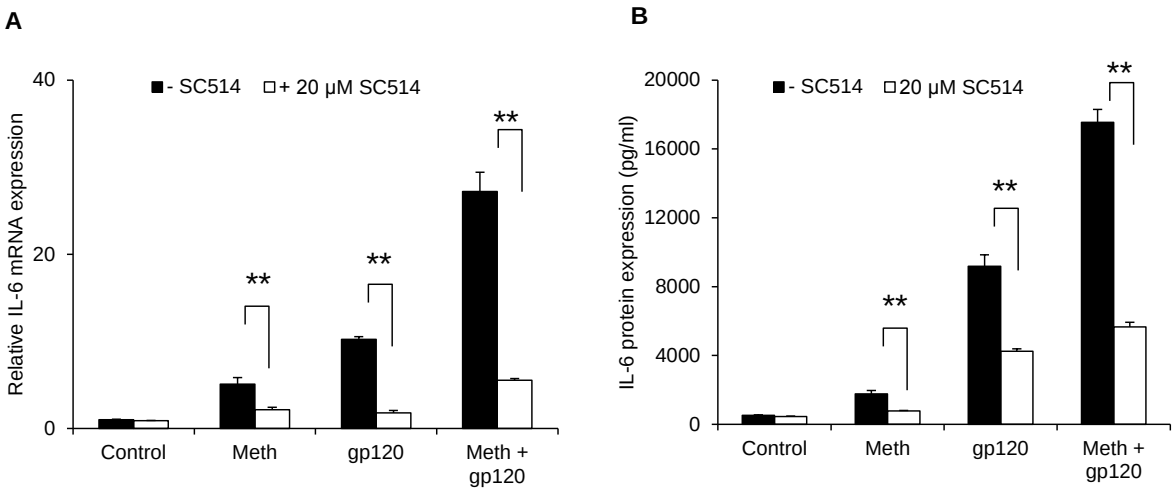

Figure 32: The NF-κB pathway is involved in the induction of IL-6 by MA and gp120. SVGA astrocytes were treated with 500 μM of MA once a day for 3 days for MA treatment. The cells were then seeded in 6-well plates with 8 X 10^5 cells and transfected with 2 μg of plasmid expressing gp120. Untreated cells were also transfected with 2μg of plasmid expressing gp120. For inhibitor treatments, cells were treated with the specific inhibitors for the NF-κB pathway (SC514) 1 hour prior to addition of MA and/or gp120. The cells were harvested 6 hours post-transfection to quantify the mRNA expression levels of IL-6 in the presence of SC514 (A). In order to determine the levels of IL-6 protein, the cell culture supernatants were collected 24 hours post-transfection (B). Each bar shows the mean ± SE of 3 independent experiment with each performed in triplicates. The p-value of ≤ 0.01 (**) was considered to be statistically significant as calculated using student's t-test.

We also investigated the potential role of PI3K/Akt in the increase of IL-6 expression since both MA and gp120 utilized PI3K/Akt in inducing the expression of IL-6. SVGA astrocytes were treated with either MA or gp120 alone or both gp120 and MA, and the whole-cell lysates were collected after 0, 5, 10, 20, 40 and 60 min. The proteins were separated using SDS-PAGE electrophoresis and the expression of phosphorylated Akt was measured in western blot assay. Both gp120 and MA showed increased expression of p-Akt with MA and gp120 showing higher expressions of p-Akt than either of the agents alone (Fig. 33A). Furthermore, the levels of PI3K/Akt-activation was observed to be more than additive in the astrocytes, treated with gp120 and MA as opposed to those treated with either MA or gp120 alone (Fig. 33B). Additionally, the area under curve for gp120 and MA was significantly higher than either MA or gp120 alone (Fig. 33C). Furthermore, LY294002 (an inhibitor of the PI3K/Akt pathway) abrogated IL-6 expression (Fig. 33D). Taken together, these results suggest that both the NF-κB and PI3K/Akt pathways are responsible for the increase of IL-6 levels observed with the combined treatment with gp120 and MA in astrocytes.

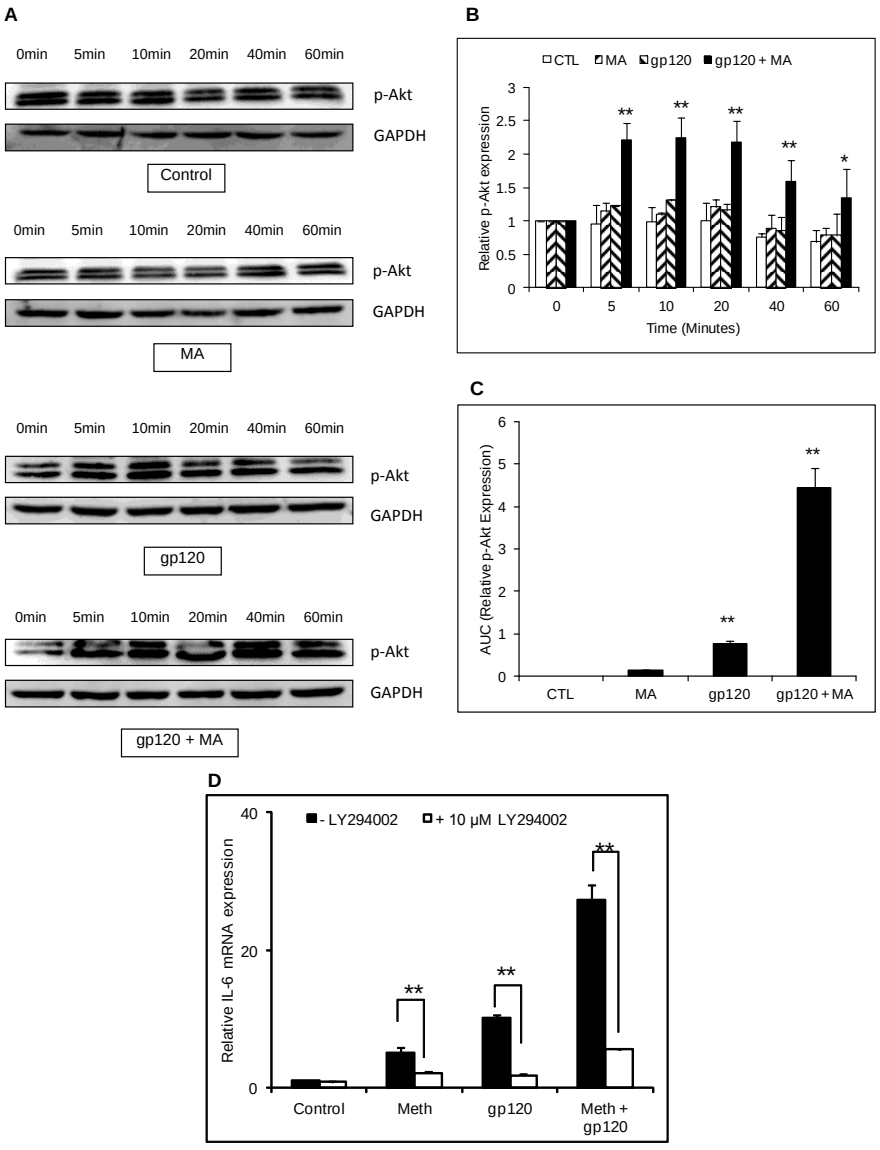

Figure 33: gp120 and/or MA activate PI3K/Akt signaling in astrocytes. SVGA astrocytes were treated with 500µM MA and/or 50ng/ml recombinant gp120 protein for 0, 5, 10, 20, 40 and 60 minutes. The cells were lysed using RIPA buffer and homogenized to prepare whole-cell lysate. The protein was electrophoresed and p-Akt was detected in western blotting. GAPDH was used as a loading control (A). The bar chart represents the normalized densitometry values measured using GAPDH as control. The expression of p-Akt observed at 0 min was considered as basal expression (B). The area under the curve of the normalized p-Akt expression was calculated by adding the expression levels at different time-points shown in (A) and (B) in the kinetics. The values were normalized with untreated control as basal expression levels (C). For inhibitor treatments, cells were treated with the specific inhibitors for the PI3K/Akt pathway (LY294002) 1 hour prior to addition of MA and/or gp120. The cells were harvested 6 hours post-transfection to quantify the mRNA expression levels of IL-6 (D).Each bar shows the mean ± SE of 3 independent experiment with each performed in triplicates. The p-value of ≤0.05 (*) and ≤ 0.01 (**) were considered to be statistically significant as calculated using student's t-test.

5.3. Discussion:

One of the features of many CNS diseases is the presence of elevated levels of cytokines. For example, increased levels of cytokines and chemokines have been found in CNS diseases such as Parkinson's disease (PD), Alzheimer's disease (AD) and Multiple Sclerosis (MS) (reviewed in Mogi et al., 1996; Steinman, 2008). Altered levels of cytokines and chemokines also play an important role in the pathology of HAND (reviewed in Kaul & Lipton, 2006). MA, and most other drugs of abuse, are associated with both a greater risk in the acquisition of HIV infection and more rapid disease progression. Although, several reports have documented the deleterious effects of various drugs of abuse in the CNS, the mechanism by which these drugs exacerbate HIV infection of the CNS remains unclear. In an early study, Nath et al. reported that an HIV-infected abuser of MA and cocaine exhibited CNS complications that developed more rapidly and was more severe than those observed in non-abusing HIV+ patients (Nath, Maragos, Avison, Schmitt, & Berger, 2001). MA has also been found to act synergistically with Tat in producing CNS damage in a rat model (reviewed in Nath et al., 2002). Furthermore, studies have documented the effects of MA on increased viral load/infectivity in different biological compartments using either *in vitro* or *in vivo* models (Liang et al., 2008; Marcondes, Flynn, Watry, Zandonatti, & Fox, 2010; Nair et al., 2009; Toussi et al., 2009).

We hypothesized that, MA and gp120 might exacerbate the neuroinflammatory response via overlapping signaling pathways. Our previous work demonstrated that HIV gp120 induces IL-6 expression in astrocytes through an NF-κB-dependent mechanism (Shah, Singh, et al., 2011; Shah, Verma, et al., 2011; Silverstein et al., 2012). In addition, we have shown that MA can increase the expression of IL-6 and IL-8 in astrocytes (Shah et al., 2012).

We therefore, wished to investigate the combined effects of gp120 and MA on the induction of proinflammatory cytokines in astrocytes. The present study shows for the first time that, when administered simultaneously, gp120 and MA can increase the expression of IL-6 to levels that are significantly higher than that induced by either agent alone. Thus, our data suggests that gp120 and MA act synergistically to induce IL-6. Our earlier reports, along with this study, show that the effects of both gp120 and MA are mediated by the PI3K/Akt and the NF-κB pathways. Therefore, we hypothesized that these two pathways interact in tandem to increase expression of IL-6 after simultaneous administration of MA and gp120 in astrocytes. Indeed, we found increased phosphorylation of Akt and IκB-α upon treatments with either MA or gp120 alone as well as both of them together. The phosphorylation of Akt was observed to be higher in the cells treated with MA and gp120 together. Furthermore, the p-IκB-α levels were observed to be not only higher but also the activation was observed earlier than the cells treated with either MA or gp120 alone. The involvement of either PI3K/Akt or NF-κB was further confirmed by the fact that specific inhibitors abrogated the synergy in MA and gp120-mediated IL-6 production. Although gp120 was found to increase the expression of IL-6 through activation of the p38-MAPK pathway, the MA-mediated increase of IL-6 did not involve the p38-MAPK pathway. Our work confirms a previous study using a human neuroblastoma cell line that showed that MA exposure did not activate the p38-MAPK pathway in these cells (Guillot et al., 2008). Therefore, we ruled out the possibility of the involvement of the p38-MAPK pathway in the MA-mediated exacerbation of the expression levels of IL-6 induced by gp120. On the contrary we did not observe synergy in IL-8 production whereas both MA and gp120 individually increased the expression of IL-8 in astrocytes.

In conclusion, we have demonstrated that both MA and gp120 could induce the expression of IL-6 in astrocytes by utilizing common signaling pathways. The results from this study suggest a model for synergistic IL-6 production in astrocytes (Figure 32). When in the CNS, MA and gp120 can activate the PI3K/Akt pathway via their action on mGluR5 (Osborne & Olive, 2008; Ribeiro et al., 2011; Tata & Yamamoto, 2008) and the HIV-1 co-receptors that bind gp120 (i.e. CXCR4 or CCR5). The activation of PI3K/Akt can further activate the NF-κB pathway via phosphorylation of IKK, which can lead to the increased expression of IL-6. Additionally, the p38-MAPK pathway is involved in the increased expression levels of IL-6 due to gp120. The p38-MAPK pathway is known to activate the NF-κB pathway in addition to other transcription factors such as AP-1, STAT1 and ATF2. However, this pathway may not be involved in the MA-gp120 interaction that results in increased expression of IL-6 in astrocytes. This study, therefore, provides key information with regard to molecular pathways involved in MA-mediated exacerbation of the induction of IL-6 by gp120. Previously, MA has been shown to potentiate the oxidative stress induced by HIV-1 proteins, including gp120, which may result in disruption of tight junction proteins in the BBB (Mahajan et al., 2008; Ramirez et al., 2009). Additionally, MA has been shown to act as a co-factor in the alteration of BBB permeability induced by gp120 (Banerjee et al., 2010). Taken together with the results of the present work, these findings indicate possible synergistic interactions between MA and gp120 at several different levels that may exacerbate the neuro-toxicity related to neuroAIDS. Understanding the mechanisms involved in these interactions will be of help in development of therapeutic strategies for the treatment of HAND among MA abusers.

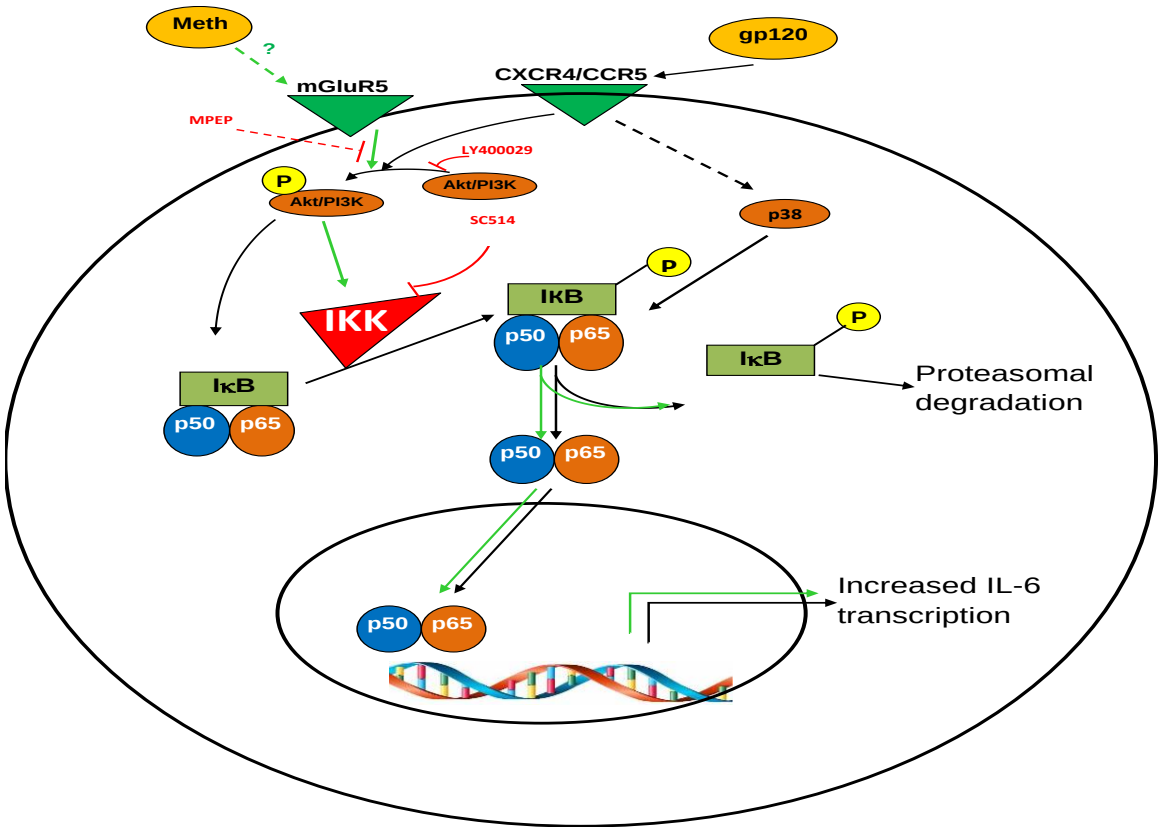

Figure 34: Schematic illustrations of the signaling pathways that mediate the induction of IL-6 by MA and gp120 in astrocytes. Treatment of astrocytes with gp120 results in the binding of gp120 by the CCR5 or CXCR4 chemokine receptors and the subsequent activation of PI3K/Akt and p38-MAPK. The activation of these two pathways may lead to increased activation of NF-κB. The activated NF-κB then translocates into the nucleus and increases the transcription of IL-6. Treatment of astrocytes with MA results in activation of metabotropic glutamate receptor 5 (mGluR5). The mechanism of mGluR5 activation by MA is unclear, but one possibility is that the increase in extracellular glutamate caused by MA treatment may activate the receptor. mGluR5 then activates the PI3K/Akt pathway which can lead to activation of NF-κB and increased expression of IL-6. Thus, gp120 and MA can induce higher expression levels of IL-6 as compared to the levels observed in the presence of either agent alone.

5.4. Acknowledgement:

Chapter 5 contains figures and text of the manuscript accepted in PLOSONE 2012 by Shah et. al.The dissertation author was the lead author of the published manuscript.

CHAPTER-6

HIV gp120 AND METHAMPHETAMINE-MEDIATED OXIDATIVE STRESS INDUCES ASTROCYTE APOPTOSIS VIA CYTOCHROME P450 2E1

6.1. Introduction:

The HIV-1 envelope protein, gp120, mediates entry of the virus into host cells, including T cells and monocytes. Infected monocytes can traffic across the blood-brain barrier (BBB) into the CNS where the virus can replicate in microglia and astrocytes (Carroll-Anzinger et al., 2007; Kaul et al., 2005). The neurotoxic effects of HIV-1 proteins, including gp120, can be either through direct or indirect mechanisms (Gonzalez-Scarano & Martin-Garcia, 2005). In terms of indirect mechanisms, HIV-1 gp120 has been shown to induce the expression of proinflammatory chemokines and cytokines (Shah & Kumar, 2010; Shah, Singh, et al., 2011; Shah, Verma, et al., 2011), and to induce oxidative stress in astrocytes and microglia (P. V. Reddy et al., 2012; Ronaldson & Bendayan, 2008). Both in vitro and in vivo models have been used to demonstrate that gp120 can directly induce apoptosis in neurons (Silverstein et al., 2012).

Variety of illicit substances such as morphine, cocaine and methamphetamine (MA), have been shown to exacerbate HIV-associated neurotoxicity (Silverstein et al., 2011; Silverstein et al., 2012; Yao, Allen, Zhu, Callen, & Buch, 2009). In the central nervous system (CNS), MA has been shown to increase excitotoxicity (Yamamoto & Raudensky, 2008), BBB damage (M. Park, Hennig, & Toborek, 2012; Yamamoto & Raudensky, 2008), the expression of pro-inflammatory cytokines (Shah et al., 2012), and oxidative stress (M. Park et al., 2012; Ramirez et al., 2009). Due to its structural similarity to dopamine, MA has

been shown to increase dopaminergic activity leading to increased intracellular oxidative stress and neurotoxicity (LaVoie & Hastings, 1999). These findings are consistent with the protective effect of various antioxidants against MA-induced neurotoxicity (Banerjee et al., 2010; M. J. Park et al., 2006; Zhang, Banerjee, Banks, & Ercal, 2009). Thus, oxidative stress is suggested to play an important role in MA-mediated neurotoxicity. Furthermore, it is likely that concurrent HIV infection and substance abuse may cause enhanced neurotoxicity. We have recently shown that gp120 and MA co-operate synergistically to induce the pro-inflammatory cytokine IL-6 in astrocytes (Shah et al., 2012). However, it is not known whether such cooperation exist at oxidative stress level.

Recent advances suggest the involvement of various cytochrome P450 (CYP) enzymes in neurotoxicity, perhaps as the result of production of reactive oxygen species (ROS) and/or reactive metabolites. The involvement of CYP46 in Alzheimer's disease (Brown et al., 2004) and CYP2D6 in PD (Elbaz et al., 2004) illustrate the contributions of these enzymes to neurodegenerative disorders. Although the role of CYPs in drug abuse and HIV-1 neuropathogenesis is unexplored, a recent study suggests a potential role for CYP2E1 in alcohol-mediated neurotoxicity (Jin, Ande, Kumar, & Kumar, 2013). Furthermore, NADPH oxidase (NOX) has been shown to induce ROS, both independently as well as in association with CYP-mediated drug metabolism. Therefore, we hypothesize that CYP and NOX pathways are involved in HIV- and/or MA-induced neurotoxicity.

The present study was undertaken to determine whether viral protein gp120 and methamphetamine cooperates to cause enhanced oxidative stress leading to increased cell death and whether CYP is involved in gp120/MA-mediated oxidative stress and astrocyte apoptosis.

6.2. Results:

6.2.1. HIV-1 gp120 and MA independently increase oxidative stress in astrocytes.

Several studies have reported gp120-mediated induction of oxidative stress in astrocytes (P. V. Reddy et al., 2012; Ronaldson & Bendayan, 2008; Visalli et al., 2007). In this study, we used SVGA astrocytic cells and transfected them with a plasmid containing a gp120 expression vector. Astrocytes were transfected for different lengths of time and ROS was measured using H_2DC-FDA on flow cytometer. As shown in Fig. 35A, gp120 induced ROS production with a peak increase (75.2 ± 10.6 %) at 24 hours compared to mock-transfected cells. In order to confirm the effect of exogenous gp120, we used recombinant gp120IIIB protein and obtained similar results that showed an increase in ROS production as early as 6 hours. The peak ROS production (21.7 ± 5.1 %) was observed at 12 hours of exposure (Fig. 35B). The increase in ROS production was also found to be concentration-dependent as 2 nM gp120IIIB showed 22.1 ± 3.2 % increase compared to the control (Fig. 35C).

MA is known to induce oxidative stress in various cell types in the brain mainly via dopaminergic mechanism (Beauvais, Atwell, Jayanthi, Ladenheim, & Cadet, 2011; Shin et al., 2012). In order to determine the effect of MA on ROS production, we treated the astrocytes with varying concentrations of MA. The results showed a concentration-dependent increase in ROS with 500 μM showing maximal ROS (37.3 ± 2.4 %) at 24 hours (Fig. 35D). Furthermore, in order to test the effect of single dose of MA on ROS production, astrocytes were treated with 500 μM MA for various lengths of time. This dose of MA was based on the blood concentrations and tissue/serum compartmentalization as reported in literatures (Melega et al., 2007; Riviere et al., 2000; Talloczy et al., 2008). Furthermore, the binge

administration of MA in the range of 250mg-1g has been found to produce brain concentrations of MA between 164μM-776μM (Riviere et al., 2000). As expected, MA increased ROS production in a time-dependent manner and peak ROS production (29.4 ± 3.0 %) was observed at 24 hours (Fig. 35E).

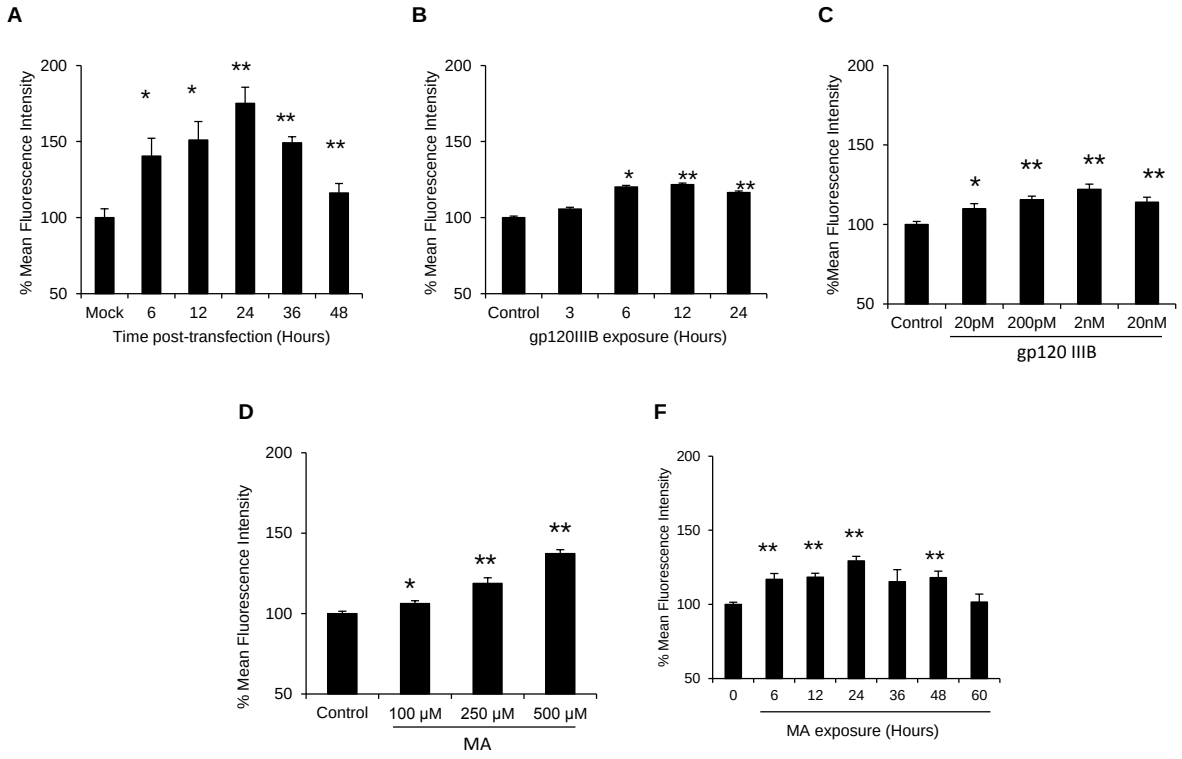

Figure 35: HIV-1 gp120 and MA increase oxidative stress in time-dependent manner. SVGA astrocytes were seeded at 2.75 X 10^5/well in 12-well plates and treated with appropriate agents. The cells were then washed twice with PBS and incubated with 5μM solution of H2DC-FDA for 30 min at 37ºC. This was followed by 2 washes with PBS and fluorescence intensity was measured using flow cytometer. (A) Cells were transfected with 2 μg of plasmid expressing gp120 for 5 hours using Lipofectamine 2000TM followed by replacement of the transfection mix with complete medium. ROS was measured after 6, 12, 24, 36 and 48 hours post-transfection. (B) Cells were treated with 200μM of recombinant gp120 IIIB and ROS was measured after 3, 6, 12 and 24 hours after the treatment. (C) Cells were treated at varying concentration of gp120IIIB and ROS was measured after 24 hours of exposure. (D) Cells were treated with different concentration of MA and ROS was measured after 24 hours of exposure. (E) Cells were treated with 500 μM MA and ROS was measured. The bars represent mean ± SE of at least 2 independent experiments with each treatment in triplicates. The p-value ≤ 0.05 (*) and ≤ 0.01(**) were considered statistically significant using two-tailed student's t-test.

6.2.2. HIV-1 gp120 and MA additively increase oxidative stress in astrocytes.

Upon demonstrating that both MA and gp120 independently induced ROS in SVGA astrocytes; we examined whether MA and gp120 interact additively or synergistically to increase oxidative stress. We treated SVGA astrocytes with 500 μM MA and transfected with 2 μg of gp120-plasmid followed by measurement of ROS at 24 hours post-treatment. Clearly, astrocytes treated with both MA and gp120 showed ROS levels (107.1 ± 12.9 %) higher than either MA (41.8 ± 4.4 %) or gp120 alone (67.7 ± 11.0 %) (Fig. 36A). Furthermore, two-factor ANOVA model suggested an additive effect rather than synergistic (p=0.91). In order to confirm the finding in primary astrocyte culture, we used 2 nM recombinant gp120IIIB protein in combination with 500 μM MA. We observed similar results in terms of ROS production in primary human fetal astrocytes using flowcytometry (5.9 ± 2.5 % for MA; 24.3 ± 4.0 % for gp120 and 54.8 ± 13.1 % for MA+gp120)(Fig. 36B). Similarly, the fluorescence observed using microscopy was significantly higher when cells were treated with both gp120 and MA as compared to cells treated with either agent alone in SVGA astrocytes (Fig. 36C) and primary astrocytes (Fig. 36D).

Since oxidative stress is known to be associated with both cell death (Cohen & d'Arcy Doherty, 1987) and cell proliferation (Klaunig & Kamendulis, 2004), depending on the extent of the ROS production, we analyzed the functional consequences of MA and gp120 treatments in SVGA astrocytes. Clearly, the treatment with MA and gp120 significantly increased the level of terminal deoxynucleotidyltransferase-mediated dUTP-nick end labeling (TUNEL)-positive astrocytes when compared to MA or gp120 alone (Fig. 36E). In parallel experiments, we quantified the level of cell death induced by MA and/or gp120 using 3-(4,5-

Dimethylthiazol-2-yl)-2,5-diphenyltetrazolium bromide (MTT) assay and found that cells treated with gp120 and MA showed an additive effect and significantly higher ($p \leq 0.01$) cell death was observed (14.1 ± 2.9 %) when compared to either MA (6.8 ± 1.5 %) or gp120 (8.3 ± 1.8 %) alone (Fig 36F). These observations indicated that the oxidative stress induced by gp120 and/or MA was lethal to astrocytes and MA and gp120 additively increase the cellular toxicity.

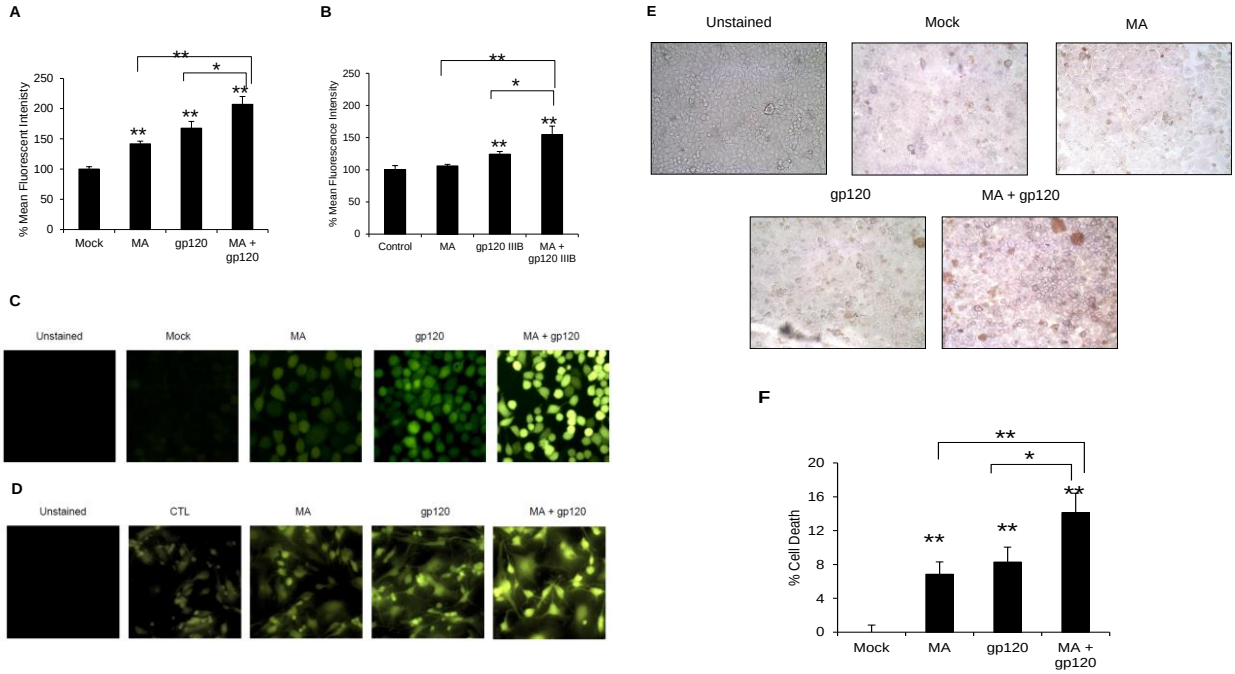

Figure 36: HIV-1 gp120 and MA additively increase oxidative stress in astrocytes. (A,C) SVGA astrocytes were seeded at 2.75 X 10^5 cells/well in 12-well plates and treated with or without 500 μM MA concomitantly with transfection mix containing 2 μg of gp120-plasmid for 24 hours. Mean fluorescence intensity was measured to quantify ROS production (A) and fluorescence was observed using fluorescent microscope (C). (B, D) Primary human fetal astrocytes were seeded at 1 X 106/well in 12-well plates and treated with either 2 nM gp120IIIB or 500 μM MA as well as both MA and gp120IIIB for 24 hours. The ROS production was quantified using flow cytometer (B) and fluorescence was observed using fluorescent microscope (D). SVGA astrocytes treated with MA and/or gp120 were stained for TUNEL (E) as shown with arrows or treated with MTT (F) to measure cell death. For MTT assay, cell viability in mock-transfected cells was considered as control and cell death was expressed as % death in control. The bars represent mean ± SE of at least 3 independent experiments with each treatment in triplicates. The p-value ≤ 0.01(**) were considered statistically significant using student's t-test and two-way ANOVA.

Since the combination of MA and gp120 showed increased oxidative stress, we sought to address the molecular mechanism responsible for these effects. First, we pre-treated SVGA cells with 100 μM vitamin C, a common antioxidant, followed by treatments with gp120 and MA. As expected, vitamin C alone reduced basal levels of ROS production. However, it also abolished the ROS generated by either MA or gp120 alone, as well as MA+gp120 (Fig. 37A). In addition, vitamin C also abrogated cell death caused by MA and gp120 alone and also in combination (Fig. 37B). Similarly, we also used vitamin E, another canonical ROS quencher to confirm our results with vitamin C. Surprisingly, TROLOX, a water soluble form of vitamin E, did not reduce ROS production (Fig. 37C). However, when we used vitamin E in its native form (α-tocopherol), it reduced ROS generated by MA or gp120 alone, as well as MA+gp120 (Fig. 37D). It also rescued the astrocytes from cell death (Fig. 37E). Although N-Acetyl cysteine (NAC) has been shown to abrogate gp120-mediated ROS production in astrocytes (Visalli et al., 2007), in our studies NAC did not show any reduction in ROS production (Fig. 37F). This observation is similar to our previous report, where we showed that NAC did not reduce alcohol-mediated ROS in astrocytes (Jin et al., 2013).

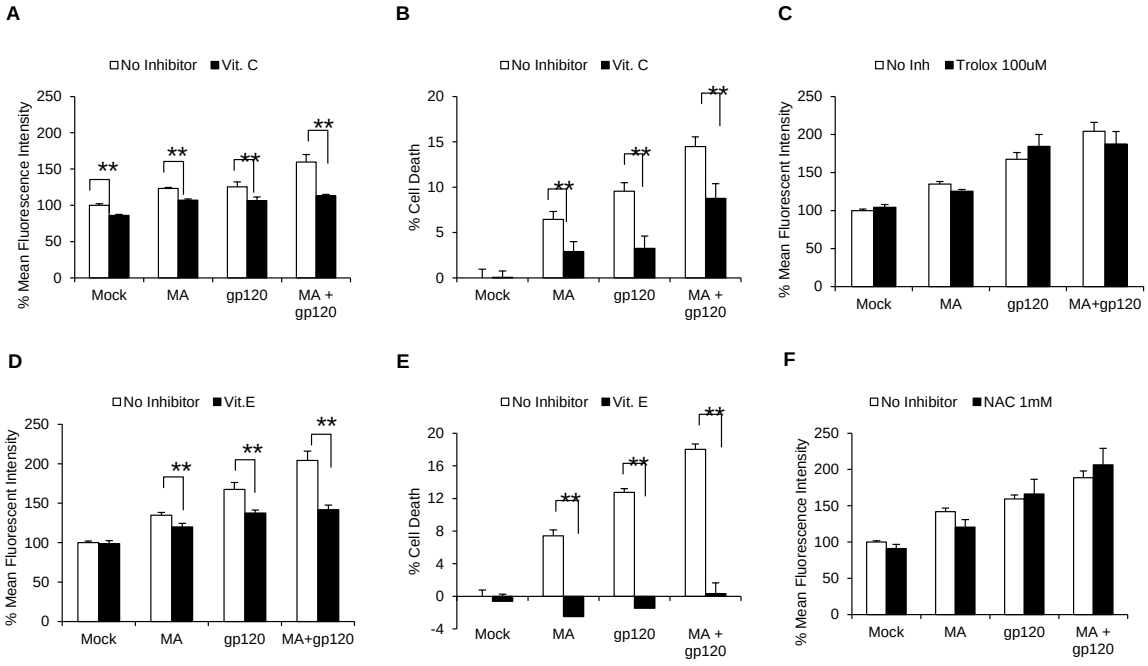

Figure 37: ROS quenchers reduced MA±gp120-induced oxidative stress and cell death. SVGA astrocytes were treated with or without vitamin C (vit. C) and vitamin E (vit. E) 1 hour prior to treatments with MA and/or gp120. ROS (A and D) was measured using flow cytometer 24 hours after the treatments and effect on cell death (B and E) was measured 48 hours after the treatments. C and F show the effect of TROLOX and NAC on the ROS production, respectively. The bars represent mean ± SE of at least 3 independent experiments with each treatment in triplicates. The p-value ≤ 0.05 (*) and ≤ 0.01 (*) were considered significant using two-tailed student's t-test and two-way ANOVA.

6.2.3. MA and gp120 induced the expression of cytochrome P450.

Since CYP has been shown to be involved in oxidative stress in many organs/tissues including the brain, we measured the mRNA expression levels of various CYPs in astrocytes treated with MA and/or gp120. Both MA and gp120 induced different isozymes of CYP at variable levels (Fig. 38A). Among the isozymes induced, CYP2E1 (1.7 ± 0.2 fold), CYP2D6 (2.3 ± 0.3 fold) and CYP2B6 (3.2 ± 03. Fold) clearly showed additive increases (two-way ANOVA showed p-value = 0.34 and 0.18 and 0.84, respectively suggesting absence of synergy) in the levels of mRNA expression with gp120+MA when compared to either MA (non-significant change for CYP2E1 and CYP2D6 and 2.8± 0.3 fold for CYP2B6) or gp120 (1.3 ± 0.1 fold for CYP2E1 and 1.8 ± 0.3 fold for CYP2D6 and non-significant for CYP2B6) alone (Fig. 38A). These results were further confirmed at the protein level for CYP2E1 (1.3 ± 0.1 fold for gp120 + MA), CYP2D6 (1.7 ± 0.2 fold for gp120 + MA) and CYP2B6 (1.4 ± 0.1 fold for gp120+MA) (Fig. 38B). Furthermore, in order to confirm that this phenomenon in primary astrocytes, HFA were treated with gp120 IIIB and/or MA and the protein and mRNA expression levels of the CYPs were measured. Similar to SVGA astrocytes, gp120 and MA also showed additive increase in the levels of CYP2E1, CYP2B6 and CYP2D6 mRNA (Fig. 39A) and protein (Fig. 39B) in HFA primary cells. The analysis run for synergy using two-way ANOVA showed non-significant p-values, suggesting no synergistic interaction.

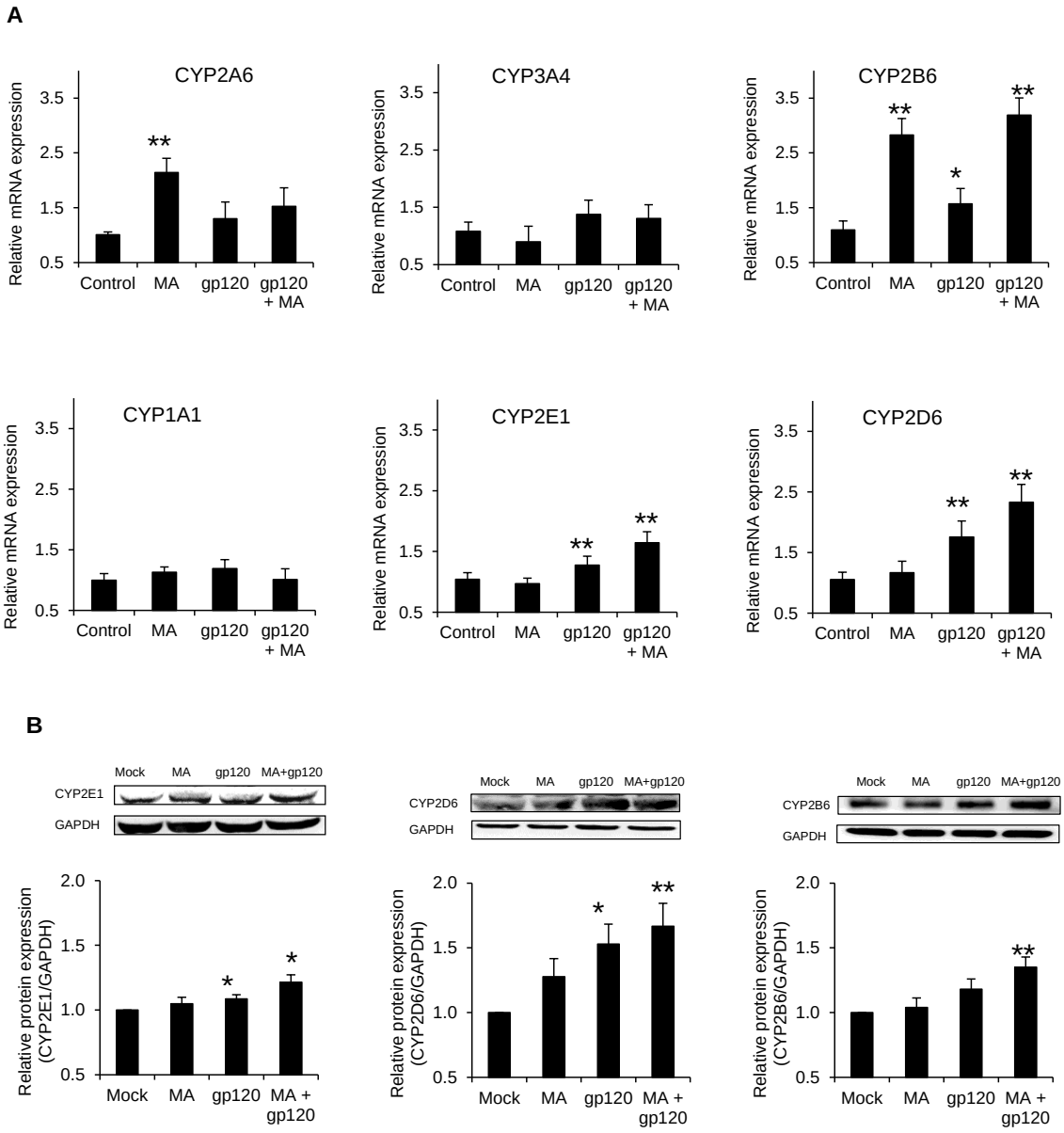

Figure 38: MA and gp120 induced the expression of various isozymes of cytochrome P450 in SVGA. (A-B) SVGA astrocytes were treated with or without 500 μM MA and transfected with gp120 for 6 hours post-transfection. Upon termination of the treatments, mRNA was isolated its expressions for various isozymes of CYP were measured (A) as described in Materials and Methods. Similarly, cells harvested 12 hours post-treatment protein was isolated and the levels of CYPs were measured using western blotting (B) with GAPDH used as housekeeping gene. (C-D) Primary human fetal astrocytes were treated with MA and/or gp120IIIB for 6 or 12 hours and expressions of CYPs were measured at the levels of mRNA (C) and protein (D), respectively. The p-value ≤ 0.05 (*) and ≤ 0.01(**) were considered statistically significant using two-tailed student's t-test and ANOVA.

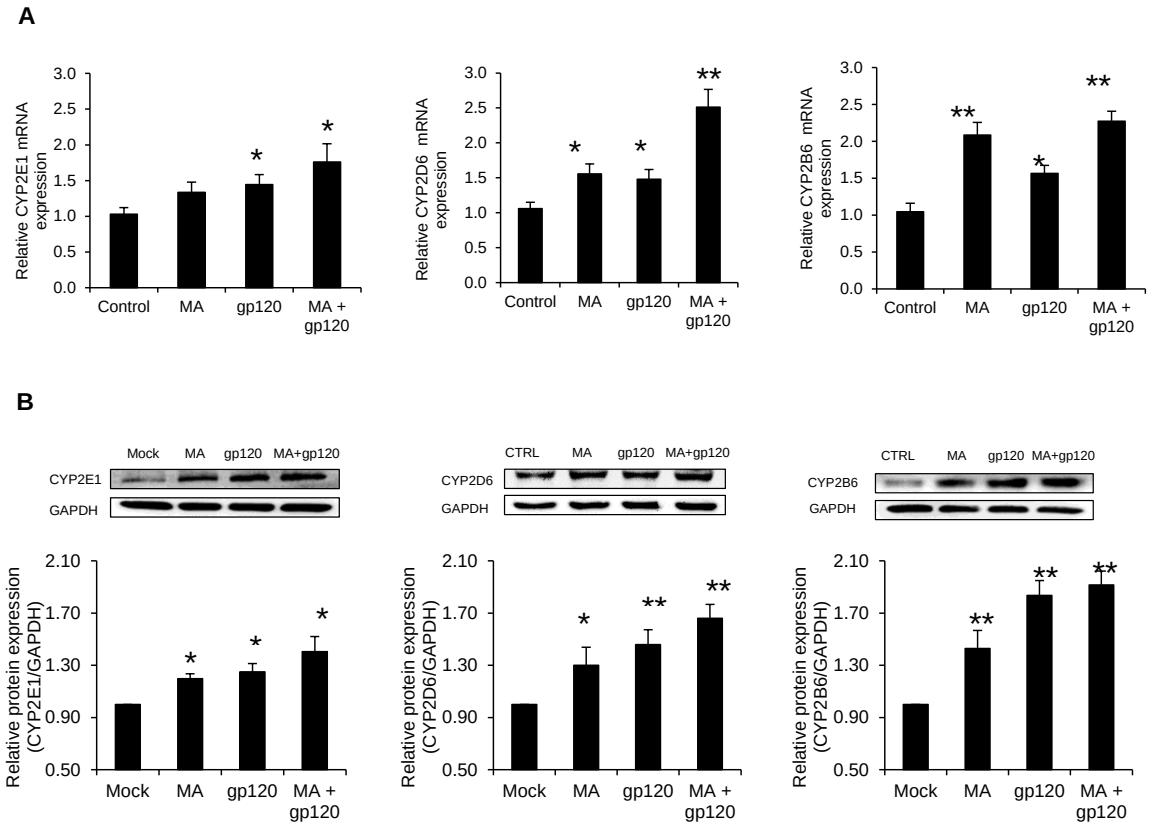

Figure 39: MA and gp120 induced the expression of various isozymes of cytochrome P450 in HFA. (A-B) Primary human fetal astrocytes were treated with MA and/or gp120IIIB for 6 or 12 hours and expressions of CYPs were measured at the levels of mRNA (A) and protein (B), respectively. The p-value ≤ 0.05 (*) and ≤ 0.01(**) were considered statistically significant using two-tailed student's t-test and ANOVA.

6.2.4. Role of CYP2E1 in gp120 and/or MA-mediated oxidative stress.

In order to examine the role of CYP2E1 in oxidative stress, we pre-treated astrocytes with different concentrations of diallylsulfide (DAS), a selective inhibitor of CYP2E1. Clearly, both 10 and 25 μM DAS reduced the ROS generated by either MA and/or gp120 (Fig. 40A). It is of note that DAS alone showed some decrease in the basal ROS production but its efficacy against MA and/or gp120-mediated oxidative stress was significant and dose-dependent (p for trend = 0.01). Although DAS did not significantly rescue the cell from death caused by MA alone, it significantly rescued the cell-death ($p \leq 0.01$) caused by gp120 alone and MA+gp120 (Fig. 40B). In parallel experiments, DAS was also found to reduce the TUNEL staining in the cells treated with MA and/or gp120 (Fig. 40C). Furthermore, we also specifically knocked-down CYP2E1 using siRNA in order to confirm our findings with chemical inhibitor. As expected, the knock-down of CYP2E1 resulted into reduction of ROS (Fig. 40D) and it also showed reduced TUNEL staining in the cells treated with MA and/or gp120 (Fig. 40E). The specific knockdown of CYP2E1 was confirmed using western blotting, which showed 75-80% knock-down of CYP2E1 (Fig. 40D). These results clearly suggest the involvement of CYP2E1 in oxidative stress and cell death induced by gp120, MA or both. We also tested fluoxetine and paroxetine, specific inhibitors for CYP2D6, and orphenadrine (OP), specific inhibitor for CYP2B6, on MA+gp120-mediated ROS generation. However, these antagonists failed to reduce the ROS formation, rather paroxetine and OP further increased oxidative stress (Fig. 41A-C). In addition, we also specifically knocked-down CYP2B6 and CYP2D6 using siRNA. However, as observed with chemical inhibitors, these siRNA did not show any effect on ROS production (Fig. 42A-B). Although, oxidative stress is one of the functional consequences of cytochrome P450 enzyme activity, the

possible role of CYP2D6 and CYP2B6 in other physiological functions cannot be disregarded.

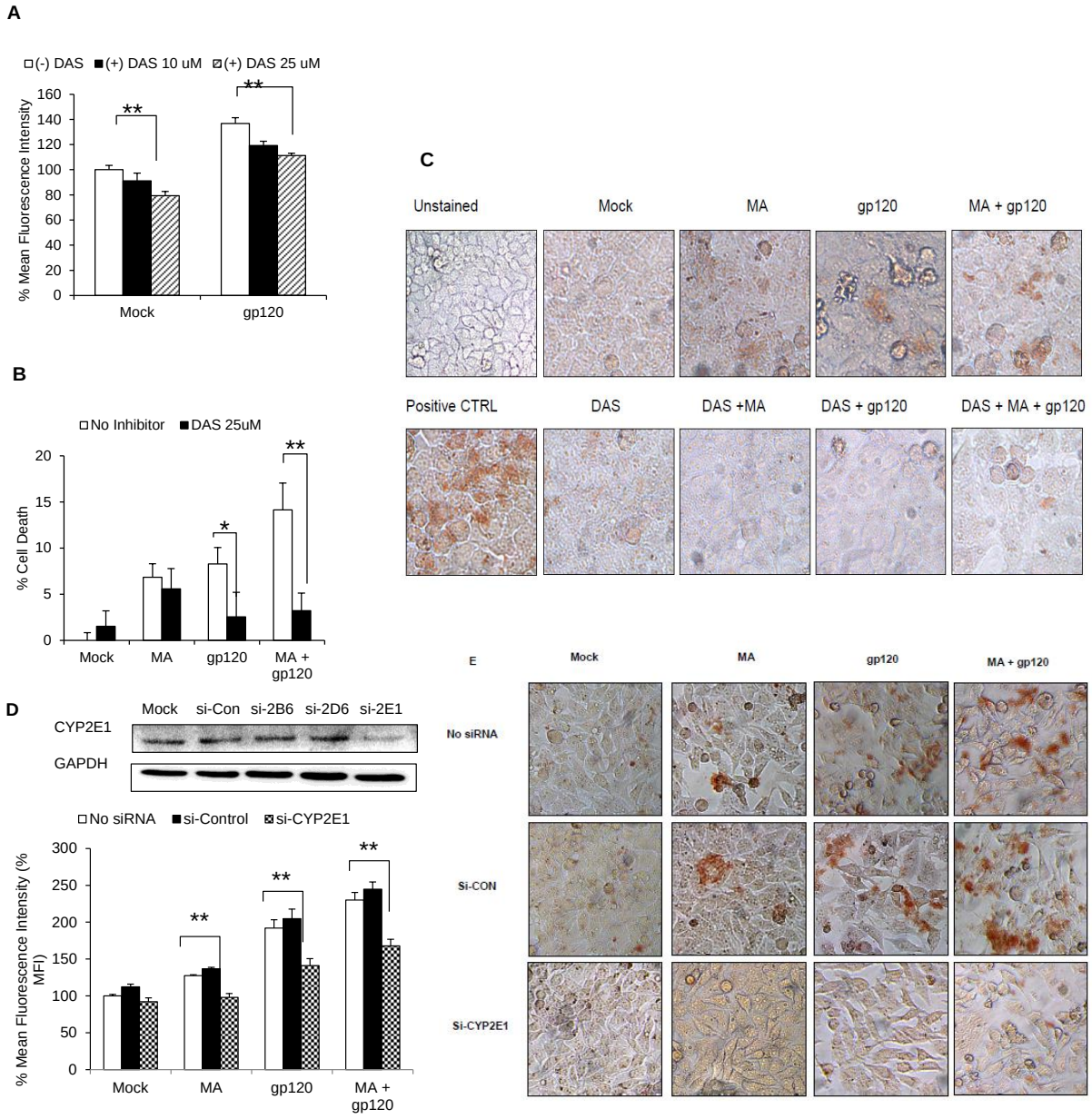

Figure 40: CYP2E1 played an important role in oxidative stress. (A-C) The effect of DAS, a selective CYP2E1 inhibitor, on ROS production (A), cell death (B) and TUNEL labeling (C) in astrocytes treated with MA and/or gp120. (D-E) The effect of siRNA-mediated knockdown of CYP2E1 on ROS (D) and TUNEL labeling (E) in MA and/or gp120 treated SVGA astrocytes. The ROS production and cell death were compared with untreated control that was normalized at 100%. Bar graphs show mean of at least 3 independent experiments. The blot is representative of 3 independent experiments. GAPDH was used to normalize the expressions of CYPs. The bars represent mean ± SE of at least 3 independent experiments with each treatment in triplicates. The p-value ≤ 0.05 (*) and ≤ 0.01(**) were considered statistically significant using two-tailed student's t-test and ANOVA.

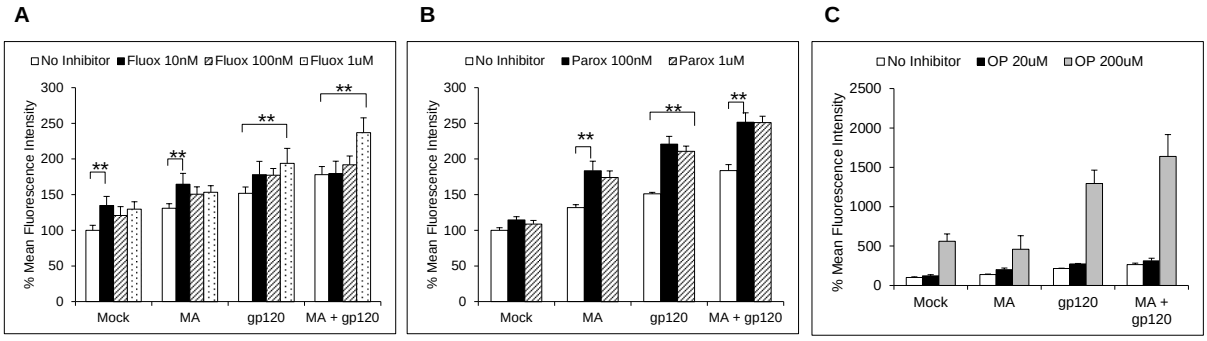

Figure 41: The inhibitors for CYP2B6 and CYP2D6 did not reduce the ROS production via MA and/or gp120. SVGA astrocytes were treated with or without the inhibitor 1 hour prior to treatments with MA and/or gp120. The effect of CYP2D6 inhibitors, fluoxetine (A) and paroxetine (B) and CYP2B6 inhibitor, Orphenadrine (OP) (C), on ROS production by MA and/or gp120. The higher doses of the respective inhibitors significantly increased ROS production. The ROS production and cell death were compared with untreated control that was normalized at 100%. The bars represent mean ± SE of 2 independent experiments with each treatment in triplicates. The p-value ≤ 0.05 (*) and ≤ 0.01(**) were considered statistically significant using two-tailed student's t-test and multiple ANOVA.

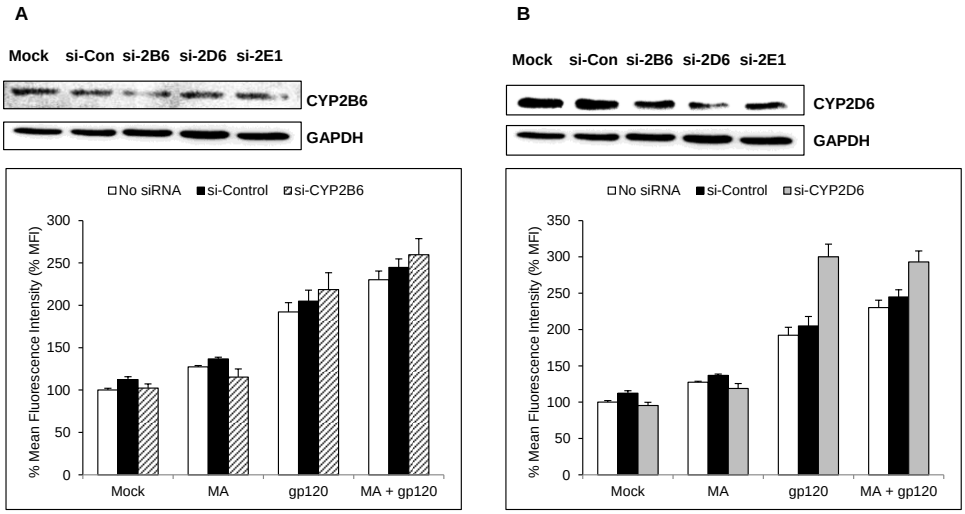

Figure 42: The siRNA against CYP2B6 and CYP2D6 did not reduce the ROS production via MA and/or gp120. SVGA astrocytes were transfected with 20 pmole CYP2B6 or CYP2D6 siRNA for 48 hours. The cells were then reseeded for optimal confluence and treated with MA and/or gp120. The effect of CYP2B6 (A) and CYP2D6 (B) knockdown on ROS production was measured. The specificity of siRNA on gene knockdown was confirmed with western blotting (insets). ROS production was compared with control that was normalized at 100%. Scrambled sequence of siRNA, an internal control, showed no effect on gene knockdown or ROS production. The bars represent mean ± SE of 3 independent experiments with each treatment in triplicates.

6.2.5. NADPH oxidase and metal chelation are involved in MA/gp120-mediated oxidative stress and cell death.

The NOX family NADPH oxidase enzymes are responsible for the transfer of electrons across biological membranes and generation of ROS (Bedard & Krause, 2007). In addition, various NOX also serve as essential co-enzymes coupled with CYP2E1-mediated electron transfer in the generation of ROS (Haorah et al., 2008). In order to examine the involvement of NOX in gp120±MA-mediated oxidative stress, we treated the SVGA astrocytes with various concentrations of DPI, an inhibitor for NADPH oxidase. DPI significantly reduced the ROS production observed with either MA or gp120 alone and MA+gp120 (Fig. 43A) in dose dependent manner (p for trend = 0.01). Furthermore, 25nM DPI rescued the cell death induced by MA and/or gp120 (Fig. 43B), thereby confirming the role of NADPH oxidase in MA/gp120-mediated cell toxicity. Among the NOX family of enzymes, NOX2 and NOX4 isozymes are predominantly responsible for NOX-derived ROS in astrocytes (Abramov et al., 2005; Pawate, Shen, Fan, & Bhat, 2004). Therefore, we knocked-down NOX2 and NOX4 using siRNA, which also abrogated the ROS produced by MA and gp120, either alone or in combination (MA±gp120) (Fig. 43C-D). Furthermore, control-siRNA transfected cells did not show any significant change in the ROS production, when compared with no-siRNA control for the respective treatment groups ($p > 0.3$ when measured using two-way ANOVA).

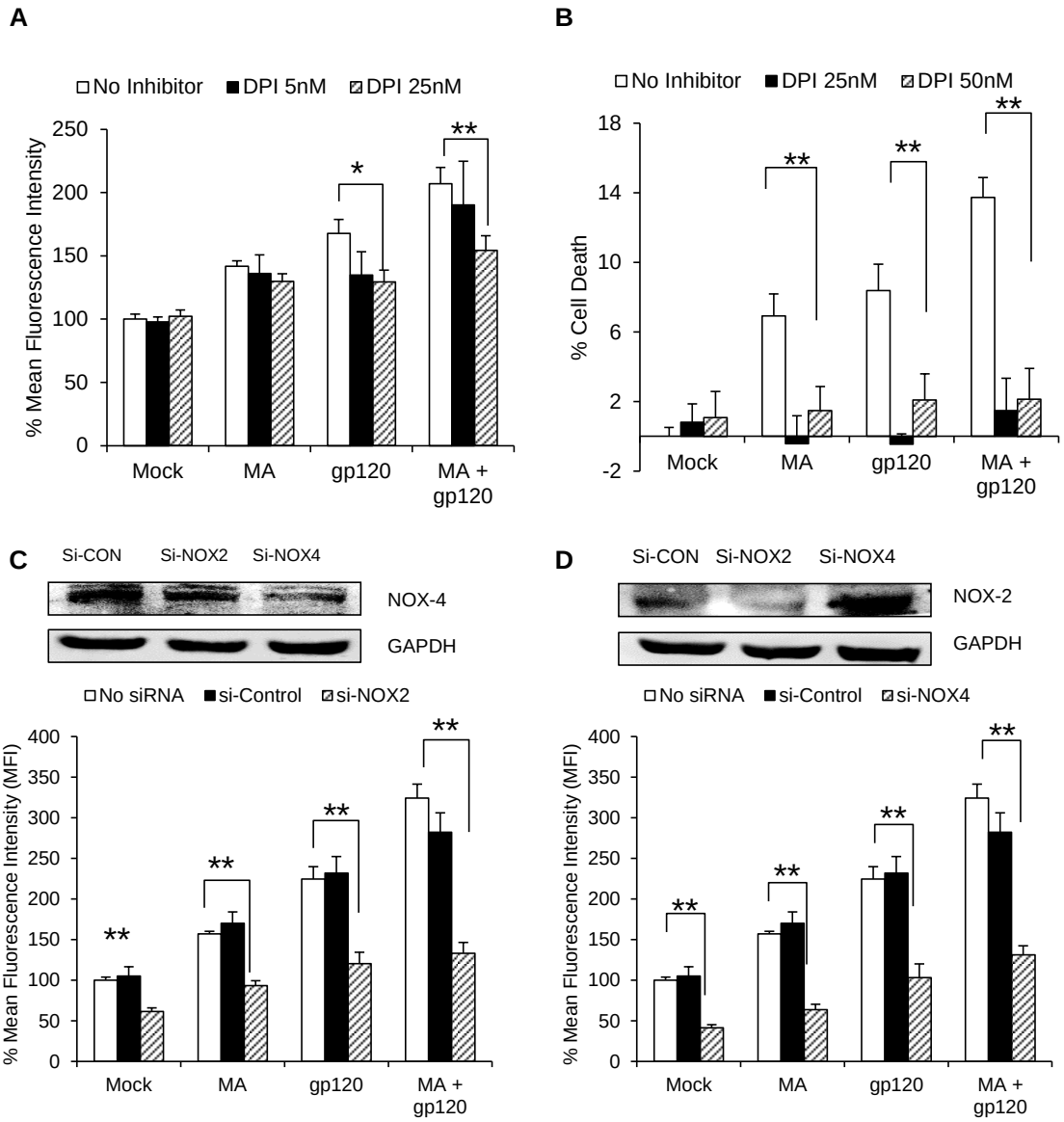

Figure 43: Role of NADPH oxidase in MA and/or gp120-induced oxidative stress and cell death. (A-B) SVGA cells were treated with DPI, a selective inhibitor for NADPH oxidase, at various concentrations 1 hour prior to the treatments with MA and/or gp120 and the effect was observed on ROS production (A) and cell death (B). (C-D) Astrocytes were transfected with 10nM siRNA targeting either NOX2 or NOX4 subunit of NOX family for 48 hours. These cells were further treated with MA and/or gp120. The effect of gene knock-down on ROS production was measured for NOX2 (C) and NOX4 (D). The gene knockdown was confirmed using western-blotting for the efficiency of each siRNA. The cells transfected with 10 nM of control siRNA was used as control, which showed no significant change in ROS production. The bars represent mean ± SE of at least 3 independent experiments with each treatment in triplicates (except DPI 5nM in Aand DPI 25nM in B). The p-value ≤ 0.05 (*) and ≤ 0.01(**) were considered statistically two-tailed significant using student's t-test and multiple ANOVA.

Superoxides ($O_2^{\cdot-}$) generated via NOX are converted into H_2O_2, which is further converted into tertiary effector species such as hydroxyl radical (·OH) via the Fenton-Weiss-Haber (FWH) reaction (Fridovich, 1989; van Golen, van Gulik, & Heger, 2012). We therefore hypothesized that FWH reaction is a downstream mechanism of NOX-mediated ROS production. Since increased expression of ferritin is an indicator of oxidative stress (Friedman, Arosio, Finazzi, Koziorowski, & Galazka-Friedman, 2011), we measured the expression of ferritin heavy chain in the cells treated with MA and/or gp120. We observed higher ferritin expressions in astrocytes treated with MA and/or gp120 than untreated controls (Fig. 44A), which suggested involvement of $Fe^{+2} \leftrightarrow Fe^{+3}$ cycle. Therefore, we treated astrocytes with various concentrations of deferoxamine (DFO), an inhibitor of FWH reaction, 1 hour prior to the treatments with either MA or gp120 alone and MA+gp120. Among various doses used, 50 nM DFO was found to reduce the ROS generated by gp120 alone as well as gp120 + MA (Fig. 44B). Furthermore, 50 nM DFO also rescued the astrocytes from cell death induced by oxidative stress (Fig. 44C). The involvement of iron cycle can also lead to increased protein carbonylation, which can further lead to apoptotic cell death (Cattaruzza & Hecker, 2008; Suzuki, Carini, & Butterfield, 2010). Therefore, we measured the levels of carbonylated protein in the astrocytes treated with MA and/or gp120. As expected, we observed increased levels of protein carbonylation (Fig. 44D) upon treatments. Overall, these data suggested that NOX2 and NOX4 produced superoxides, which further underwent FWH chemistry to produce peroxides, leading to increased protein carbonylation. Together these resulted into increased oxidative stress and consequently cell death.

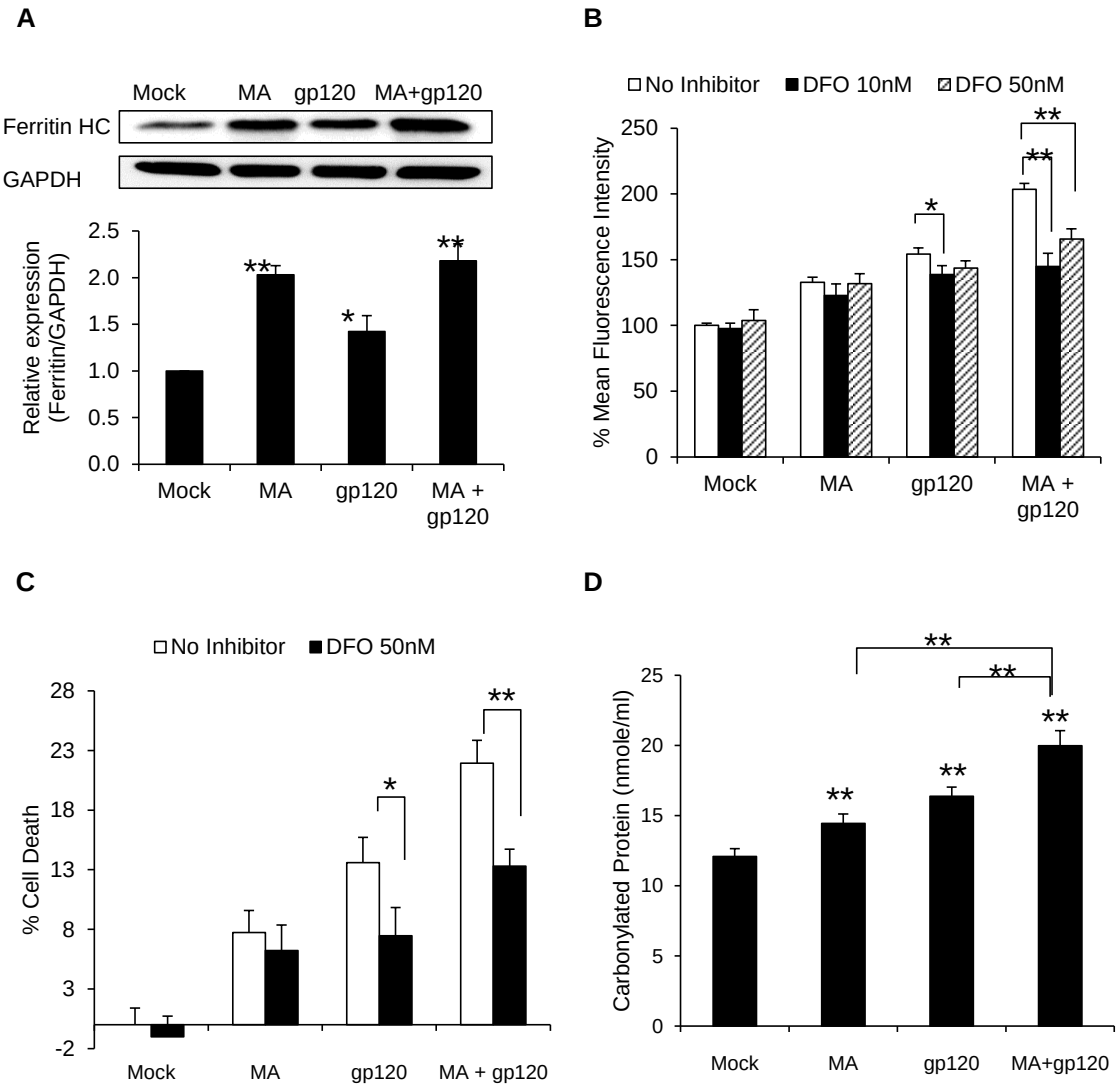

Figure 44: The expression of ferritin and role of FWH chemistry in MA and/or gp120-mediated oxidative stress and cell death. SVGA astrocytes were treated with MA and/or gp120 and the expressions of ferritin heavy chain (Ferritin HC) were measured using western blotting (A) and representative image is shown. Cells were treated with varying concentrations of DFO, an iron chelator used as FWH reaction antagonist, for 1 hour prior to treatments with MA and/or gp120 and the effect was observed on ROS (B) and cell death (C). (D) shows the amount of carbonylated proteins after 24 hours as a result of treatment with MA and/or gp120. The ROS production and cell death were compared with untreated control that was normalized at 100%. The bars represent mean ± SE of at least 3 independent experiments with each treatment in triplicates. The p-value ≤ 0.05 (*) and ≤ 0.01(**) were considered statistically significant using two-tailed student's t-test and multiple ANOVA.

6.2.6. Caspase-3 is involved in MA- and/or gp120-mediated apoptosis in astrocytes.

Involvement of caspase-3 is a classical mechanism of apoptosis in a variety of cells. We therefore examined the effect of MA and/or gp120 on caspase-3 protein expression and activity. Our results show increased protein expressions of caspase-3 when astrocytes were treated with MA and/or gp120. The immunoblots showed significantly increased expression of cleaved caspase-3 (17 kDa) in the cells treated with MA, gp120 and MA+gp120. However, pro-caspase-3 isoform (35 kDa) was slightly reduced in the cells treated with gp120+MA (Fig. 45A). Furthermore, astrocytes treated with either MA or gp120 alone showed increased caspase-3 cleavage activity as compared to untreated cells. In addition, cells treated with gp120 and MA showed significantly higher ($p \leq 0.01$) caspase-3 cleavage activity as compared to either of the agents alone and the effect was found to be additive (Fig. 45B). Furthermore, the inhibitors for ROS (Fig. 45C), CYP2E1 (Fig. 45D), NADPH oxidase (Fig. 45E), and FWH reaction (Fig. 45F) significantly reduced MA/gp120-mediated caspase-3 activity. These findings clearly suggested that pathways involving CYP2E1, NOX family of NADPH oxidase, and FWH reaction are responsible for MA- and/or gp120-mediated apoptosis in SVGA astrocytes.

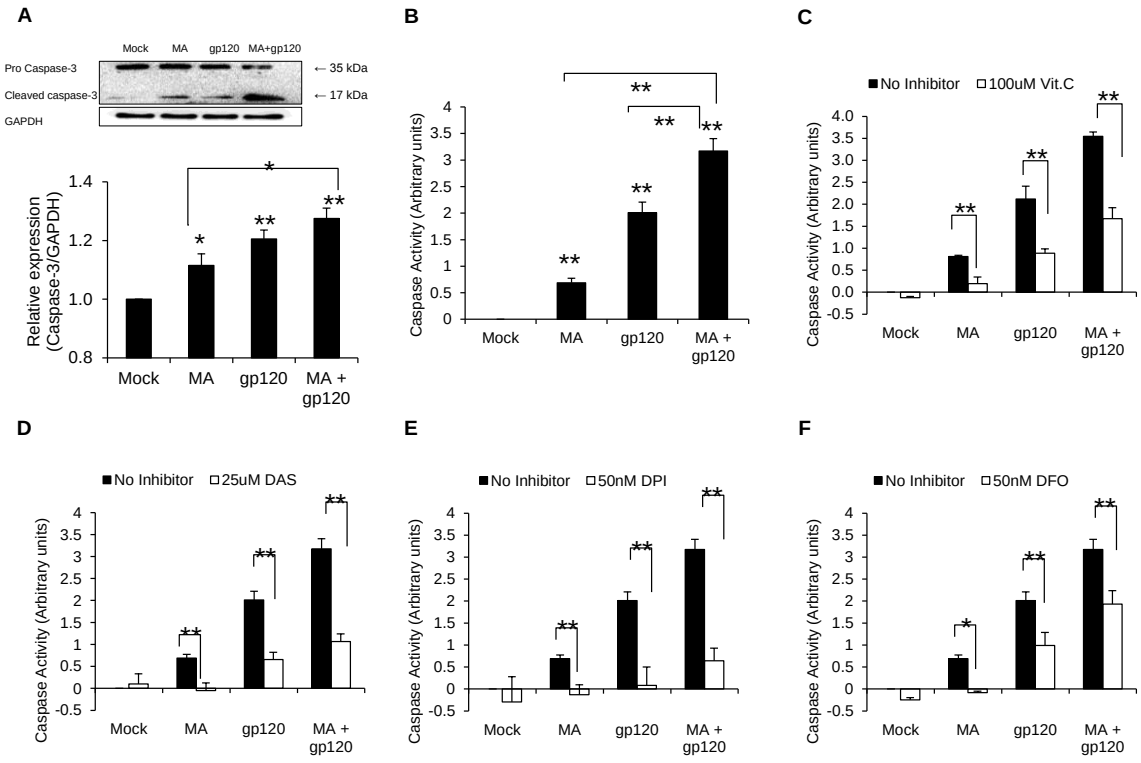

Figure 45: Caspase-3 activation is involved in the MA and/or gp120-mediated apoptosis in astrocytes. (A-B) SVGA cells were treated with MA and/or gp120 for 24 hours and the cytoplasmic proteins were obtained, which were used to measure pro-caspase-3 (35 kDa) and cleaved caspase-3 (17 kDa) protein expressions (A) and caspase-3 cleavage activity (B). The cells were also treated with either 100 μM vitamin C (C), 25 μM DAS (D), 50 nM DPI (E) or 50 nM DFO (F) 1 hour prior to the treatments with MA and/or gp120 and the effect on caspase-3 cleavage activity was measured. The activity was normalized with basal levels in untreated control and reported as change in the activity. The bars represent mean ± SE of 3 independent experiments with each treatment in triplicates. The p-value ≤ 0.05 (*) and ≤ 0.01(**) were considered statistically significant using two-tailed student's t-test and multiple ANOVA. The significant values shown above the bars were calculated using student's t-test for comparison between the treatment and mock transfected control.

6.3. Discussion:

Substance abuse such as MA is thought to be an additional risk factor in worsening the HIV-associated neurodegeneration (Silverstein et al., 2012). Viral proteins such as gp120 and Tat have been shown to interplay co-operatively with MA and damage BBB integrity in mouse brain (Banerjee et al., 2010). Additionally, MA alone is also known to induce behavioral impairment in gp120 transgenic mice (Henry et al., 2013). However, there is no direct evidence that elucidates the mechanism responsible for the combined effect of MA- and gp120-induced toxicities in the brain. We have recently shown that MA and gp120 can induce pro-inflammatory cytokine IL-6 via common signaling mechanism involving PI3K/Akt and NF-κB pathways (Shah et al., 2012; Shah, Verma, et al., 2011). On the other hand, an increasing body of literatures clearly suggests oxidative stress as one of the mediators of neurotoxicity induced by HIV-1 gp120 as well as MA independently. However, no attempt has been made to determine the role of oxidative stress in a possible situation where HIV-infected individuals were methamphetamine users as well. This study was undertaken with the idea of determining whether gp120 and MA-mediated oxidative stress would cause increased apoptosis in astrocytes and whether CYP450 has any role in oxidative stress.

Oxidative stress is associated with cell toxicity in various neurodegenerative disorders such as AD and PD (Dasuri et al., 2013). In addition, several reports have highlighted the role of oxidative stress in the pathology of HIV associated neurocognitive disorders (HAND) (Mollace et al., 2001). This was further confirmed by our studies with morphine wherein we showed morphine-mediated increased virus replication (Kumar et al., 2004), accelerated disease progression (Kumar et al., 2006) and increased oxidative stress (Perez-Casanova,

Husain, Noel, Rivera-Amill, & Kumar, 2008; Perez-Casanova, Noel, Rivera-Amill, Husain, & Kumar, 2007) in macaque model of HIV/AIDS. The oxidative stress produced by either MA or gp120 has also been shown to have neurotoxic potential via various intermediates. MA, in particular, is found to increase oxidative stress predominantly via dopaminergic and glutamatergic mechanisms (Silverstein et al., 2011). The dopaminergic toxicity observed with MA is attributed to its structural similarity with dopamine. Furthermore, gp120 is shown to increase oxidative stress via glutathione and lipid peroxidation (Louboutin & Strayer, 2012; Ronaldson & Bendayan, 2008). Concurrent with the existing literatures, we also observed increased oxidative stress in astrocytes treated with gp120 and MA individually, in time- and concentration-dependent manners.

Recently dopamine has been shown to regulate the expression of various CYP isozymes in the liver (Wojcikowski & Daniel, 2009). Furthermore, Bromek et al. has shown that CYP2D increases dopamine formation in the brain (Bromek et al., 2011). In addition to the metabolism of xenobiotics including substances of abuse, the role of CYPs in oxidative stress is unequivocally accepted in various tissues/organs including the brain (Hedlund, Gustafsson, & Warner, 2001). Specifically, the roles of CYP2E1 for alcohol metabolism-mediated toxicity and CYP2A6 (Jin et al., 2013) for tobacco/nicotine metabolism-mediated toxicity (Ande et al., 2012) have been implicated through the oxidative stress pathway in many tissues/organs. Our group along with others has previously reported that astrocytes also express many CYPs at variable levels, and they have demonstrated the role of CYPs in alcohol- and nicotine-mediated oxidative stress and toxicities (Ande et al., 2012; Meyer, Gehlhaus, Knoth, & Volk, 2007). Similarly, MA has been shown to induce mRNA expression of CYP2E1 and activity of CYP2C6 in rats (Dostalek et al., 2007; Takimoto,

Ujike, Nakamura, & Iwahashi, 2002). Our observations with regard to increased expressions of CYP2A6, 2B6, and 2D6 by MA and CYP2E1, 2B6, and 2D6 by gp120 are important to elucidate the roles of these CYPs in oxidative stress, metabolism of certain xenobiotics, and homeostasis of other resident molecules such as dopamine in the brain. More importantly, the additive increase in the expressions of CYP2D6 and CYP2E1 by gp120+MA is intriguing, which suggests a possibility for that CYPs might have been involved in oxidative stress. This is the first evidence that shows an additive effect between MA or gp120 and CYP expression in central nervous system.

Amphetamine analogues including MA are known to interact with CYP2D6 and alters its activity (D. Wu, Otton, Inaba, Kalow, & Sellers, 1997), which is further supported by the finding that selective inhibitors of CYP2D6 reduces the metabolism of ecstacy (methamphetamine analog) in-vitro (Ramamoorthy et al., 2002). However, the role of CYP2E1 in the metabolism of MA is largely unknown, except a few recent reports that have shown an involvement of CYP2E1 and CYP2B in the metabolism of either MA or pyrolysis product of MA (Sanga et al., 2006; Valoti et al., 2000). CYP2E1 is mainly known for the metabolic activity in presence of ethanol; however, it's involvement in MA-mediated production of ROS leading to increased cell death is not known. We are able to confirm involvement of CYP2E1 in oxidative stress because DAS, a selective inhibitor for CYP2E1, significantly abrogated not only gp120/MA-mediated production of ROS but also cell death caused by these two stimulants individually or in combination. Unlike CYP2E1 inhibitor, the CYP2D6 and CYP2B6 inhibitors increased MA/gp120-induced ROS suggesting lack of its role in MA/gp120-mediated oxidative stress. The increased oxidative stress by CYP2D6

inhibitors has been observed before and has been attributed to the direct effect of these inhibitors (C. S. Lee, Kim, Jang, Kim, & Myung, 2010)

The interaction of various CYPs with NADPH system is tightly regulated by NADPH oxidase enzymes (Eid et al., 2009). CYP2E1 is specifically involved in the metabolism of R-OH compounds into aldehydes, which is coupled with the conversion of NADPH to $NADP^+$ and the released electron is consumed in the process. This $NADP^+$ is converted via non-CYP mechanism into NADPH, which is recycled back to NADPH by NOX family of NADPH oxidase (Fig. 46). The NOX family, particularly NOX2 and NOX4, is potentially known to increase ROS in astrocytes independently as well as in association with FWH chemistry (Bedard & Krause, 2007; van Golen et al., 2012). Furthermore, the superoxides and peroxides generated via NOX enzymes can result into increased expressions of ferritin and protein carbonylation (Cattaruzza & Hecker, 2008) as shown in this study as well. The role of NOX in substance abuse such as alcohol (X. Wang et al., 2012) and methamphetamine (M. J. Park et al., 2006) is known in neuronal toxicity. Furthermore, the NOX enzymes have been implicated in therapeutic intervention of CNS disorders such as strokes and Alzheimer's disease (Cairns, Kim, Tang, & Yenari, 2012; Sorce, Krause, & Jaquet, 2012). Our observations with NOX2 and NOX4 knockdown to rescue cells from oxidative damage support the possibility of using NOX as a target for developing potential therapeutics for the treatment of neuroAIDS, especially among MA users.

Various free radicals, generated during oxidative stress may lead to multifactorial physiological effects in the cells via DNA-damage, lipid-peroxidation or activation of apoptotic mechanisms. The ROS-mediated BBB damage has been shown to cause lipid peroxidation and loss of tight junction protein (Banerjee et al., 2010; M. Park et al., 2012).

MA and gp120 in combination are specifically shown to alter the levels of tight junction proteins to create a "leaky" BBB, which may enhance the invasion of infected monocytes into the brain (Banerjee et al., 2010). Similarly, cocaine in association with gp120 has also been shown to increase ROS, which involves caspase-3 and NF-κB activation to induce apoptosis in astrocytes (Yao et al., 2009). In our prior studies we have shown an overlapping mechanism between MA and gp120 involving NF-κB activation (Shah et al., 2012). We have further shown the induction of pro-inflammatory cytokines as a result of NF-κB activation. In the present study, we observed an increase in the expression of cleaved caspase-3 protein in MA and/or gp120, which were further confirmed with increased in caspase-3 cleavage activity. Our results are consistent with the recent finding that apoptosis is involved in gp120-mediated toxicity (Hu et al., 2009; Visalli et al., 2007). Furthermore, caspase-3 cleavage activity was inhibited by selective inhibitors for CYP2E1, NADPH oxidase, and FWH reaction. Together these findings suggest that increase in caspase-3 expression and activity via ROS and cytokines via NF-κB activation may lead to toxicity in astrocytes. Thus, there is a possibility of a cross-talk between these two mechanisms and therefore further studies are needed to investigate the effect of CYP-mediated ROS on cytokine production or vice-versa. Our TUNEL staining was also consistent with this notion since both MA and gp120 independently as well as in combination led to increased DNA damage. Our observations with MTT assay further confirmed the toxic consequences of ROS production as a result of MA/gp120 interaction. Additionally, inhibitors for CYP2E1, NADPH oxidase, and FWH reaction abolished caspase-3 activity and apoptotic cell death, which clearly suggested that ROS, induced by gp120/MA interaction, was responsible for the apoptotic cell death.

In summary, results from our present study indicate that in the astrocytes, MA potentiates the gp120-mediated oxidative stress that may worsen the neurodegenerative complications in HIV-infected MA users. The involvement of CYP2E1 in interaction between gp120 and MA present a novel opportunity to explore their further roles in neurotoxicity. Furthermore, it provides an opportunity to use this pathway as a target to find potentially novel pharmaceuticals. Specific inhibitors such as DAS, which is also a food additive (Jin et al., 2013), may potentially be used as food supplements/drugs in HIV-infected MA users to reduce neurotoxicity. The oxidative stress-mediated increased toxicity by MA/gp120 in astrocytic cells also provides an opportunity to potentially use anti-oxidants in reducing MA-mediated HIV-1 pathogenesis in the patients who abuse MA. Finally, since peptide inhibitors against NADPH oxidase have been shown to be protective in animal models, these inhibitors may potentially be used to reduce MA-induced HIV-1 pathogenesis in the humans.

6.4. Acknowledgement:

The figures and text in chapter 6 were originally published in Cell death and disease 2013 by Shah et. al. The author of the dissertation was the first author of the published work.

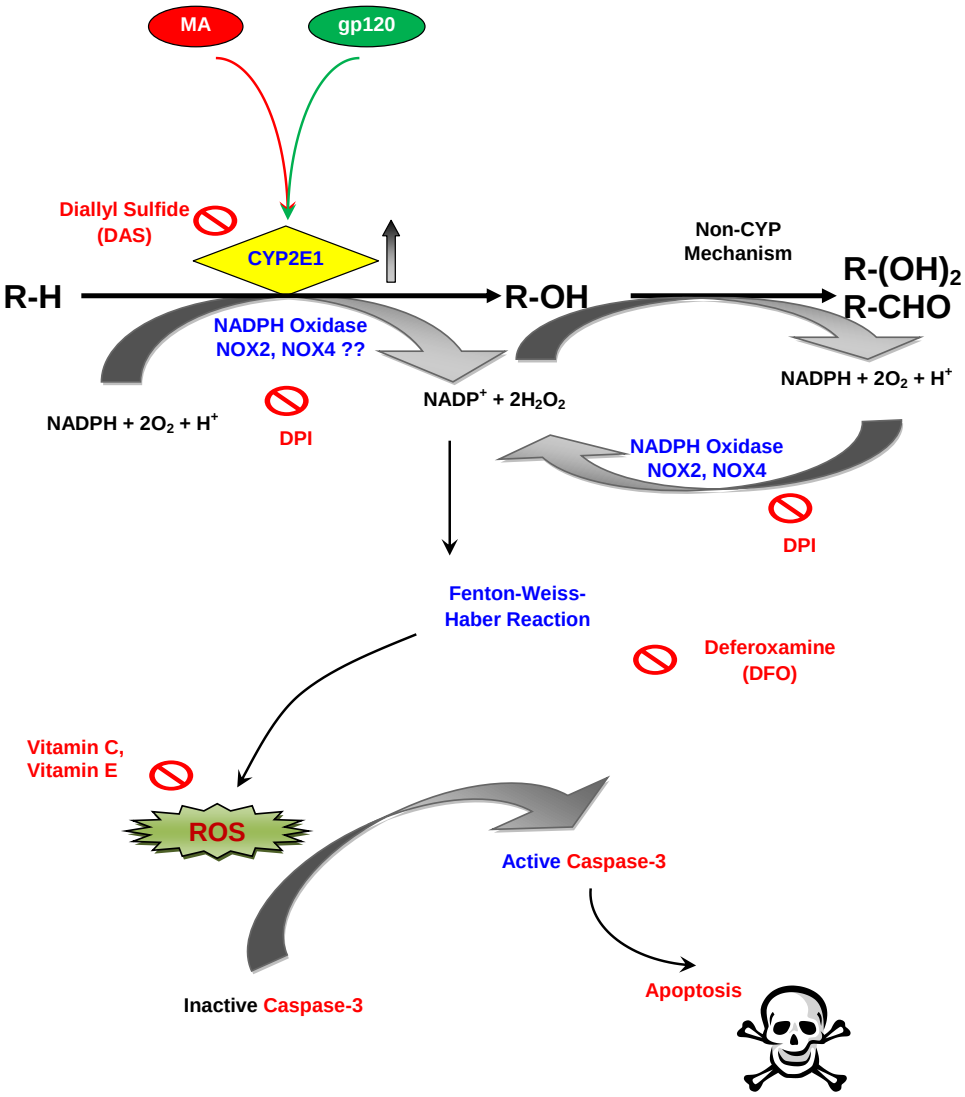

Figure 46: Schematic illustration of MA and/or gp120-mediated oxidative stress. MA and/or gp120 increase the expressions of CYP2E1, which generates free electrons via conversion of NADPH to NADP+. The CYP2E1 reaction cycle produces ROS as a result of uncoupling of the reaction. In addition, the NADP+ generated during this process is recycled via NADPH oxidase to produce superoxides and peroxides. The superoxides can further generate peroxides through Fenton chemistry. The ROS generated via this mechanism increases the caspase-3 activity, which then induces DNA fragmentation ultimately leading to apoptosis in astrocytes. The combination of MA and gp120 thus exacerbates the toxicity through common molecular mechanism(s). R-H represents MA or physiological substrates, such as dopamine. R-H may be oxidized to R-OH, which may further be oxidized to R-(OH)2 or R-CHO.

CHAPTER-7

FUTURE DIRECTIONS

The neuroinflammation is an extremely broad field to explore and a lot of work is needed in order to comprehensively understand the mechanisms underlying the pathology associated with neuroinflammation. The role of gp120 in oxidative stress and cytotoxicity strongly suggest its role in the cellular toxicity in the brain. However, our study might prove to be tip of the iceberg in the field of neuroAIDS. Evidently, several reports are emerging that suggest an intricate cooperation between the cell death mechanisms and cell survival mechanisms. Autophagy for instance is an intracellular repair mechanism that degrades the damaged organelles and also serves as a means of immune function to destroy intracellular pathogens. The role of gp120 in the autophagy is largely unknown. In the future, the complex interaction between the oxidative stress and autophagy would be an important aspect to study the mechanistic explanation of the gp120-mediated cytotoxicity. Furthermore, protein mis-folding is known to be associated with the cell death and the ER-stress is closely associated with the oxidative stress in the normal physiology. Therefore, a study in the direction of the triad comprised of oxidative stress, ER-stress and autophagy can be undertaken to move one step forward in the current understanding.

In the current era, transgenic animal model is considered as an important tool to understand the pathophysiology of the disease. Such a transgenic model for gp120 can provide vital information in the current understanding of the gp120-mediated neurotoxicity. Therefore, in future studies inclusion of gp120-transgenic mice would be a key approach.

Our study with the role of CYP enzymes in the gp120-and MA-mediated oxidative stress has opened a new horizon towards the possibility of CYP-mediated toxicity. The fact

that gp120 can alter the expression levels of CYP enzymes clearly indicates a possible role in drug-drug interaction and alteration in the drug metabolism in the brain cells. In future, a study in the HIV-infected population with or without methamphetamine abuse may provide new perspectives towards the understanding of patient responsiveness to the HAART therapy.

APPENDIX

SPRINGER LICENSE
TERMS AND CONDITIONS

Sep 24, 2013

This is a License Agreement between ANKIT SHAH ("You") and Springer ("Springer") provided by Copyright Clearance Center ("CCC"). The license consists of your order details, the terms and conditions provided by Springer, and the payment terms and conditions.

All payments must be made in full to CCC. For payment instructions, please see information listed at the bottom of this form.

License Number	3230910598246
License date	Sep 16, 2013
Licensed content publisher	Springer
Licensed content publication	Journal of NeuroVirology
Licensed content title	Methamphetamine toxicity and its implications during HIV-1 infection
Licensed content author	Peter S. Silverstein
Licensed content date	Jan 1, 2011
Volume number	17
Issue number	5
Type of Use	Thesis/Dissertation
Portion	Full text
Number of copies	1
Author of this Springer article	Yes and you are a contributor of the new work
Order reference number	
Title of your thesis / dissertation	HIV-1 gp120 and methamphetamine: implications in neuroAIDS
Expected completion date	Jan 2014
Estimated size(pages)	120
Total	0.00 USD

ELSEVIER LICENSE
TERMS AND CONDITIONS

Sep 24, 2013

This is a License Agreement between ANKIT SHAH ("You") and Elsevier ("Elsevier") provided by Copyright Clearance Center ("CCC"). The license consists of your order details, the terms and conditions provided by Elsevier, and the payment terms and conditions.

All payments must be made in full to CCC. For payment instructions, please see information listed at the bottom of this form.

Supplier	Elsevier Limited The Boulevard,Langford Lane Kidlington,Oxford,OX5 1GB,UK
Registered Company Number	1982084
Customer name	ANKIT SHAH
Customer address	2464 CHARLOTTE ST KANSAS CITY, MO 64108
License number	3194420084447
License date	Jul 22, 2013
Licensed content publisher	Elsevier
Licensed content publication	Biochemical and Biophysical Research Communications
Licensed content title	HIV-1 envelope protein gp120 up regulates CCL5 production in astrocytes which can be circumvented by inhibitors of NF-κB pathway
Licensed content author	Ankit Shah,Dhirendra P. Singh,Shilpa Buch,Anil Kumar
Licensed content date	14 October 2011
Licensed content volume number	414
Licensed content issue number	1
Number of pages	6
Start Page	112
End Page	117
Type of Use	reuse in a thesis/dissertation
Portion	full article
Format	electronic
Are you the author of this	Yes

Elsevier article?	
Will you be translating?	No
Order reference number	
Title of your thesis/dissertation	HIV-1 gp120 and methamphetamine: implications in neuroAIDS
Expected completion date	Jan 2014
Estimated size (number of pages)	
Elsevier VAT number	GB 494 6272 12
Permissions price	0.00 USD
VAT/Local Sales Tax	0.0 USD / 0.0 GBP
Total	0.00 USD

BioMed Central copyright and license agreement

In submitting a research article ('article') to any of the journals published by BioMed Central I certify that:

1. I am authorized by my co-authors to enter into these arrangements.

2. I warrant, on behalf of myself and my co-authors, that:

    1. the article is original, has not been formally published in any other peer-reviewed journal, is not under consideration by any other journal and does not infringe any existing copyright or any other third party rights;
    2. I am/we are the sole author(s) of the article and have full authority to enter into this agreement and in granting rights to BioMed Central are not in breach of any other obligation. If the law requires that the article be published in the public domain, I/we will notify BioMed Central at the time of submission upon which clauses 3 through 6 inclusive do not apply;
    3. the article contains nothing that is unlawful, libellous, or which would, if published, constitute a breach of contract or of confidence or of commitment given to secrecy;
    4. I/we have taken due care to ensure the integrity of the article. To my/our - and currently accepted scientific - knowledge all statements contained in it purporting to be facts are true and any formula or instruction contained in the article will not, if followed accurately, cause any injury, illness or damage to the user.
    5. I agree to BioMed Central's Open Data policy

And I agree to the following license agreement:

BioMed Central Open Access license agreement
Brief summary of the agreement

Anyone is free:

- to copy, distribute, and display the work;
- to make derivative works;
- to make commercial use of the work;

Under the following conditions: Attribution

- the original author must be given credit;
- for any reuse or distribution, it must be made clear to others what the license terms of this work are;
- any of these conditions can be waived if the authors gives permission.

Statutory fair use and other rights are in no way affected by the above.

Full BioMed Central Open Access license agreement

(Identical to the 'Creative Commons Attribution License')

License

PLOSONE:

Open-Access License

No Permission Required

PLOS applies the Creative Commons Attribution License (CCAL) to all works we publish (read the human-readable summary or the full license legal code). Under the CCAL, authors retain ownership of the copyright for their article, but authors allow anyone to download, reuse, reprint, modify, distribute, and/or copy articles in PLOS journals, so long as the original authors and source are cited. **No permission is required from the authors or the publishers.**

In most cases, appropriate attribution can be provided by simply citing the original article (e.g., Kaltenbach LS et al. (2007) Huntingtin Interacting Proteins Are Genetic Modifiers of Neurodegeneration. *PLOS Genet* 3(5): e82. doi:10.1371/journal.pgen.0030082). If the item you plan to reuse is not part of a published article (e.g., a featured issue image), then please indicate the originator of the work, and the volume, issue, and date of the journal in which the item appeared. For any reuse or redistribution of a work, you must also make clear the license terms under which the work was published.

This broad license was developed to facilitate open access to, and free use of, original works of all types. Applying this standard license to your own work will ensure your right to make your work freely and openly available. Learn more about open access. For queries about the license, please contact us.

Grant of Permission

Dear Dr. Shah:

Thank you for your interest in our copyrighted material, and for requesting permission for its use.

Permission is granted for the following subject to the conditions outlined below:

Title: HIV-1 gp120 and Drugs of Abuse: Interactions in the Central Nervous System
Author(s): Peter S. Silverstein, Ankit Shah, James Weemhoff, Santosh Kumar, D. P. Singh and Anil Kumar
Pages 369-383 (15)

To be used in the following manner:

1. Bentham Science Publishers grants you the right to reproduce the material indicated above on a one-time, non-exclusive basis, solely for the purpose described. Permission must be requested separately for any future or additional use.

2. For an article, the copyright notice must be printed on the first page of article or book chapter. For figures, photographs, covers, or tables, the notice may appear with the material, in a footnote, or in the reference list.

REFERENCES

Abramov, A. Y., Jacobson, J., Wientjes, F., Hothersall, J., Canevari, L., & Duchen, M. R. (2005). Expression and modulation of an NADPH oxidase in mammalian astrocytes. *J Neurosci, 25*(40), 9176-9184. doi: 10.1523/JNEUROSCI.1632-05.2005

Adamson, D. C., Dawson, T. M., Zink, M. C., Clements, J. E., & Dawson, V. L. (1996). Neurovirulent simian immunodeficiency virus infection induces neuronal, endothelial, and glial apoptosis. *Mol Med, 2*(4), 417-428.

Agrawal, L., Louboutin, J. P., Marusich, E., Reyes, B. A., Van Bockstaele, E. J., & Strayer, D. S. (2010). Dopaminergic neurotoxicity of HIV-1 gp120: reactive oxygen species as signaling intermediates. *Brain Res, 1306*, 116-130. doi: 10.1016/j.brainres.2009.09.113

Aksenov, M. Y., Aksenova, M. V., Nath, A., Ray, P. D., Mactutus, C. F., & Booze, R. M. (2006). Cocaine-mediated enhancement of Tat toxicity in rat hippocampal cell cultures: the role of oxidative stress and D1 dopamine receptor. *Neurotoxicology, 27*(2), 217-228. doi: 10.1016/j.neuro.2005.10.003

Alvarez, S., Serramia, M. J., Fresno, M., & Munoz-Fernandez, M. (2005). Human immunodeficiency virus type 1 envelope glycoprotein 120 induces cyclooxygenase-2 expression in neuroblastoma cells through a nuclear factor-kappaB and activating protein-1 mediated mechanism. *J Neurochem, 94*(3), 850-861. doi: 10.1111/j.1471-4159.2005.03267.x

Ande, A., Earla, R., Jin, M., Silverstein, P. S., Mitra, A. K., Kumar, A., & Kumar, S. (2012). An LC-MS/MS method for concurrent determination of nicotine metabolites and the role of CYP2A6 in nicotine metabolite-mediated oxidative stress in SVGA astrocytes. *Drug Alcohol Depend, 125*(1-2), 49-59. doi: 10.1016/j.drugalcdep.2012.03.015

Anthony, I. C., & Bell, J. E. (2008). The Neuropathology of HIV/AIDS. *Int Rev Psychiatry, 20*(1), 15-24. doi: 10.1080/09540260701862037

Archibald, S. L., Masliah, E., Fennema-Notestine, C., Marcotte, T. D., Ellis, R. J., McCutchan, J. A., . . . Jernigan, T. L. (2004). Correlation of in vivo neuroimaging abnormalities with postmortem human immunodeficiency virus encephalitis and dendritic loss. *Arch Neurol, 61*(3), 369-376. doi: 10.1001/archneur.61.3.369

Arora, P. K., Fride, E., Petitto, J., Waggie, K., & Skolnick, P. (1990). Morphine-induced immune alterations in vivo. *Cell Immunol, 126*(2), 343-353.

Ascher, M. S., & Sheppard, H. W. (1988). AIDS as immune system activation: a model for pathogenesis. *Clin Exp Immunol, 73*(2), 165-167.

Avdoshina, V., Biggio, F., Palchik, G., Campbell, L. A., & Mocchetti, I. (2010). Morphine induces the release of CCL5 from astrocytes: potential neuroprotective mechanism against the HIV protein gp120. *Glia, 58*(13), 1630-1639. doi: 10.1002/glia.21035

Bachis, A., Aden, S. A., Nosheny, R. L., Andrews, P. M., & Mocchetti, I. (2006). Axonal transport of human immunodeficiency virus type 1 envelope protein glycoprotein 120 is found in association with neuronal apoptosis. *J Neurosci, 26*(25), 6771-6780. doi: 10.1523/JNEUROSCI.1054-06.2006

Bachis, A., Cruz, M. I., & Mocchetti, I. (2010). M-tropic HIV envelope protein gp120 exhibits a different neuropathological profile than T-tropic gp120 in rat striatum. *Eur J Neurosci, 32*(4), 570-578. doi: 10.1111/j.1460-9568.2010.07325.x

Banerjee, A., Zhang, X., Manda, K. R., Banks, W. A., & Ercal, N. (2010). HIV proteins (gp120 and Tat) and methamphetamine in oxidative stress-induced damage in the brain: potential role of the thiol antioxidant N-acetylcysteine amide. *Free Radic Biol Med, 48*(10), 1388-1398. doi: 10.1016/j.freeradbiomed.2010.02.023

Bardi, G., Sengupta, R., Khan, M. Z., Patel, J. P., & Meucci, O. (2006). Human immunodeficiency virus gp120-induced apoptosis of human neuroblastoma cells in the absence of CXCR4 internalization. *J Neurovirol, 12*(3), 211-218. doi: 10.1080/13550280600848373

Battaglia, G., Fornai, F., Busceti, C. L., Aloisi, G., Cerrito, F., De Blasi, A., . . . Nicoletti, F. (2002). Selective blockade of mGlu5 metabotropic glutamate receptors is protective against methamphetamine neurotoxicity. *J Neurosci, 22*(6), 2135-2141.

Beauvais, G., Atwell, K., Jayanthi, S., Ladenheim, B., & Cadet, J. L. (2011). Involvement of dopamine receptors in binge methamphetamine-induced activation of endoplasmic reticulum and mitochondrial stress pathways. *PLoS One, 6*(12), e28946. doi: 10.1371/journal.pone.0028946

Bedard, K., & Krause, K. H. (2007). The NOX family of ROS-generating NADPH oxidases: physiology and pathophysiology. *Physiol Rev, 87*(1), 245-313. doi: 10.1152/physrev.00044.2005

Beg, A. A., & Baltimore, D. (1996). An essential role for NF-kappaB in preventing TNF-alpha-induced cell death. *Science, 274*(5288), 782-784.

Berger, J. R., Kumar, M., Kumar, A., Fernandez, J. B., & Levin, B. (1994). Cerebrospinal fluid dopamine in HIV-1 infection. *AIDS, 8*(1), 67-71.

Bowie, A., & O'Neill, L. A. (2000). Oxidative stress and nuclear factor-kappaB activation: a reassessment of the evidence in the light of recent discoveries. *Biochem Pharmacol, 59*(1), 13-23. doi: S0006-2952(99)00296-8 [pii]

Bowyer, J. F., & Ali, S. (2006). High doses of methamphetamine that cause disruption of the blood-brain barrier in limbic regions produce extensive neuronal degeneration in mouse hippocampus. *Synapse, 60*(7), 521-532. doi: 10.1002/syn.20324

Broderick, D. F., Wippold, F. J., 2nd, Clifford, D. B., Kido, D., & Wilson, B. S. (1993). White matter lesions and cerebral atrophy on MR images in patients with and without AIDS dementia complex. *AJR Am J Roentgenol, 161*(1), 177-181. doi: 10.2214/ajr.161.1.8517298

Bromek, E., Haduch, A., Golembiowska, K., & Daniel, W. A. (2011). Cytochrome P450 mediates dopamine formation in the brain in vivo. *J Neurochem, 118*(5), 806-815. doi: 10.1111/j.1471-4159.2011.07339.x

Brown, J., 3rd, Theisler, C., Silberman, S., Magnuson, D., Gottardi-Littell, N., Lee, J. M., . . . Wolozin, B. (2004). Differential expression of cholesterol hydroxylases in Alzheimer's disease. *J Biol Chem, 279*(33), 34674-34681. doi: 10.1074/jbc.M402324200

Buch, S., Yao, H., Guo, M., Mori, T., Mathias-Costa, B., Singh, V., . . . Su, T. P. (2012). Cocaine and HIV-1 interplay in CNS: cellular and molecular mechanisms. *Curr HIV Res, 10*(5), 425-428.

Buchacz, K., McFarland, W., Kellogg, T. A., Loeb, L., Holmberg, S. D., Dilley, J., & Klausner, J. D. (2005). Amphetamine use is associated with increased HIV incidence among men who have sex with men in San Francisco. *AIDS, 19*(13), 1423-1424.

Cadet, J. L., & Krasnova, I. N. (2009). Molecular bases of methamphetamine-induced neurodegeneration. *Int Rev Neurobiol, 88*, 101-119. doi: 10.1016/S0074-7742(09)88005-7

Cadet, J. L., Sheng, P., Ali, S., Rothman, R., Carlson, E., & Epstein, C. (1994). Attenuation of methamphetamine-induced neurotoxicity in copper/zinc superoxide dismutase transgenic mice. *J Neurochem, 62*(1), 380-383.

Cairns, B., Kim, J. Y., Tang, X. N., & Yenari, M. A. (2012). NOX inhibitors as a therapeutic strategy for stroke and neurodegenerative disease. *Curr Drug Targets, 13*(2), 199-206.

Carroll-Anzinger, D., & Al-Harthi, L. (2006). Gamma interferon primes productive human immunodeficiency virus infection in astrocytes. *J Virol, 80*(1), 541-544. doi: 10.1128/JVI.80.1.541-544.2006

Carroll-Anzinger, D., Kumar, A., Adarichev, V., Kashanchi, F., & Al-Harthi, L. (2007). Human immunodeficiency virus-restricted replication in astrocytes and the ability of gamma interferon to modulate this restriction are regulated by a downstream effector of the Wnt signaling pathway. *J Virol, 81*(11), 5864-5871. doi: 10.1128/JVI.02234-06

Cass, W. A., Harned, M. E., Peters, L. E., Nath, A., & Maragos, W. F. (2003). HIV-1 protein Tat potentiation of methamphetamine-induced decreases in evoked overflow of dopamine in the striatum of the rat. *Brain Res, 984*(1-2), 133-142. doi: S0006899303031226 [pii]

Cattaruzza, M., & Hecker, M. (2008). Protein carbonylation and decarboylation: a new twist to the complex response of vascular cells to oxidative stress. *Circ Res, 102*(3), 273-274. doi: 10.1161/CIRCRESAHA.108.172148

Checkley, M. A., Luttge, B. G., & Freed, E. O. (2011). HIV-1 envelope glycoprotein biosynthesis, trafficking, and incorporation. *J Mol Biol, 410*(4), 582-608. doi: 10.1016/j.jmb.2011.04.042

Chen, T., Zhang, L., Qu, Y., Huo, K., Jiang, X., & Fei, Z. (2012). The selective mGluR5 agonist CHPG protects against traumatic brain injury in vitro and in vivo via ERK and Akt pathway. *Int J Mol Med, 29*(4), 630-636. doi: 10.3892/ijmm.2011.870

Cheung, R., Ravyn, V., Wang, L., Ptasznik, A., & Collman, R. G. (2008). Signaling mechanism of HIV-1 gp120 and virion-induced IL-1beta release in primary human macrophages. *J Immunol, 180*(10), 6675-6684. doi: 180/10/6675 [pii]

Churchill, M. J., Wesselingh, S. L., Cowley, D., Pardo, C. A., McArthur, J. C., Brew, B. J., & Gorry, P. R. (2009). Extensive astrocyte infection is prominent in human

immunodeficiency virus-associated dementia. *Ann Neurol, 66*(2), 253-258. doi: 10.1002/ana.21697

Clapham, P. R., & McKnight, A. (2001). HIV-1 receptors and cell tropism. *Br Med Bull, 58*, 43-59.

Clavel, F. (1987). HIV-2, the West African AIDS virus. *AIDS, 1*(3), 135-140.

Cochran, S. D., Ackerman, D., Mays, V. M., & Ross, M. W. (2004). Prevalence of non-medical drug use and dependence among homosexually active men and women in the US population. *Addiction, 99*(8), 989-998. doi: 10.1111/j.1360-0443.2004.00759.x

Coelho-Santos, V., Goncalves, J., Fontes-Ribeiro, C., & Silva, A. P. (2012). Prevention of methamphetamine-induced microglial cell death by TNF-alpha and IL-6 through activation of the JAK-STAT pathway. *J Neuroinflammation, 9*, 103. doi: 10.1186/1742-2094-9-103

Cohen, G. M., & d'Arcy Doherty, M. (1987). Free radical mediated cell toxicity by redox cycling chemicals. *Br J Cancer Suppl, 8*, 46-52.

Colfax, G., & Guzman, R. (2006). Club drugs and HIV infection: a review. *Clin Infect Dis, 42*(10), 1463-1469. doi: 10.1086/503259

Coulthard, L. R., White, D. E., Jones, D. L., McDermott, M. F., & Burchill, S. A. (2009). p38(MAPK): stress responses from molecular mechanisms to therapeutics. *Trends Mol Med, 15*(8), 369-379. doi: 10.1016/j.molmed.2009.06.005

Dairaghi, D. J., Soo, K. S., Oldham, E. R., Premack, B. A., Kitamura, T., Bacon, K. B., & Schall, T. J. (1998). RANTES-induced T cell activation correlates with CD3 expression. *J Immunol, 160*(1), 426-433.

Dasuri, K., Zhang, L., & Keller, J. N. (2013). Oxidative stress, neurodegeneration, and the balance of protein degradation and protein synthesis. *Free Radic Biol Med, 62*, 170-185. doi: 10.1016/j.freeradbiomed.2012.09.016

Davidson, C., Gow, A. J., Lee, T. H., & Ellinwood, E. H. (2001). Methamphetamine neurotoxicity: necrotic and apoptotic mechanisms and relevance to human abuse and treatment. *Brain Res Brain Res Rev, 36*(1), 1-22.

Davis, C. B., Dikic, I., Unutmaz, D., Hill, C. M., Arthos, J., Siani, M. A., . . . Littman, D. R. (1997). Signal transduction due to HIV-1 envelope interactions with chemokine receptors CXCR4 or CCR5. *J Exp Med, 186*(10), 1793-1798.

De Cock, K. M., Adjorlolo, G., Ekpini, E., Sibailly, T., Kouadio, J., Maran, M., . . . Gayle, H. D. (1993). Epidemiology and transmission of HIV-2. Why there is no HIV-2 pandemic. *JAMA, 270*(17), 2083-2086.

Diaz-Ruiz, O., Navarro, L., Mendez-Diaz, M., Galicia, O., Elder, J. H., Sanna, P. P., . . . Prospero-Garcia, O. (2001). Inhibition of the ERK pathway prevents HIVgp120-induced REM sleep increase. *Brain Res, 913*(1), 78-81.

Dostalek, M., Jurica, J., Pistovcakova, J., Hanesova, M., Tomandl, J., Linhart, I., & Sulcova, A. (2007). Effect of methamphetamine on cytochrome P450 activity. *Xenobiotica, 37*(12), 1355-1366. doi: 10.1080/00498250701652877

Drouin-Ouellet, J., Brownell, A. L., Saint-Pierre, M., Fasano, C., Emond, V., Trudeau, L. E., . . . Cicchetti, F. (2011). Neuroinflammation is associated with changes in glial mGluR5 expression and the development of neonatal excitotoxic lesions. *Glia, 59*(2), 188-199. doi: 10.1002/glia.21086

Edelman, D. A., Jiang, Y., Tyburski, J. G., Wilson, R. F., & Steffes, C. P. (2007). Cytokine production in lipopolysaccharide-exposed rat lung pericytes. *J Trauma, 62*(1), 89-93. doi: 10.1097/TA.0b013e31802dd712

Eggert, D., Dash, P. K., Serradji, N., Dong, C. Z., Clayette, P., Heymans, F., . . . Gendelman, H. E. (2009). Development of a platelet-activating factor antagonist for HIV-1 associated neurocognitive disorders. *J Neuroimmunol, 213*(1-2), 47-59. doi: 10.1016/j.jneuroim.2009.06.002

Eid, A. A., Gorin, Y., Fagg, B. M., Maalouf, R., Barnes, J. L., Block, K., & Abboud, H. E. (2009). Mechanisms of podocyte injury in diabetes: role of cytochrome P450 and NADPH oxidases. *Diabetes, 58*(5), 1201-1211. doi: 10.2337/db08-1536

Elbaz, A., Levecque, C., Clavel, J., Vidal, J. S., Richard, F., Amouyel, P., . . . Tzourio, C. (2004). CYP2D6 polymorphism, pesticide exposure, and Parkinson's disease. *Ann Neurol, 55*(3), 430-434. doi: 10.1002/ana.20051

Everall, I., Luthert, P., & Lantos, P. (1993). A review of neuronal damage in human immunodeficiency virus infection: its assessment, possible mechanism and relationship to dementia. *J Neuropathol Exp Neurol, 52*(6), 561-566.

Farber, K., & Kettenmann, H. (2005). Physiology of microglial cells. *Brain Res Brain Res Rev, 48*(2), 133-143. doi: 10.1016/j.brainresrev.2004.12.003

Filippi, C. G., Ulug, A. M., Ryan, E., Ferrando, S. J., & van Gorp, W. (2001). Diffusion tensor imaging of patients with HIV and normal-appearing white matter on MR images of the brain. *AJNR Am J Neuroradiol, 22*(2), 277-283.

Flora, G., Lee, Y. W., Nath, A., Maragos, W., Hennig, B., & Toborek, M. (2002). Methamphetamine-induced TNF-alpha gene expression and activation of AP-1 in discrete regions of mouse brain: potential role of reactive oxygen intermediates and lipid peroxidation. *Neuromolecular Med, 2*(1), 71-85. doi: 10.1385/NMM:2:1:71

Fox, L., Alford, M., Achim, C., Mallory, M., & Masliah, E. (1997). Neurodegeneration of somatostatin-immunoreactive neurons in HIV encephalitis. *J Neuropathol Exp Neurol, 56*(4), 360-368.

Frankel, A. D., & Young, J. A. (1998). HIV-1: fifteen proteins and an RNA. *Annu Rev Biochem, 67*, 1-25. doi: 10.1146/annurev.biochem.67.1.1

Fridovich, I. (1989). Superoxide dismutases. An adaptation to a paramagnetic gas. *J Biol Chem, 264*(14), 7761-7764.

Friedman, A., Arosio, P., Finazzi, D., Koziorowski, D., & Galazka-Friedman, J. (2011). Ferritin as an important player in neurodegeneration. *Parkinsonism Relat Disord, 17*(6), 423-430. doi: 10.1016/j.parkreldis.2011.03.016

Fumagalli, F., Gainetdinov, R. R., Valenzano, K. J., & Caron, M. G. (1998). Role of dopamine transporter in methamphetamine-induced neurotoxicity: evidence from mice lacking the transporter. *J Neurosci, 18*(13), 4861-4869.

Gabuzda, D. H., Ho, D. D., de la Monte, S. M., Hirsch, M. S., Rota, T. R., & Sobel, R. A. (1986). Immunohistochemical identification of HTLV-III antigen in brains of patients with AIDS. *Ann Neurol, 20*(3), 289-295. doi: 10.1002/ana.410200304

Gabuzda, D., & Wang, J. (2000). Chemokine receptors and mechanisms of cell death in HIV neuropathogenesis. *J Neurovirol, 6 Suppl 1*, S24-32.

Golembiowska, K., Konieczny, J., Wolfarth, S., & Ossowska, K. (2003). Neuroprotective action of MPEP, a selective mGluR5 antagonist, in methamphetamine-induced dopaminergic neurotoxicity is associated with a decrease in dopamine outflow and inhibition of hyperthermia in rats. *Neuropharmacology, 45*(4), 484-492.

Goncalves, J., Baptista, S., Martins, T., Milhazes, N., Borges, F., Ribeiro, C. F., . . . Silva, A. P. (2010). Methamphetamine-induced neuroinflammation and neuronal dysfunction in the mice hippocampus: preventive effect of indomethacin. *Eur J Neurosci, 31*(2), 315-326. doi: 10.1111/j.1460-9568.2009.07059.x

Goncalves, J., Martins, T., Ferreira, R., Milhazes, N., Borges, F., Ribeiro, C. F., . . . Silva, A. P. (2008). Methamphetamine-induced early increase of IL-6 and TNF-alpha mRNA expression in the mouse brain. *Ann N Y Acad Sci, 1139*, 103-111. doi: 10.1196/annals.1432.043

Gonzales, R., Ang, A., Marinelli-Casey, P., Glik, D. C., Iguchi, M. Y., Rawson, R. A., & Methamphetamine Treatment Project Corporate, Authors. (2009). Health-related quality of life trajectories of methamphetamine-dependent individuals as a function of treatment completion and continued care over a 1-year period. *J Subst Abuse Treat, 37*(4), 353-361. doi: 10.1016/j.jsat.2009.04.001

Gonzalez-Scarano, F., & Martin-Garcia, J. (2005). The neuropathogenesis of AIDS. *Nat Rev Immunol, 5*(1), 69-81. doi: 10.1038/nri1527

Gordon, C. J., Muesing, M. A., Proudfoot, A. E., Power, C. A., Moore, J. P., & Trkola, A. (1999). Enhancement of human immunodeficiency virus type 1 infection by the CC-chemokine RANTES is independent of the mechanism of virus-cell fusion. *J Virol, 73*(1), 684-694.

Gorry, P., Purcell, D., Howard, J., & McPhee, D. (1998). Restricted HIV-1 infection of human astrocytes: potential role of nef in the regulation of virus replication. *J Neurovirol, 4*(4), 377-386.

Grundner, C., Li, Y., Louder, M., Mascola, J., Yang, X., Sodroski, J., & Wyatt, R. (2005). Analysis of the neutralizing antibody response elicited in rabbits by repeated inoculation with trimeric HIV-1 envelope glycoproteins. *Virology, 331*(1), 33-46. doi: 10.1016/j.virol.2004.09.022

Guillot, T. S., Shepherd, K. R., Richardson, J. R., Wang, M. Z., Li, Y., Emson, P. C., & Miller, G. W. (2008). Reduced vesicular storage of dopamine exacerbates methamphetamine-induced neurodegeneration and astrogliosis. *J Neurochem, 106*(5), 2205-2217. doi: 10.1111/j.1471-4159.2008.05568.x

Haorah, J., Ramirez, S. H., Floreani, N., Gorantla, S., Morsey, B., & Persidsky, Y. (2008). Mechanism of alcohol-induced oxidative stress and neuronal injury. *Free Radic Biol Med, 45*(11), 1542-1550. doi: 10.1016/j.freeradbiomed.2008.08.030

Haughey, N. J., & Mattson, M. P. (2002). Calcium dysregulation and neuronal apoptosis by the HIV-1 proteins Tat and gp120. *J Acquir Immune Defic Syndr, 31 Suppl 2,* S55-61.

Hawkins, P. G., Santoso, S., Adams, C., Anest, V., & Morris, K. V. (2009). Promoter targeted small RNAs induce long-term transcriptional gene silencing in human cells. *Nucleic Acids Res, 37*(9), 2984-2995. doi: 10.1093/nar/gkp127

Hebert, M. A., & O'Callaghan, J. P. (2000). Protein phosphorylation cascades associated with methamphetamine-induced glial activation. *Ann N Y Acad Sci, 914*, 238-262.

Hedlund, E., Gustafsson, J. A., & Warner, M. (2001). Cytochrome P450 in the brain; a review. *Curr Drug Metab, 2*(3), 245-263.

Henry, B. L., Geyer, M. A., Buell, M., Perry, W., Young, J. W., Minassian, A., & Translational Methamphetamine, Aids Research Center Group. (2013). Behavioral effects of chronic methamphetamine treatment in HIV-1 gp120 transgenic mice. *Behav Brain Res, 236*(1), 210-220. doi: 10.1016/j.bbr.2012.08.037

Hesselgesser, J., & Horuk, R. (1999). Chemokine and chemokine receptor expression in the central nervous system. *J Neurovirol, 5*(1), 13-26.

Hesselgesser, J., Taub, D., Baskar, P., Greenberg, M., Hoxie, J., Kolson, D. L., & Horuk, R. (1998). Neuronal apoptosis induced by HIV-1 gp120 and the chemokine SDF-1 alpha is mediated by the chemokine receptor CXCR4. *Curr Biol, 8*(10), 595-598. doi: S0960-9822(98)70230-1 [pii]

Hou, L., & Klann, E. (2004). Activation of the phosphoinositide 3-kinase-Akt-mammalian target of rapamycin signaling pathway is required for metabotropic glutamate receptor-dependent long-term depression. *J Neurosci, 24*(28), 6352-6361. doi: 10.1523/JNEUROSCI.0995-04.2004

Howard, S. A., Nakayama, A. Y., Brooke, S. M., & Sapolsky, R. M. (1999). Glucocorticoid modulation of gp120-induced effects on calcium-dependent degenerative events in primary hippocampal and cortical cultures. *Exp Neurol, 158*(1), 164-170. doi: 10.1006/exnr.1999.7080

Hsieh, H. L., Wang, H. H., Wu, W. B., Chu, P. J., & Yang, C. M. (2010). Transforming growth factor-beta1 induces matrix metalloproteinase-9 and cell migration in astrocytes: roles of ROS-dependent ERK- and JNK-NF-kappaB pathways. *J Neuroinflammation, 7*, 88. doi: 10.1186/1742-2094-7-88

Hu, S., Sheng, W. S., Lokensgard, J. R., Peterson, P. K., & Rock, R. B. (2009). Preferential sensitivity of human dopaminergic neurons to gp120-induced oxidative damage. *J Neurovirol, 15*(5-6), 401-410. doi: 10.3109/13550280903296346

Iskander, S., Walsh, K. A., & Hammond, R. R. (2004). Human CNS cultures exposed to HIV-1 gp120 reproduce dendritic injuries of HIV-1-associated dementia. *J Neuroinflammation, 1*(1), 7. doi: 10.1186/1742-2094-1-7

Jaerve, A., & Muller, H. W. (2012). Chemokines in CNS injury and repair. *Cell Tissue Res, 349*(1), 229-248. doi: 10.1007/s00441-012-1427-3

Jayanthi, S., Ladenheim, B., & Cadet, J. L. (1998). Methamphetamine-induced changes in antioxidant enzymes and lipid peroxidation in copper/zinc-superoxide dismutase transgenic mice. *Ann N Y Acad Sci, 844*, 92-102.

Jin, M., Ande, A., Kumar, A., & Kumar, S. (2013). Regulation of cytochrome P450 2e1 expression by ethanol: role of oxidative stress-mediated pkc/jnk/sp1 pathway. *Cell Death Dis, 4*, e554. doi: 10.1038/cddis.2013.78

Johnson, R. T., McArthur, J. C., & Narayan, O. (1988). The neurobiology of human immunodeficiency virus infections. *FASEB J, 2*(14), 2970-2981.

Kaltschmidt, B., Baeuerle, P. A., & Kaltschmidt, C. (1993). Potential involvement of the transcription factor NF-kappa B in neurological disorders. *Mol Aspects Med, 14*(3), 171-190.

Kao, S. J., Lei, H. C., Kuo, C. T., Chang, M. S., Chen, B. C., Chang, Y. C., . . . Lin, C. H. (2005). Lipoteichoic acid induces nuclear factor-kappaB activation and nitric oxide synthase expression via phosphatidylinositol 3-kinase, Akt, and p38 MAPK in RAW

264.7 macrophages. *Immunology, 115*(3), 366-374. doi: 10.1111/j.1365-2567.2005.02160.x

Kato, H., Araki, T., Imai, Y., Takahashi, A., & Itoyama, Y. (2003). Protection of dopaminergic neurons with a novel astrocyte modulating agent (R)-(-)-2-propyloctanoic acid (ONO-2506) in an MPTP-mouse model of Parkinson's disease. *J Neurol Sci, 208*(1-2), 9-15. doi: S0022510X02004112 [pii]

Kaul, M., & Lipton, S. A. (1999). Chemokines and activated macrophages in HIV gp120-induced neuronal apoptosis. *Proc Natl Acad Sci U S A, 96*(14), 8212-8216.

Kaul, M., & Lipton, S. A. (2006). Mechanisms of neuroimmunity and neurodegeneration associated with HIV-1 infection and AIDS. *J Neuroimmune Pharmacol, 1*(2), 138-151. doi: 10.1007/s11481-006-9011-9

Kaul, M., Ma, Q., Medders, K. E., Desai, M. K., & Lipton, S. A. (2007). HIV-1 coreceptors CCR5 and CXCR4 both mediate neuronal cell death but CCR5 paradoxically can also contribute to protection. *Cell Death Differ, 14*(2), 296-305. doi: 10.1038/sj.cdd.4402006

Kaul, M., Zheng, J., Okamoto, S., Gendelman, H. E., & Lipton, S. A. (2005). HIV-1 infection and AIDS: consequences for the central nervous system. *Cell Death Differ, 12 Suppl 1*, 878-892. doi: 10.1038/sj.cdd.4401623

Ketzler, S., Weis, S., Haug, H., & Budka, H. (1990). Loss of neurons in the frontal cortex in AIDS brains. *Acta Neuropathol, 80*(1), 92-94.

Khan, N. A., Di Cello, F., Stins, M., & Kim, K. S. (2007). Gp120-mediated cytotoxicity of human brain microvascular endothelial cells is dependent on p38 mitogen-activated protein kinase activation. *J Neurovirol, 13*(3), 242-251. doi: 10.1080/13550280701286531

Kim, S. S., Subramanya, S., Peer, D., Shimaoka, M., & Shankar, P. (2011). Antibody-mediated delivery of siRNAs for anti-HIV therapy. *Methods Mol Biol, 721*, 339-353. doi: 10.1007/978-1-61779-037-9_21

Kita, T., Miyazaki, I., Asanuma, M., Takeshima, M., & Wagner, G. C. (2009). Dopamine-induced behavioral changes and oxidative stress in methamphetamine-induced neurotoxicity. *Int Rev Neurobiol, 88*, 43-64. doi: 10.1016/S0074-7742(09)88003-3

Klaunig, J. E., & Kamendulis, L. M. (2004). The role of oxidative stress in carcinogenesis. *Annu Rev Pharmacol Toxicol, 44*, 239-267. doi: 10.1146/annurev.pharmtox.44.101802.121851

Koutsilieri, E., ter Meulen, V., & Riederer, P. (2001). Neurotransmission in HIV associated dementia: a short review. *J Neural Transm, 108*(6), 767-775.

Kuhle, J., Lindberg, R. L., Regeniter, A., Mehling, M., Steck, A. J., Kappos, L., & Czaplinski, A. (2009). Increased levels of inflammatory chemokines in amyotrophic lateral sclerosis. *Eur J Neurol, 16*(6), 771-774. doi: 10.1111/j.1468-1331.2009.02560.x

Kumar, R., Orsoni, S., Norman, L., Verma, A. S., Tirado, G., Giavedoni, L. D., . . . Kumar, A. (2006). Chronic morphine exposure causes pronounced virus replication in cerebral compartment and accelerated onset of AIDS in SIV/SHIV-infected Indian rhesus macaques. *Virology, 354*(1), 192-206. doi: 10.1016/j.virol.2006.06.020

Kumar, R., Torres, C., Yamamura, Y., Rodriguez, I., Martinez, M., Staprans, S., . . . Kumar, A. (2004). Modulation by morphine of viral set point in rhesus macaques infected with simian immunodeficiency virus and simian-human immunodeficiency virus. *J Virol, 78*(20), 11425-11428. doi: 10.1128/JVI.78.20.11425-11428.2004

Kunsch, C., & Rosen, C. A. (1993). NF-kappa B subunit-specific regulation of the interleukin-8 promoter. *Mol Cell Biol, 13*(10), 6137-6146.

Kutsch, O., Oh, J., Nath, A., & Benveniste, E. N. (2000). Induction of the chemokines interleukin-8 and IP-10 by human immunodeficiency virus type 1 tat in astrocytes. *J Virol, 74*(19), 9214-9221.

Langford, D., Adame, A., Grigorian, A., Grant, I., McCutchan, J. A., Ellis, R. J., . . . Group, H. I. V. Neurobehavioral Research Center. (2003). Patterns of selective neuronal damage in methamphetamine-user AIDS patients. *J Acquir Immune Defic Syndr, 34*(5), 467-474.

Laurenzi, M. A., Siden, A., Persson, M. A., Norkrans, G., Hagberg, L., & Chiodi, F. (1990). Cerebrospinal fluid interleukin-6 activity in HIV infection and inflammatory and noninflammatory diseases of the nervous system. *Clin Immunol Immunopathol, 57*(2), 233-241.

Lavi, E., Kolson, D. L., Ulrich, A. M., Fu, L., & Gonzalez-Scarano, F. (1998). Chemokine receptors in the human brain and their relationship to HIV infection. *J Neurovirol, 4*(3), 301-311.

LaVoie, M. J., & Hastings, T. G. (1999). Dopamine quinone formation and protein modification associated with the striatal neurotoxicity of methamphetamine: evidence against a role for extracellular dopamine. *J Neurosci, 19*(4), 1484-1491.

Lazzerini, P. E., Lorenzini, S., Selvi, E., Capecchi, P. L., Chindamo, D., Bisogno, S., . . . Laghi-Pasini, F. (2007). Simvastatin inhibits cytokine production and nuclear factor-kB activation in interleukin 1beta-stimulated synoviocytes from rheumatoid arthritis patients. *Clin Exp Rheumatol, 25*(5), 696-700. doi: 2179 [pii]

Lee, C. S., Kim, Y. J., Jang, E. R., Kim, W., & Myung, S. C. (2010). Fluoxetine induces apoptosis in ovarian carcinoma cell line OVCAR-3 through reactive oxygen species-dependent activation of nuclear factor-kappaB. *Basic Clin Pharmacol Toxicol, 106*(6), 446-453. doi: 10.1111/j.1742-7843.2009.00509.x

Lee, C., Tomkowicz, B., Freedman, B. D., & Collman, R. G. (2005). HIV-1 gp120-induced TNF-{alpha} production by primary human macrophages is mediated by phosphatidylinositol-3 (PI-3) kinase and mitogen-activated protein (MAP) kinase pathways. *J Leukoc Biol, 78*(4), 1016-1023. doi: 10.1189/jlb.0105056

Lee, E., Yin, Z., Sidoryk-Wegrzynowicz, M., Jiang, H., & Aschner, M. (2012). 15-Deoxy-Delta12,14-prostaglandin J(2) modulates manganese-induced activation of the NF-kappaB, Nrf2, and PI3K pathways in astrocytes. *Free Radic Biol Med, 52*(6), 1067-1074. doi: 10.1016/j.freeradbiomed.2011.12.016

Lee, Y. W., Hennig, B., Yao, J., & Toborek, M. (2001). Methamphetamine induces AP-1 and NF-kappaB binding and transactivation in human brain endothelial cells. *J Neurosci Res, 66*(4), 583-591. doi: 10.1002/jnr.1248 [pii]

Lee, Y. W., Son, K. W., Flora, G., Hennig, B., Nath, A., & Toborek, M. (2002). Methamphetamine activates DNA binding of specific redox-responsive transcription factors in mouse brain. *J Neurosci Res, 70*(1), 82-89. doi: 10.1002/jnr.10370

Levy, J. A., Shimabukuro, J., Hollander, H., Mills, J., & Kaminsky, L. (1985). Isolation of AIDS-associated retroviruses from cerebrospinal fluid and brain of patients with neurological symptoms. *Lancet, 2*(8455), 586-588.

Li, J., Bentsman, G., Potash, M. J., & Volsky, D. J. (2007). Human immunodeficiency virus type 1 efficiently binds to human fetal astrocytes and induces neuroinflammatory responses independent of infection. *BMC Neurosci, 8,* 31. doi: 10.1186/1471-2202-8-31

Liang, H., Wang, X., Chen, H., Song, L., Ye, L., Wang, S. H., . . . Ho, W. Z. (2008). Methamphetamine enhances HIV infection of macrophages. *Am J Pathol, 172*(6), 1617-1624. doi: 10.2353/ajpath.2008.070971

Liu, Y., Liu, H., Kim, B. O., Gattone, V. H., Li, J., Nath, A., . . . He, J. J. (2004). CD4-independent infection of astrocytes by human immunodeficiency virus type 1: requirement for the human mannose receptor. *J Virol, 78*(8), 4120-4133.

Livak, K. J., & Schmittgen, T. D. (2001). Analysis of relative gene expression data using real-time quantitative PCR and the 2(-Delta Delta C(T)) Method. *Methods, 25*(4), 402-408. doi: 10.1006/meth.2001.1262

Louboutin, J. P., Agrawal, L., Reyes, B. A., Van Bockstaele, E. J., & Strayer, D. S. (2009). HIV-1 gp120 neurotoxicity proximally and at a distance from the point of exposure: protection by rSV40 delivery of antioxidant enzymes. *Neurobiol Dis, 34*(3), 462-476. doi: 10.1016/j.nbd.2009.03.003

Louboutin, J. P., & Strayer, D. S. (2012). Blood-brain barrier abnormalities caused by HIV-1 gp120: mechanistic and therapeutic implications. *ScientificWorldJournal, 2012*, 482575. doi: 10.1100/2012/482575

Lu, D. Y., Tang, C. H., Yeh, W. L., Wong, K. L., Lin, C. P., Chen, Y. H., . . . Fu, W. M. (2009). SDF-1alpha up-regulates interleukin-6 through CXCR4, PI3K/Akt, ERK, and NF-kappaB-dependent pathway in microglia. *Eur J Pharmacol, 613*(1-3), 146-154. doi: S0014-2999(09)00212-X [pii]
10.1016/j.ejphar.2009.03.001

Madani, N., Kozak, S. L., Kavanaugh, M. P., & Kabat, D. (1998). gp120 envelope glycoproteins of human immunodeficiency viruses competitively antagonize signaling by coreceptors CXCR4 and CCR5. *Proc Natl Acad Sci U S A, 95*(14), 8005-8010.

Mahajan, S. D., Aalinkeel, R., Sykes, D. E., Reynolds, J. L., Bindukumar, B., Adal, A., . . . Schwartz, S. A. (2008). Methamphetamine alters blood brain barrier permeability via the modulation of tight junction expression: Implication for HIV-1 neuropathogenesis

in the context of drug abuse. *Brain Res, 1203*, 133-148. doi: 10.1016/j.brainres.2008.01.093

Mahajan, S. D., Hu, Z., Reynolds, J. L., Aalinkeel, R., Schwartz, S. A., & Nair, M. P. (2006). Methamphetamine modulates gene expression patterns in monocyte derived mature dendritic cells: implications for HIV-1 pathogenesis. *Mol Diagn Ther, 10*(4), 257-269.

Major, E. O., Miller, A. E., Mourrain, P., Traub, R. G., de Widt, E., & Sever, J. (1985). Establishment of a line of human fetal glial cells that supports JC virus multiplication. *Proc Natl Acad Sci U S A, 82*(4), 1257-1261.

Marcondes, M. C., Flynn, C., Watry, D. D., Zandonatti, M., & Fox, H. S. (2010). Methamphetamine increases brain viral load and activates natural killer cells in simian immunodeficiency virus-infected monkeys. *Am J Pathol, 177*(1), 355-361. doi: 10.2353/ajpath.2010.090953

Masliah, E., Achim, C. L., Ge, N., DeTeresa, R., Terry, R. D., & Wiley, C. A. (1992). Spectrum of human immunodeficiency virus-associated neocortical damage. *Ann Neurol, 32*(3), 321-329. doi: 10.1002/ana.410320304

Masliah, E., Ge, N., Achim, C. L., Hansen, L. A., & Wiley, C. A. (1992). Selective neuronal vulnerability in HIV encephalitis. *J Neuropathol Exp Neurol, 51*(6), 585-593.

McArthur, J. C., Brew, B. J., & Nath, A. (2005). Neurological complications of HIV infection. *Lancet Neurol, 4*(9), 543-555. doi: 10.1016/S1474-4422(05)70165-4

McDermott, D. H., Beecroft, M. J., Kleeberger, C. A., Al-Sharif, F. M., Ollier, W. E., Zimmerman, P. A., . . . Murphy, P. M. (2000). Chemokine RANTES promoter polymorphism affects risk of both HIV infection and disease progression in the Multicenter AIDS Cohort Study. *AIDS, 14*(17), 2671-2678.

McGeer, E. G., & McGeer, P. L. (1998). The importance of inflammatory mechanisms in Alzheimer disease. *Exp Gerontol, 33*(5), 371-378.

Medders, K. E., Sejbuk, N. E., Maung, R., Desai, M. K., & Kaul, M. (2010). Activation of p38 MAPK is required in monocytic and neuronal cells for HIV glycoprotein 120-induced neurotoxicity. *J Immunol, 185*(8), 4883-4895. doi: 10.4049/jimmunol.0902535

Melega, W. P., Cho, A. K., Harvey, D., & Lacan, G. (2007). Methamphetamine blood concentrations in human abusers: application to pharmacokinetic modeling. *Synapse, 61*(4), 216-220. doi: 10.1002/syn.20365

Mennicken, F., Maki, R., de Souza, E. B., & Quirion, R. (1999). Chemokines and chemokine receptors in the CNS: a possible role in neuroinflammation and patterning. *Trends Pharmacol Sci, 20*(2), 73-78. doi: S0165-6147(99)01308-5 [pii]

Mette, M. F., Aufsatz, W., van der Winden, J., Matzke, M. A., & Matzke, A. J. (2000). Transcriptional silencing and promoter methylation triggered by double-stranded RNA. *EMBO J, 19*(19), 5194-5201. doi: 10.1093/emboj/19.19.5194

Meucci, O., Fatatis, A., Simen, A. A., Bushell, T. J., Gray, P. W., & Miller, R. J. (1998). Chemokines regulate hippocampal neuronal signaling and gp120 neurotoxicity. *Proc Natl Acad Sci U S A, 95*(24), 14500-14505.

Meucci, O., Fatatis, A., Simen, A. A., & Miller, R. J. (2000). Expression of CX3CR1 chemokine receptors on neurons and their role in neuronal survival. *Proc Natl Acad Sci U S A, 97*(14), 8075-8080. doi: 10.1073/pnas.090017497

Meyer, R. P., Gehlhaus, M., Knoth, R., & Volk, B. (2007). Expression and function of cytochrome p450 in brain drug metabolism. *Curr Drug Metab, 8*(4), 297-306.

Miljkovic, D., Timotijevic, G., & Mostarica Stojkovic, M. (2011). Astrocytes in the tempest of multiple sclerosis. *FEBS Lett, 585*(23), 3781-3788. doi: 10.1016/j.febslet.2011.03.047

Mogi, M., Harada, M., Narabayashi, H., Inagaki, H., Minami, M., & Nagatsu, T. (1996). Interleukin (IL)-1 beta, IL-2, IL-4, IL-6 and transforming growth factor-alpha levels are elevated in ventricular cerebrospinal fluid in juvenile parkinsonism and Parkinson's disease. *Neurosci Lett, 211*(1), 13-16. doi: 0304394096127063 [pii]

Mollace, V., Nottet, H. S., Clayette, P., Turco, M. C., Muscoli, C., Salvemini, D., & Perno, C. F. (2001). Oxidative stress and neuroAIDS: triggers, modulators and novel antioxidants. *Trends Neurosci, 24*(7), 411-416.

Monji, A., Kato, T., & Kanba, S. (2009). Cytokines and schizophrenia: Microglia hypothesis of schizophrenia. *Psychiatry Clin Neurosci, 63*(3), 257-265.

Morgan, J. E. (2000). Optic nerve head structure in glaucoma: astrocytes as mediators of axonal damage. *Eye (Lond), 14 (Pt 3B)*, 437-444. doi: 10.1038/eye.2000.128

Nagatsu, T., Mogi, M., Ichinose, H., & Togari, A. (2000). Changes in cytokines and neurotrophins in Parkinson's disease. *J Neural Transm Suppl*(60), 277-290.

Nair, M. P., & Saiyed, Z. M. (2011). Effect of methamphetamine on expression of HIV coreceptors and CC-chemokines by dendritic cells. *Life Sci, 88*(21-22), 987-994. doi: 10.1016/j.lfs.2010.09.019

Nair, M. P., Saiyed, Z. M., Nair, N., Gandhi, N. H., Rodriguez, J. W., Boukli, N., . . . Miguez-Burbano, M. J. (2009). Methamphetamine enhances HIV-1 infectivity in monocyte derived dendritic cells. *J Neuroimmune Pharmacol, 4*(1), 129-139. doi: 10.1007/s11481-008-9128-0

Narita, M., Miyatake, M., Narita, M., Shibasaki, M., Shindo, K., Nakamura, A., . . . Suzuki, T. (2006). Direct evidence of astrocytic modulation in the development of rewarding effects induced by drugs of abuse. *Neuropsychopharmacology, 31*(11), 2476-2488. doi: 10.1038/sj.npp.1301007

Nath, A., Hartloper, V., Furer, M., & Fowke, K. R. (1995). Infection of human fetal astrocytes with HIV-1: viral tropism and the role of cell to cell contact in viral transmission. *J Neuropathol Exp Neurol, 54*(3), 320-330.

Nath, A., Hauser, K. F., Wojna, V., Booze, R. M., Maragos, W., Prendergast, M., . . . Turchan, J. T. (2002). Molecular basis for interactions of HIV and drugs of abuse. *J Acquir Immune Defic Syndr, 31 Suppl 2*, S62-69.

Nath, A., Maragos, W. F., Avison, M. J., Schmitt, F. A., & Berger, J. R. (2001). Acceleration of HIV dementia with methamphetamine and cocaine. *J Neurovirol, 7*(1), 66-71. doi: 10.1080/135502801300069737

Navia, B. A., Cho, E. S., Petito, C. K., & Price, R. W. (1986). The AIDS dementia complex: II. Neuropathology. *Ann Neurol, 19*(6), 525-535. doi: 10.1002/ana.410190603

Osborne, M. P., & Olive, M. F. (2008). A role for mGluR5 receptors in intravenous methamphetamine self-administration. *Ann N Y Acad Sci, 1139*, 206-211. doi: 10.1196/annals.1432.034

Ozdener, H. (2005). Molecular mechanisms of HIV-1 associated neurodegeneration. *J Biosci, 30*(3), 391-405.

Pajoohesh-Ganji, A., & Byrnes, K. R. (2011). Novel neuroinflammatory targets in the chronically injured spinal cord. *Neurotherapeutics, 8*(2), 195-205. doi: 10.1007/s13311-011-0036-2

Park, M., Hennig, B., & Toborek, M. (2012). Methamphetamine alters occludin expression via NADPH oxidase-induced oxidative insult and intact caveolae. *J Cell Mol Med, 16*(2), 362-375. doi: 10.1111/j.1582-4934.2011.01320.x

Park, M. J., Lee, S. K., Lim, M. A., Chung, H. S., Cho, S. I., Jang, C. G., & Lee, S. M. (2006). Effect of alpha-tocopherol and deferoxamine on methamphetamine-induced neurotoxicity. *Brain Res, 1109*(1), 176-182. doi: 10.1016/j.brainres.2006.06.030

Pawate, S., Shen, Q., Fan, F., & Bhat, N. R. (2004). Redox regulation of glial inflammatory response to lipopolysaccharide and interferongamma. *J Neurosci Res, 77*(4), 540-551. doi: 10.1002/jnr.20180

Perez-Casanova, A., Husain, K., Noel, R. J., Jr., Rivera-Amill, V., & Kumar, A. (2008). Interaction of SIV/SHIV infection and morphine on plasma oxidant/antioxidant balance in macaque. *Mol Cell Biochem, 308*(1-2), 169-175. doi: 10.1007/s11010-007-9625-0

Perez-Casanova, A., Noel, R. J., Jr., Rivera-Amill, V., Husain, K., & Kumar, A. (2007). Morphine-mediated deterioration of oxidative stress leads to rapid disease progression in SIV/SHIV-infected macaques. *AIDS Res Hum Retroviruses, 23*(8), 1004-1007. doi: 10.1089/aid.2006.0286

Perrella, O., Finelli, L., & Carrieri, P. B. (1992). The role of cytokines in AIDS-dementia complex. *Acta Neurol (Napoli), 14*(4-6), 342-344.

Persidsky, Y., Ramirez, S. H., Haorah, J., & Kanmogne, G. D. (2006). Blood-brain barrier: structural components and function under physiologic and pathologic conditions. *J Neuroimmune Pharmacol, 1*(3), 223-236. doi: 10.1007/s11481-006-9025-3

Potula, R., Hawkins, B. J., Cenna, J. M., Fan, S., Dykstra, H., Ramirez, S. H., . . . Persidsky, Y. (2010). Methamphetamine causes mitrochondrial oxidative damage in human T lymphocytes leading to functional impairment. *J Immunol, 185*(5), 2867-2876. doi: 10.4049/jimmunol.0903691

Price, T. O., Ercal, N., Nakaoke, R., & Banks, W. A. (2005). HIV-1 viral proteins gp120 and Tat induce oxidative stress in brain endothelial cells. *Brain Res, 1045*(1-2), 57-63. doi: 10.1016/j.brainres.2005.03.031

Pu, C., & Vorhees, C. V. (1995). Protective effects of MK-801 on methamphetamine-induced depletion of dopaminergic and serotonergic terminals and striatal astrocytic response: an immunohistochemical study. *Synapse, 19*(2), 97-104. doi: 10.1002/syn.890190205

Ramamoorthy, Y., Yu, A. M., Suh, N., Haining, R. L., Tyndale, R. F., & Sellers, E. M. (2002). Reduced (+/-)-3,4-methylenedioxymethamphetamine ("Ecstasy") metabolism with cytochrome P450 2D6 inhibitors and pharmacogenetic variants in vitro. *Biochem Pharmacol, 63*(12), 2111-2119.

Ramirez, S. H., Potula, R., Fan, S., Eidem, T., Papugani, A., Reichenbach, N., . . . Persidsky, Y. (2009). Methamphetamine disrupts blood-brain barrier function by induction of oxidative stress in brain endothelial cells. *J Cereb Blood Flow Metab, 29*(12), 1933-1945. doi: 10.1038/jcbfm.2009.112

Reddy, P. V., Gandhi, N., Samikkannu, T., Saiyed, Z., Agudelo, M., Yndart, A., . . . Nair, M. P. (2012). HIV-1 gp120 induces antioxidant response element-mediated expression in primary astrocytes: role in HIV associated neurocognitive disorder. *Neurochem Int, 61*(5), 807-814. doi: 10.1016/j.neuint.2011.06.011

Reddy, S. A., Huang, J. H., & Liao, W. S. (2000). Phosphatidylinositol 3-kinase as a mediator of TNF-induced NF-kappa B activation. *J Immunol, 164*(3), 1355-1363. doi: ji_v164n3p1355 [pii]

Reichel, C. M., Schwendt, M., McGinty, J. F., Olive, M. F., & See, R. E. (2011). Loss of object recognition memory produced by extended access to methamphetamine self-administration is reversed by positive allosteric modulation of metabotropic glutamate receptor 5. *Neuropsychopharmacology, 36*(4), 782-792. doi: 10.1038/npp.2010.212

Ribeiro, F. M., Paquet, M., Cregan, S. P., & Ferguson, S. S. (2010). Group I metabotropic glutamate receptor signalling and its implication in neurological disease. *CNS Neurol Disord Drug Targets, 9*(5), 574-595.

Ribeiro, F. M., Paquet, M., Ferreira, L. T., Cregan, T., Swan, P., Cregan, S. P., & Ferguson, S. S. (2010). Metabotropic glutamate receptor-mediated cell signaling pathways are

altered in a mouse model of Huntington's disease. *J Neurosci, 30*(1), 316-324. doi: 10.1523/JNEUROSCI.4974-09.2010

Ribeiro, F. M., Pires, R. G., & Ferguson, S. S. (2011). Huntington's disease and Group I metabotropic glutamate receptors. *Mol Neurobiol, 43*(1), 1-11. doi: 10.1007/s12035-010-8153-1

Ricci, G., Volpi, L., Pasquali, L., Petrozzi, L., & Siciliano, G. (2009). Astrocyte-neuron interactions in neurological disorders. *J Biol Phys, 35*(4), 317-336. doi: 10.1007/s10867-009-9157-9

Riviere, G. J., Gentry, W. B., & Owens, S. M. (2000). Disposition of methamphetamine and its metabolite amphetamine in brain and other tissues in rats after intravenous administration. *J Pharmacol Exp Ther, 292*(3), 1042-1047.

Ronaldson, P. T., Ashraf, T., & Bendayan, R. (2010). Regulation of multidrug resistance protein 1 by tumor necrosis factor alpha in cultured glial cells: involvement of nuclear factor-kappaB and c-Jun N-terminal kinase signaling pathways. *Mol Pharmacol, 77*(4), 644-659. doi: 10.1124/mol.109.059410

Ronaldson, P. T., & Bendayan, R. (2006). HIV-1 viral envelope glycoprotein gp120 triggers an inflammatory response in cultured rat astrocytes and regulates the functional expression of P-glycoprotein. *Mol Pharmacol, 70*(3), 1087-1098. doi: 10.1124/mol.106.025973

Ronaldson, P. T., & Bendayan, R. (2008). HIV-1 viral envelope glycoprotein gp120 produces oxidative stress and regulates the functional expression of multidrug resistance protein-1 (Mrp1) in glial cells. *J Neurochem, 106*(3), 1298-1313. doi: 10.1111/j.1471-4159.2008.05479.x

Saha, R. N., & Pahan, K. (2003). Tumor necrosis factor-alpha at the crossroads of neuronal life and death during HIV-associated dementia. *J Neurochem, 86*(5), 1057-1071. doi: 1942 [pii]

Saile, B., Matthes, N., El Armouche, H., Neubauer, K., & Ramadori, G. (2001). The bcl, NFkappaB and p53/p21WAF1 systems are involved in spontaneous apoptosis and in the anti-apoptotic effect of TGF-beta or TNF-alpha on activated hepatic stellate cells. *Eur J Cell Biol, 80*(8), 554-561.

Sanga, M., Younis, I. R., Tirumalai, P. S., Bland, T. M., Banaszewska, M., Konat, G. W., . . . Callery, P. S. (2006). Epoxidation of the methamphetamine pyrolysis product, trans-phenylpropene, to trans-phenylpropylene oxide by CYP enzymes and stereoselective glutathione adduct formation. *Toxicol Appl Pharmacol, 211*(2), 148-156. doi: 10.1016/j.taap.2005.06.017

Sather, D. N., Armann, J., Ching, L. K., Mavrantoni, A., Sellhorn, G., Caldwell, Z., . . . Stamatatos, L. (2009). Factors associated with the development of cross-reactive neutralizing antibodies during human immunodeficiency virus type 1 infection. *J Virol, 83*(2), 757-769. doi: 10.1128/JVI.02036-08

Schoeniger-Skinner, D. K., Ledeboer, A., Frank, M. G., Milligan, E. D., Poole, S., Martin, D., . . . Watkins, L. R. (2007). Interleukin-6 mediates low-threshold mechanical allodynia induced by intrathecal HIV-1 envelope glycoprotein gp120. *Brain Behav Immun, 21*(5), 660-667. doi: 10.1016/j.bbi.2006.10.010

Sellhorn, G., Caldwell, Z., Mineart, C., & Stamatatos, L. (2009). Improving the expression of recombinant soluble HIV Envelope glycoproteins using pseudo-stable transient transfection. *Vaccine, 28*(2), 430-436. doi: 10.1016/j.vaccine.2009.10.028

Shah, A., & Kumar, A. (2010). HIV-1 gp120-mediated increases in IL-8 production in astrocytes are mediated through the NF-kappaB pathway and can be silenced by gp120-specific siRNA. *J Neuroinflammation, 7*, 96. doi: 10.1186/1742-2094-7-96

Shah, A., Silverstein, P. S., Singh, D. P., & Kumar, A. (2012). Involvement of metabotropic glutamate receptor 5, AKT/PI3K signaling and NF-kappaB pathway in methamphetamine-mediated increase in IL-6 and IL-8 expression in astrocytes. *J Neuroinflammation, 9*, 52. doi: 10.1186/1742-2094-9-52

Shah, A., Singh, D. P., Buch, S., & Kumar, A. (2011). HIV-1 envelope protein gp120 up regulates CCL5 production in astrocytes which can be circumvented by inhibitors of NF-kappaB pathway. *Biochem Biophys Res Commun, 414*(1), 112-117. doi: 10.1016/j.bbrc.2011.09.033

Shah, A., Verma, A. S., Patel, K. H., Noel, R., Rivera-Amill, V., Silverstein, P. S., . . . Kumar, A. (2011). HIV-1 gp120 induces expression of IL-6 through a nuclear factor-kappa B-dependent mechanism: suppression by gp120 specific small interfering RNA. *PLoS One, 6*(6), e21261. doi: 10.1371/journal.pone.0021261

Shin, E. J., Duong, C. X., Nguyen, X. K., Li, Z., Bing, G., Bach, J. H., . . . Kim, H. C. (2012). Role of oxidative stress in methamphetamine-induced dopaminergic toxicity

mediated by protein kinase Cdelta. *Behav Brain Res, 232*(1), 98-113. doi: 10.1016/j.bbr.2012.04.001

Siebenlist, U., Franzoso, G., & Brown, K. (1994). Structure, regulation and function of NF-kappa B. *Annu Rev Cell Biol, 10*, 405-455. doi: 10.1146/annurev.cb.10.110194.002201

Silva, A. P., Martins, T., Baptista, S., Goncalves, J., Agasse, F., & Malva, J. O. (2010). Brain injury associated with widely abused amphetamines: neuroinflammation, neurogenesis and blood-brain barrier. *Curr Drug Abuse Rev, 3*(4), 239-254.

Silverstein, P. S., Shah, A., Gupte, R., Liu, X., Piepho, R. W., Kumar, S., & Kumar, A. (2011). Methamphetamine toxicity and its implications during HIV-1 infection. *J Neurovirol, 17*(5), 401-415. doi: 10.1007/s13365-011-0043-4

Silverstein, P. S., Shah, A., Weemhoff, J., Kumar, S., Singh, D. P., & Kumar, A. (2012). HIV-1 gp120 and drugs of abuse: interactions in the central nervous system. *Curr HIV Res, 10*(5), 369-383.

Sinke, A. P., Jayakumar, A. R., Panickar, K. S., Moriyama, M., Reddy, P. V., & Norenberg, M. D. (2008). NFkappaB in the mechanism of ammonia-induced astrocyte swelling in culture. *J Neurochem, 106*(6), 2302-2311. doi: 10.1111/j.1471-4159.2008.05549.x

Sorce, S., Krause, K. H., & Jaquet, V. (2012). Targeting NOX enzymes in the central nervous system: therapeutic opportunities. *Cell Mol Life Sci, 69*(14), 2387-2407. doi: 10.1007/s00018-012-1014-5

Sparacio, S. M., Zhang, Y., Vilcek, J., & Benveniste, E. N. (1992). Cytokine regulation of interleukin-6 gene expression in astrocytes involves activation of an NF-kappa B-like nuclear protein. *J Neuroimmunol, 39*(3), 231-242.

Spargo, E., Everall, I. P., & Lantos, P. L. (1993). Neuronal loss in the hippocampus in Huntington's disease: a comparison with HIV infection. *J Neurol Neurosurg Psychiatry, 56*(5), 487-491.

Sriram, K., Miller, D. B., & O'Callaghan, J. P. (2006). Minocycline attenuates microglial activation but fails to mitigate striatal dopaminergic neurotoxicity: role of tumor necrosis factor-alpha. *J Neurochem, 96*(3), 706-718. doi: 10.1111/j.1471-4159.2005.03566.x

Steinman, L. (2008). Nuanced roles of cytokines in three major human brain disorders. *J Clin Invest, 118*(11), 3557-3563. doi: 10.1172/JCI36532

Stephans, S., & Yamamoto, B. (1996). Methamphetamines pretreatment and the vulnerability of the striatum to methamphetamine neurotoxicity. *Neuroscience, 72*(3), 593-600.

Suzuki, Y. J., Carini, M., & Butterfield, D. A. (2010). Protein carbonylation. *Antioxid Redox Signal, 12*(3), 323-325. doi: 10.1089/ars.2009.2887

Takimoto, T., Ujike, H., Nakamura, K., & Iwahashi, K. (2002). [Increase expression of CYP2E1 mRNA after methamphetamine administration in rats]. *Nihon Arukoru Yakubutsu Igakkai Zasshi, 37*(3), 163-167.

Talloczy, Z., Martinez, J., Joset, D., Ray, Y., Gacser, A., Toussi, S., . . . Santambrogio, L. (2008). Methamphetamine inhibits antigen processing, presentation, and phagocytosis. *PLoS Pathog, 4*(2), e28. doi: 10.1371/journal.ppat.0040028

Tang, C. H., Chiu, Y. C., Tan, T. W., Yang, R. S., & Fu, W. M. (2007). Adiponectin enhances IL-6 production in human synovial fibroblast via an AdipoR1 receptor, AMPK, p38, and NF-kappa B pathway. *J Immunol, 179*(8), 5483-5492. doi: 179/8/5483 [pii]

Tata, D. A., & Yamamoto, B. K. (2007). Interactions between methamphetamine and environmental stress: role of oxidative stress, glutamate and mitochondrial dysfunction. *Addiction, 102 Suppl 1*, 49-60. doi: 10.1111/j.1360-0443.2007.01770.x

Tata, D. A., & Yamamoto, B. K. (2008). Chronic stress enhances methamphetamine-induced extracellular glutamate and excitotoxicity in the rat striatum. *Synapse, 62*(5), 325-336. doi: 10.1002/syn.20497

Theodore, S., Stolberg, S., Cass, W. A., & Maragos, W. F. (2006). Human immunodeficiency virus-1 protein tat and methamphetamine interactions. *Ann N Y Acad Sci, 1074*, 178-190. doi: 10.1196/annals.1369.018

Thompson, K. A., Churchill, M. J., Gorry, P. R., Sterjovski, J., Oelrichs, R. B., Wesselingh, S. L., & McLean, C. A. (2004). Astrocyte specific viral strains in HIV dementia. *Ann Neurol, 56*(6), 873-877. doi: 10.1002/ana.20304

Thompson, K. A., McArthur, J. C., & Wesselingh, S. L. (2001). Correlation between neurological progression and astrocyte apoptosis in HIV-associated dementia. *Ann Neurol, 49*(6), 745-752.

Thompson, W. L., & Van Eldik, L. J. (2009). Inflammatory cytokines stimulate the chemokines CCL2/MCP-1 and CCL7/MCP-3 through NFkB and MAPK dependent pathways in rat astrocytes [corrected]. *Brain Res, 1287*, 47-57. doi: 10.1016/j.brainres.2009.06.081

Tocharus, J., Khonthun, C., Chongthammakun, S., & Govitrapong, P. (2010). Melatonin attenuates methamphetamine-induced overexpression of pro-inflammatory cytokines in microglial cell lines. *J Pineal Res, 48*(4), 347-352. doi: 10.1111/j.1600-079X.2010.00761.x

Toussi, S. S., Joseph, A., Zheng, J. H., Dutta, M., Santambrogio, L., & Goldstein, H. (2009). Short communication: Methamphetamine treatment increases in vitro and in vivo HIV replication. *AIDS Res Hum Retroviruses, 25*(11), 1117-1121. doi: 10.1089/aid.2008.0282

Trkola, A., Gordon, C., Matthews, J., Maxwell, E., Ketas, T., Czaplewski, L., . . . Moore, J. P. (1999). The CC-chemokine RANTES increases the attachment of human immunodeficiency virus type 1 to target cells via glycosaminoglycans and also activates a signal transduction pathway that enhances viral infectivity. *J Virol, 73*(8), 6370-6379.

Turchan, J., Anderson, C., Hauser, K. F., Sun, Q., Zhang, J., Liu, Y., . . . Nath, A. (2001). Estrogen protects against the synergistic toxicity by HIV proteins, methamphetamine and cocaine. *BMC Neurosci, 2*, 3.

Tyor, W. R., Glass, J. D., Griffin, J. W., Becker, P. S., McArthur, J. C., Bezman, L., & Griffin, D. E. (1992). Cytokine expression in the brain during the acquired immunodeficiency syndrome. *Ann Neurol, 31*(4), 349-360. doi: 10.1002/ana.410310402

Valoti, M., Fusi, F., Frosini, M., Pessina, F., Tipton, K. F., & Sgaragli, G. P. (2000). Cytochrome P450-dependent N-dealkylation of L-deprenyl in C57BL mouse liver microsomes: effects of in vivo pretreatment with ethanol, phenobarbital, beta-naphthoflavone and L-deprenyl. *Eur J Pharmacol, 391*(3), 199-206.

van Golen, R. F., van Gulik, T. M., & Heger, M. (2012). Mechanistic overview of reactive species-induced degradation of the endothelial glycocalyx during hepatic

ischemia/reperfusion injury. *Free Radic Biol Med, 52*(8), 1382-1402. doi: 10.1016/j.freeradbiomed.2012.01.013

van Marle, G., Henry, S., Todoruk, T., Sullivan, A., Silva, C., Rourke, S. B., . . . Power, C. (2004). Human immunodeficiency virus type 1 Nef protein mediates neural cell death: a neurotoxic role for IP-10. *Virology, 329*(2), 302-318. doi: 10.1016/j.virol.2004.08.024

Vanden Berghe, W., Plaisance, S., Boone, E., De Bosscher, K., Schmitz, M. L., Fiers, W., & Haegeman, G. (1998). p38 and extracellular signal-regulated kinase mitogen-activated protein kinase pathways are required for nuclear factor-kappaB p65 transactivation mediated by tumor necrosis factor. *J Biol Chem, 273*(6), 3285-3290.

Visalli, V., Muscoli, C., Sacco, I., Sculco, F., Palma, E., Costa, N., . . . Mollace, V. (2007). N-acetylcysteine prevents HIV gp 120-related damage of human cultured astrocytes: correlation with glutamine synthase dysfunction. *BMC Neurosci, 8*, 106. doi: 10.1186/1471-2202-8-106

Viviani, B., Corsini, E., Binaglia, M., Galli, C. L., & Marinovich, M. (2001). Reactive oxygen species generated by glia are responsible for neuron death induced by human immunodeficiency virus-glycoprotein 120 in vitro. *Neuroscience, 107*(1), 51-58. doi: S0306-4522(01)00332-3 [pii]

Viviani, B., Gardoni, F., Bartesaghi, S., Corsini, E., Facchi, A., Galli, C. L., . . . Marinovich, M. (2006). Interleukin-1 beta released by gp120 drives neural death through tyrosine phosphorylation and trafficking of NMDA receptors. *J Biol Chem, 281*(40), 30212-30222. doi: 10.1074/jbc.M602156200

Wagner, G. C., Ricaurte, G. A., Seiden, L. S., Schuster, C. R., Miller, R. J., & Westley, J. (1980). Long-lasting depletions of striatal dopamine and loss of dopamine uptake sites following repeated administration of methamphetamine. *Brain Res, 181*(1), 151-160. doi: 0006-8993(80)91265-2 [pii]

Wallace, D. R., Dodson, S., Nath, A., & Booze, R. M. (2006). Estrogen attenuates gp120- and tat1-72-induced oxidative stress and prevents loss of dopamine transporter function. *Synapse, 59*(1), 51-60. doi: 10.1002/syn.20214

Wang, A. L., Li, Z., Yuan, M., Yu, A. C., Zhu, X., & Tso, M. O. (2007). Sinomenine inhibits activation of rat retinal microglia induced by advanced glycation end products. *Int Immunopharmacol, 7*(12), 1552-1558. doi: 10.1016/j.intimp.2007.07.030

Wang, X., Ke, Z., Chen, G., Xu, M., Bower, K. A., Frank, J. A., . . . Luo, J. (2012). Cdc42-dependent activation of NADPH oxidase is involved in ethanol-induced neuronal oxidative stress. *PLoS One, 7*(5), e38075. doi: 10.1371/journal.pone.0038075

Warny, M., Keates, A. C., Keates, S., Castagliuolo, I., Zacks, J. K., Aboudola, S., . . . Kelly, C. P. (2000). p38 MAP kinase activation by Clostridium difficile toxin A mediates monocyte necrosis, IL-8 production, and enteritis. *J Clin Invest, 105*(8), 1147-1156. doi: 10.1172/JCI7545

Wilen, C. B., Tilton, J. C., & Doms, R. W. (2012). HIV: cell binding and entry. *Cold Spring Harb Perspect Med, 2*(8). doi: 10.1101/cshperspect.a006866

Wojcikowski, J., & Daniel, W. A. (2009). The brain dopaminergic system as an important center regulating liver cytochrome P450 in the rat. *Expert Opin Drug Metab Toxicol, 5*(6), 631-645. doi: 10.1517/17425250902973703

Wu, C., Lin, J., Hong, M., Choudhury, Y., Balani, P., Leung, D., . . . Wang, S. (2009). Combinatorial control of suicide gene expression by tissue-specific promoter and microRNA regulation for cancer therapy. *Mol Ther, 17*(12), 2058-2066. doi: 10.1038/mt.2009.225

Wu, D., Otton, S. V., Inaba, T., Kalow, W., & Sellers, E. M. (1997). Interactions of amphetamine analogs with human liver CYP2D6. *Biochem Pharmacol, 53*(11), 1605-1612.

Xu, W., Zhu, J. P., & Angulo, J. A. (2005). Induction of striatal pre- and postsynaptic damage by methamphetamine requires the dopamine receptors. *Synapse, 58*(2), 110-121. doi: 10.1002/syn.20185

Yamaguchi, T., Kuraishi, Y., Minami, M., Nakai, S., Hirai, Y., & Satoh, M. (1991). Methamphetamine-induced expression of interleukin-1 beta mRNA in the rat hypothalamus. *Neurosci Lett, 128*(1), 90-92. doi: 0304-3940(91)90766-M [pii]

Yamamoto, B. K., & Raudensky, J. (2008). The role of oxidative stress, metabolic compromise, and inflammation in neuronal injury produced by amphetamine-related drugs of abuse. *J Neuroimmune Pharmacol, 3*(4), 203-217. doi: 10.1007/s11481-008-9121-7

Yang, Y., Yao, H., Lu, Y., Wang, C., & Buch, S. (2010). Cocaine potentiates astrocyte toxicity mediated by human immunodeficiency virus (HIV-1) protein gp120. *PLoS One, 5*(10), e13427. doi: 10.1371/journal.pone.0013427

Yao, H., Allen, J. E., Zhu, X., Callen, S., & Buch, S. (2009). Cocaine and human immunodeficiency virus type 1 gp120 mediate neurotoxicity through overlapping signaling pathways. *J Neurovirol, 15*(2), 164-175. doi: 10.1080/13550280902755375

Younger, S. T., & Corey, D. R. (2011). Transcriptional gene silencing in mammalian cells by miRNA mimics that target gene promoters. *Nucleic Acids Res, 39*(13), 5682-5691. doi: 10.1093/nar/gkr155

Zhang, X., Banerjee, A., Banks, W. A., & Ercal, N. (2009). N-Acetylcysteine amide protects against methamphetamine-induced oxidative stress and neurotoxicity in immortalized human brain endothelial cells. *Brain Res, 1275*, 87-95. doi: 10.1016/j.brainres.2009.04.008

Zhang, X., Song, Y., Ci, X., An, N., Ju, Y., Li, H., . . . Deng, X. (2008). Ivermectin inhibits LPS-induced production of inflammatory cytokines and improves LPS-induced survival in mice. *Inflamm Res, 57*(11), 524-529. doi: 10.1007/s00011-008-8007-8

Zhao, J., O'Connor, T., & Vassar, R. (2011). The contribution of activated astrocytes to Abeta production: implications for Alzheimer's disease pathogenesis. *J Neuroinflammation, 8*, 150. doi: 10.1186/1742-2094-8-150

Zheng, J., Ghorpade, A., Niemann, D., Cotter, R. L., Thylin, M. R., Epstein, L., . . . Gendelman, H. E. (1999). Lymphotropic virions affect chemokine receptor-mediated neural signaling and apoptosis: implications for human immunodeficiency virus type 1-associated dementia. *J Virol, 73*(10), 8256-8267.

Ziebell, J. M., & Morganti-Kossmann, M. C. (2010). Involvement of pro- and anti-inflammatory cytokines and chemokines in the pathophysiology of traumatic brain injury. *Neurotherapeutics, 7*(1), 22-30. doi: 10.1016/j.nurt.2009.10.016

Zink, M. C., Coleman, G. D., Mankowski, J. L., Adams, R. J., Tarwater, P. M., Fox, K., & Clements, J. E. (2001). Increased macrophage chemoattractant protein-1 in cerebrospinal fluid precedes and predicts simian immunodeficiency virus encephalitis. *J Infect Dis, 184*(8), 1015-1021. doi: 10.1086/323478

Zou, S., Fitting, S., Hahn, Y. K., Welch, S. P., El-Hage, N., Hauser, K. F., & Knapp, P. E. (2011). Morphine potentiates neurodegenerative effects of HIV-1 Tat through actions at mu-opioid receptor-expressing glia. *Brain, 134*(Pt 12), 3616-3631. doi: 10.1093/brain/awr281

VITA

Ankit Shah was born on April 21, 1985 in Mumbai, India. He was educated in public schools in Ahmedabad, where he was brought up. After his high school, he completed his bachelors in pharmacy in pharmaceutical sciences from North Gujarat University, Gujarat, India. After completion, he also worked as a Quality Assurance officer for 6 months in Intas Pharmaceuticals at Ahmedabad, India.

After graduation from India, Mr. Shah came to United States in 2007 and joined the interdisciplinary Ph.D. program at UMKC in fall 2008 to pursue doctoral degree. During his graduate study, Mr. Shah was awarded with several awards, including the Dean's Award, Best student Award, Robert C. Lanman award and Chancellor's Doctoral Fellowship award. Mr. Shah has presented his research findings in several national and international meetings upon receiving the travel grants and awards from various societies. As a result of his dedicated hard work, Mr. Shah has published 12 papers in peer-reviewed journals and 6 of them are as first author.